A Stochastic Space-Time Rainfall Model for Engineering Risk Assessment

by Michael Leonard

Submitted in fulfilment of the requirements for the degree of
DOCTOR OF PHILOSOPHY

April 14, 2010

FACULTY OF ENGINEERING, COMPUTER AND MATHEMATICAL SCIENCES
School of Civil Environmental and Mining Engineering
THE UNIVERSITY OF ADELAIDE
AUSTRALIA

References

Abramowitz, M., and I. Stegun (1964), *Handbook of mathematical functions*, Applied Mathematics Series, National Bureau of Standards, Washington, D.C.

Allcroft, D. J., and C. A. Glasbey (2003), A latent gaussian markov random-field model for spatiotemporal rainfall disaggregation, *Journal of the Royal Statistical Society Series C-Applied Statistics*, *52*, 487–498.

Bacchi, B., and N. T. Kottegoda (1995), Identification and calibration of spatial correlation patterns of rainfall, *Journal of Hydrology*, *165*(1-4), 311–348.

Ball, J. (1994), The influence of storm temporal patterns on catchment response, *Journal of Hydrology*, *158*, 275–303, doi:10.1016/0022-1694(95)02778-N.

Bartlett, M. S. (1963), The spectral analysis of point processes, *Journal of the Royal Statistical Society, Series B*, *25*, 264–280.

Battan, L. (1962), *Radar observes the weather*, Science study series ; no. 18, Heinemann, London, U.K.

Bell, T. (1987), A space-time stochastic model of rainfall for satellite remote sensing studies, *Journal of Geophysical Research.*, *92*, 96319643.

Bjerknes, J. (1969), Atmospheric teleconnections from the equatorial pacific, *Monthly Weather Review*, *97*(3), 163–172.

Blaikie, J., and J. Ball (2005), Loss models - /an evaluation of the probability of antecedent rainfall prior to significant/ rainfall events in sydney, australia, in *Proceedings of Urban Drainage Modelling*, Copenhagen.

BOM (1983), *Climate of Australia*, from: Year Book of Australia, No. 67, Bureau of Meteorology, Australian Government Publishing Service, Canberra, Australia.

BTE (2001), Economic cost of natural distasters in australia, *Tech. rep.*, Bureau of Transport Economics, Canberra, Australia.

Burlando, P., and R. Rosso (1996), Scaling and multiscaling models of depth-duration-frequency curves for storm precipitation, *Journal of Hydrology*, *187*(1-2), 45–64.

Chan, R., and M. Ng (1996), Conjugate gradient methods for toeplitz systems, *SIAM Review*, *38*(3), 427–482.

Chandler, R. (1997), A spectral method for estimating parameters in rainfall models, *Bernoulli*, *3*, 301–332.

Chaubey, I., C. T. Haan, S. Grunwald, and J. M. Salisbury (1999), Uncertainty in the model parameters due to spatial variability of rainfall, *Journal of Hydrology*, *220*(1-2), 48–61.

Chiew, F., T. Piechota, J. Dracup, and T. McMahon (1998), El nino southern oscillation and australian rainfall, streamflow and drought: Links and potential for forecasting, *Journal of Hydrology*, *204*, 138–149, doi:10.1016/S0022-1694(97)00121-2.

Cowpertwait, P. (1994), A generalized point process model for rainfall, *Proceedings of the Royal Society of London Series a- Mathematical and Physical Sciences*, *447*(1929), 23–27.

Cowpertwait, P. (1995), A generalized spatial-temporal model of rainfall based on a clustered point process, *Proceedings of the Royal Society of London Series a- Mathematical and Physical Sciences*, *450*(1938), 163–175.

Cowpertwait, P. (2004), Mixed rectangular pulses models of rainfall, *Hydrology and Earth System Sciences*, *8*(5), 993–1000.

Cowpertwait, P., C. G. Kilsby, and P. E. O'Connell (2002), A space-time Neyman-Scott model of rainfall: Empirical analysis of extremes, *Water Resources Research*, *38*(8), 6,1–14, doi:10.1029/2001WR000709.

Cowpertwait, P. S. P. (1991), Further developments of the Neyman-Scott clustered point process for modeling rainfall, *Water Resources Research*, *27*(7), 1431–1438.

Cowpertwait, P. S. P. (1998), A poisson-cluster model of rainfall: high-order moments and extreme value, *Proceedings of the Royal Society of London Series a- Mathematical and Physical Sciences*, *454*(1971), 885–898.

Cowpertwait, P. S. P., P. E. Oconnell, A. V. Metcalfe, and J. A. Mawdsley (1996a), Stochastic point process modelling of rainfall .1. single-site fitting and validation, *Journal of Hydrology*, *175*(1-4), 17–46.

Cowpertwait, P. S. P., P. E. Oconnell, A. V. Metcalfe, and J. A. Mawdsley (1996b), Stochastic point process modelling of rainfall .2. regionalisation and disaggregation, *Journal of Hydrology*, *175*(1-4), 47–65.

Cox, D. R., and V. Isham (1980), *Point Processes*, Chapman and Hall, London.

Cox, D. R., and V. Isham (1988), A simple spatial-temporal model of rainfall, *Proceedings of the Royal Society of London Series a- Mathematical Physical and Engineering Sciences*, *415*(1849), 317–328.

Crane, R. K. (1990), Space-time structure of rain rate fields, *Journal of Geophysical Research-Atmospheres*, *95*(D3), 2011–2020.

Dalezios, N. R., and K. Adamowski (1995), Spatiotemporal precipitation modeling in rural watersheds, *Hydrological Sciences Journal-Journal Des Sciences Hydrologiques*, *50*(5), 553–568.

De Lima, M., and J. Grasman (1999), Multifractal analysis of 15-min and daily rainfall from a semi-arid region in portugal, *Journal of Hydrology*, *220*, 1–11.

Deidda, R., G. Mascaro, E. Piga, and G. Querzoli (2007), An automatic system for rainfall signal recognition from tipping bucket gauge strip charts, *Journal of Hydrology*, *333*, 400–412.

Deitrich, C. (1993), Computationally efficient cholesky factorization of a covariance-matrix with block toeplitz structure, *Journal of Statistical Computation And Simulation*, *45*(3-4), 203–218.

Deitrich, C., and G. Newsam (1997), Fast and exact simulation of stationary gaussian processes through circulant embedding of the covariance matrix, *SIAM Journal of Scientific Computing*, *18*(4), 1088–1107.

Eagleson, P. S., N. M. Fennessey, Q. L. Wang, and I. Rodrigueziturbe (1987), Application of spatial poisson models to air-mass thunderstorm rainfall, *Journal of Geophysical Research-Atmospheres*, *92*(D8), 9661–9678.

Faures, J. M., D. C. Goodrich, D. A. Woolhiser, and S. Sorooshian (1995), Impact of small-scale spatial rainfall variability on runoff modeling, *Journal of Hydrology*, *173*(1-4), 309–326.

Franks, S. W., and G. Kuczera (2002), Flood frequency analysis: Evidence and implications of secular climate variability, new south wales, *Water Resources Research*, *38*(5), 1062, doi:10.1029/2001WR000232.

Frost, A. (2004), *Spatio-Temporal Hidden Markov Models For Incorporating Interannual Variability In Rainfall*, PhD Thesis, University of Newcastle, New South Wales, Australia.

Frost, A., R. Srikanthan, and P. Cowpertwait (2004), Stochastic generation of point rainfall data at subdaily timescales: a comparison of DRIP and NSRP, *Tech. rep.*, Cooperative Research Centre - Catchment Hydrology, Melbourne, Australia.

Georgakakos, K. P., and W. F. Krajewski (1996), Statistical-microphysical causes of rainfall variability in the tropics, *Journal of Geophysical Research-Atmospheres*, *101*(D21), 26,165–26,180.

Gneiting, T., H. Sevcikova, D. Percival, M. Schlather, and Y. Jiang (2006), Fast and exact simulation of large gaussian lattice systems in r-2: Exploring the limits, *Journal of Computational and Graphical Statistics*, *15*(3), 483–501.

Grace, R. A., and P. S. Eagleson (1967), A model for generating synthetic sequences of short-time-interval rainfall depths, in *The International Hydrology Symposium*, Colorado State University, Fort Collins, Colorado.

Green, J., D. Walland, N. Nandakumar, and R. Nathan (2003), Temporal patterns for the derivation of PMP and PMF estimates in the gtsm region of australia, in *28th Hydrology and Water Res. Symp*, pp. 1.97–1.104, Wollongong, Australia.

Green, J. R. (1965), Two probability models for sequences of wet or dry days, *Monthly Weather Review*, *93*(3), 155–156.

Gyasi-Agyei, Y., and S. Bin Mahbub (2005), Stochastic disaggregation of daily rainfall into one-hour time scale, *Journal of Hydrology*, *309*, 178–190.

Hardy, M., G. Kuczera, and P. Coombes (2005), Integrated urban water cycle management: the urbancycle model, *Water Science and Technology*, *52*(9), 1–9.

Harrold, T. I., A. Sharma, and S. Sheather (2003), A nonparametric model for stochastic generation of daily rainfall occurrence, *Water Resources Research*, *39*(10).

Heneker, T. (2002), *An Improved Engineering Design Flood Estimation Technique: Removing the Need to Estimate Initial Loss*, PhD Thesis, University of Adelaide, Adelaide, Australia.

Heneker, T. M., M. F. Lambert, and G. Kuczera (2001), A point rainfall model for risk-based design, *Journal of Hydrology*, *247*(1-2), 54–71.

Hosking, J., and J. Wallis (1997), *Regional frequency analysis: an approach based on L-moments*, Cambridge University Press, Cambridge, UK.

Hughes, G., and P. Guttorp (1999), A non-homogeneous hidden markov model for precipitation occurrence, *Applied Statistics*, *48*(1), 15–30.

Humphrey, M., J. Istok, J. Lee, A. Hevesi, and A. Flint (1997), A new method for automated dynamic calibration of tipping-bucket rain gauges, *Journal of Atmospheric and Oceanic Technology*, *14*(6), 1513–1519.

Hutchinson, M. F. (1995), Interpolating mean rainfall using thin plate smoothing splines, *International Journal of Geographic Information Systems*, *9*, 385–403.

Jennings, S., M. Lambert, and G. Kuczera (2009), A high resolution point rainfall model calibrated to short pluviograph or daily rainfall data, *Journal of Hydrology*, *submitted*.

Jordan, P. W., and A. W. Seed (2003), A stochastic model of radar measurement errors in rainfall accumulations at catchment scale, *Journal of Hydrometeorology*, *4*(5), 841–855.

Jothityangkoon, C., M. Sivapalan, and N. R. Viney (2000), Tests of a space-time model of daily rainfall in southwestern australia based on nonhomogeneous random cascades, *Water Resources Research*, *36*(1), 267–284, doi:10.1029/1999WR900253.

Kessler, E. (1969), On the distribution and continuity of water substance in atmospheric circulations, *Meteorology Monograph, American Meteorological Society*, *10*(32).

Kiem, A., S. Franks, and K. G.A. (2003), Multi-decadal variability of flood risk, *Geophysical Research Letters*, *30*(2), 1035, doi:doi:10.1029/2002GRL15992.

Krajewski, W. (1987), Cokriging radar-rainfall and rain gage data, *Journal of Geophysical Research*, *92*(D8), 9571–9580.

Kreyszig, E. (2005), *Advanced Engineering Mathematics*, Ninth Edition, Wiley, New Jersey.

Kuczera, G. (1999), Comprehensive at-site flood frequency analysis using monte carlo bayesian inference, *Water Resources Research*, *35*(5), 1551–1558, doi:10.1029/1999WR900012.

Kuczera, G., M. Lambert, T. M. Heneker, S. Jennings, A. Frost, and P. Coombes (2006), Joint probability and design storms at the crossroads, *Australian Journal of Water Resources*, *20*(2), 5–21.

Kumar, P. (1996), Role of coherent structures in the stochastic-dynamic variability of precipitation, *Journal of Geophysical Research-Atmospheres*, *101*(D21), 26,393–26,404.

Lanza, L., J. Ramirez, and E. Todini (2001), Stochastic rainfall interpolation and downscaling, *Hydrology and Earth System Sciences*, *5*(2), 139–143.

Le Cam, L. A. (1961), A stochastic description of precipitation, in *4th Berkley Symposium, Mathematics, Statistics and Probability*, University of California Press, Berkley, California.

Lewis, P. A. W. (1964), A branching poisson process model for the analysis of computer failure patterns (with discussion), *Journal of the Royal Statistical Society, Series B*, *26*, 398–456.

Lovejoy, S., and D. Schertzer (1990), Multifractals, universality classes and satellite and radar measurements of cloud and rain fields, *Journal of Geophysical Research-Atmospheres*, *95*(D3), 2021–2034.

Mackay, N. G., R. E. Chandler, C. Onof, and H. S. Wheater (2001), Disaggregation of spatial rainfall fields for hydrological modelling, *Hydrology and Earth System Sciences*, *5*(2), 165–173.

Matheron, G. (1973), The intrinsic random functions and their applications, *Advanced Applied Probability*, *5*, 439–468.

Matsoukas, C., S. Islam, and R. Kothari (1999), Fusion of radar and rain gage measurements for an accurate estimation of rainfall, *Journal of Geophysical Research-Atmospheres*, *104*(D24), 31,437–31,450.

McBride, J., and N. Nicholls (1983), Seasonal relationships between australian rainfall and the southern oscillation, *Monthly Weather Review*, *111*, 1998–2004.

Mellor, D. (1996), The modified turning bands (mtb) model for space-time rainfall .1. model definition and properties, *Journal of Hydrology*, *175*(1-4), 113–127.

Mellor, D., J. Sheffield, P. E. O'Connell, and A. V. Metcalfe (2000), A stochastic space-time rainfall forecasting system for real time flow forecasting i: Development of mtb conditional rainfall scenario generator, *Hydrology and Earth System Sciences*, *4*(4), 603–615.

Menabde, M., D. Harris, A. Seed, G. Austin, and D. Stow (1997), Multiscaling properties of rainfall and bounded random cascades, *Water Resources Research*, *33*(12), 2823–2830.

Micevski, T., S. Franks, and G. Kuczera (2006), Multidecadal variability in coastal eastern australian flood data, *Journal of Hydrology*, *327*, 219 225, doi:doi:10.1016/j.jhydrol.2005.11.017.

Mulvaney, T. (1850), On the use of self-registering rain and flood gauges in making observations on the relations of rainfall and flood discharges in a given catchment, *Trans Inst Civ Eng Irel*, *4*, 18–31.

Munroe, D. (2005), *A Stochastic Infilling Algorithm for Spatial-Temporal Rainfall Data*, PhD Thesis, Massey University, Albany, New Zealand.

Need, S., M. Lambert, and A. Metcalfe (2008), A total probability approach to flood frequency analysis in tidal river reaches, in *World Environmental and Water Resources Congress*, ASCE, Ahupua'a, Hawaii.

Neyman, J., and E. L. Scott (1958), Statistical approach to problems of cosmology, *Journal of the Royal Statistical Society*, *20*(1), 1–43.

Northrop, P. (1998), A clustered spatial-temporal model of rainfall, *Proceedings of the Royal Society of London Series a-Mathematical Physical and Engineering Sciences*, *454*(1975), 1875–1888.

Olsson, J. (1995), Limits and characteristics of the multifractal behaviour of a high resolution rainfall time-series, *Nonlinear Processes Geophysics*, *2*, 23–29.

Olsson, J., and P. Burlando (2002), Reproduction of temporal scaling by a restangular pulses rainfall model, *Hydrological Processes*, *16*, 611–630.

Onof, C., and H. S. Wheater (1993), Modelling of British rainfall using a random parameter Bartlett-Lewis rectangular pulse model, *Journal of Hydrology*, *149*, 67–95.

Onof, C., and H. S. Wheater (1994a), Improvements to the modelling of British rainfall using a modified random pulse parameter bartlett-lewis rectangular pulse model, *Journal of Hydrology*, *157*, 177–195.

Onof, C., and H. S. Wheater (1994b), Improved fitting of the bartlett-lewis rectangular pulse model for hourly rainfall, *Hydrological Sciences Journal*, *39*(6), 663–680.

Onof, C., R. E. Chandler, A. Kakou, P. Northrop, H. S. Wheater, and V. Isham (2000), Rainfall modelling using poisson-cluster processes: a review of developments, *Stochastic Environmental Research and Risk Assessment*, *14*(6), 384–411.

Over, T. M., and V. K. Gupta (1996), A space-time theory of mesoscale rainfall using random cascades, *Journal of Geophysical Research-Atmospheres*, *101*(D21), 26,319–26,331.

Pegram, G. G. S., and A. N. Clothier (2001a), High resolution space-time modelling of rainfall: the 'string of beads' model, *Journal of Hydrology*, *241*(1-2), 26–41.

Pegram, G. G. S., and A. N. Clothier (2001b), Downscaling rainfields in space and time, using the string of beads model in time series mode, *Hydrology and Earth System Sciences*, *5*(2), 175–186.

Pilgrim, D. (Ed.) (1987), *Australian Rainfall & Runoff, A guide to flood estimation.*, 1987 Revised Edition, Institution of Engineers Australia, Canberra, Australia.

Rahman, A., P. Weinmann, T. Hoang, E. Laurenson, and R. Nathan (2002), Monte carlo simulation of flood frequency curves from rainfall, *Tech. rep.*, Cooperative Research Centre for Catchment Hydrology, Melbourne, Australia.

Rodriguez-Iturbe, I., V. Gupta, and E. Waymire (1984), Scale considerations in the modeling of temporal rainfall, *Water Resources Research*, *20*(11), 1611–1619.

Rodriguez-Iturbe, I., D. R. Cox, and V. Isham (1987a), Some models for rainfall based on stochastic point processes, *Journal of the Royal Statistical Society, Series A*, *410*, 269–288.

Rodriguez-Iturbe, I., B. Febres De Power, and J. B. Valdes (1987b), Rectangular pulse point process models for rainfall: Analysis of empirical data, *Journal of Geophysical Research*, *92*(D8), 9645–9656.

Rue, H. (2001), Fast sampling of gaussian markov random fields, *Journal of The Royal Statistical Society Series B-Statistical Methodology*, *63*, 325–338.

Salas, J. (1993), Analysis and modeling of hydrologic time series, in *Handbook of Hydrology*, edited by D. Maidment, pp. 19.1–19.63, McGraw-Hill, New York.

Sanso, B., and L. Guenni (1999), Venezuelan rainfall data analysed by using a bayesian space-time model, *Journal of the Royal Statistical Society Series C-Applied Statistics*, *48*, 345–362.

Sanso, B., and L. Guenni (2000), A nonstationary multisite model for rainfall, *Journal of the American Statistical Association*, *95*(452), 1089–1100.

Sansom, J. (1999), Large-scale spatial variability of rainfall through hidden semi-markov models of breakpoint data, *Journal of Geophysical Research-Atmospheres*, *104*(D24), 31,631–31,643.

Sansom, J., and C. S. Thompson (2003), Mesoscale spatial variation of rainfall through a hidden semi- markov model of breakpoint data, *Journal of Geophysical Research-Atmospheres*, *108*(D8), art. no.–8379.

Seed, A. W., R. Srikanthan, and M. Menabde (1999), A space and time model for design storm rainfall, *Journal of Geophysical Research-Atmospheres*, *104*(D24), 31,623–31,630.

Sempere-Torres, D., C. Corral, J. Raso, and P. Malgrat (1999), Use of weather radar for combined sewer overflows monitoring and control, *Journal of Environmental Engineering - ASCE*, *125*(4), 372–380.

Shah, S. M. S., P. E. O'Connell, and J. R. M. Hosking (1996), Modelling the effects of spatial variability in rainfall on catchment response .1. formulation and calibration of a stochastic rainfall field model, *Journal of Hydrology*, *175*(1-4), 67–88.

Sih, K., P. Hill, and R. Nathan (2008), Evaluation of simple approaches to incorporating variability in design temporal patterns, in *Water Down Under*, pp. 1049 –1059.

Simmonds, I., and P. Hope (1997), Persistence characteristics of australian rainfall anomalies, *International Journal of Climatology*, *17*, 597–613.

Sinclair, S., and G. Pegram (2004), Combining radar and rain gauge rainfall estimates using conditional merging, *Atmospheric Science Letters*, *6*(1), 19–22.

Smithers, J., K. Chetty, M. Frezghi, D. Knoesen, and M. Tewolde (2007), Development and assessment of a continuous simulation modeling system for design flood estimation, *WRC Report*, *1318/1/07*.

Srikanthan, R., and T. McMahon (2001), Stochastic generation of annual, monthly and daily climate data: A review, *Hydrology and Earth System Sciences*, *5*(4), 653670.

Stern, H., G. de Hoedt, and J. Ernst (2006), Objective classification of australian climates, *Tech. rep.*, Bureau of Meteorology, Melbourne, Australia.

Sturman, A., and N. Tapper (2006), *The weather and climate of Australia and New Zealand*, Oxford University Press, Melbourne.

Tan, K., F. Chiew, and R. Grayson (2008), Stochastic event-based approach to generate concurrent hourly mean sea level pressure and wind sequences for estuarine flood risk assessment, *Journal of Hydrologic Engineering*, *13*(6), 449–460, doi:10.1061/(ASCE) 1084-0699(2008)13:6(449).

Taylor, G. I. (1938), The spectrum of turbulence, *Proceedings of the Royal Society of London Series a- Mathematical Physical and Engineering Sciences*, *164*, 476.

Tessier, Y., S. Lovejoy, and D. Schertzer (1994), Multifractal analysis and simulation of the global meteorological network, *Journal of Applied Meteorology*, *33*(12), 1572–1586.

Thiessen, A. H. (1911), Precipitation averages for large areas, *Monthly Weather Review*, *39*, 1082–1084.

Thyer, M., and G. Kuczera (2000), Modeling long-term persistence in hydroclimatic time series using a hidden state markov model, *Water Resources Research*, *36*(11), 3301–3310.

Thyer, M., and G. Kuczera (2003), A hidden markov model for modelling long-term persistence in multi-site rainfall time series. 2. real data analysis, *Journal of Hydrology*, *275*(1-2), 27–48.

Thyer, M., B. Renard, D. Kavetski, G. Kuczera, S. Franks, and S. Srikanthan (2009), Critical evaluation of parameter consistency and predictive uncertainty in hydrological modeling: A case study using bayesian total error analysis, *Water Resources Research*, *45*, W00B14, doi:10.1029/2008WR006825.

Todini, E. (2001), A bayesian technique for conditioning radar precipitation estimates to rain-gauge measurements, *Hydrology and Earth System Sciences*, *5*(2), 187–199.

Veneziano, D., R. L. Bras, and J. D. Niemann (1996), Nonlinearity and self-similarity of rainfall in time and a stochastic model, *Journal of Geophysical Research-Atmospheres*, *101*(D21), 26,371–26,392.

Verdon, D., and S. Franks (2005), Indian ocean sea surface temperature variability and winter rainfall: Eastern australia, *Water Resources Research*, *41*(6), W09,413.

Verdon, D., and S. Franks (2006), Long-term behaviour of enso: Interactions with the pdo over the past 400 years inferred from paleoclimate records, *Geophysical Research Letters*, *33*(6), L06,712.

Viney, N., and B. Bates (2004), It never rains on sunday: The prevalence and implications of untagged multi-day rainfall accumulations in the australian high quality data set, *International Journal of Climatology*, *24*(3), 1171–1192.

Waymire, E., and V. K. Gupta (1981), The mathematical structure of rainfall representations 3. some applications of the point process theory to rainfall processes, *Water Resources Research*, *17*(5), 1287–1294.

Weinmann, P., A. Rahman, T. Hoang, E. Laurenson, and R. Nathan (2002), Monte carlo simulation of flood frequency curves from rainfall the way ahead, *Australian Journal of Water Resources*, *6*(1), 71–79.

Wheater, H. S., R. E. Chandler, C. Onof, V. S. Isham, E. Bellone, C. Yang, D. Lekkas, G. Lourmas, and M. Segond (2005), Spatial-temporal rainfall modelling for flood risk estimation, *Stochastic Environmental Research and Risk Assessment*, *19*(6), 403–416, doi:10.1007/s00477-005-0011-8.

Whiting, J. (2006), *Identification and modelling of hydrological persistence with hidden Markov models*, PhD Thesis, University of Adelaide, Adelaide, Australia.

Wilks, D. (1998), Multisite generalizastoin of a daily stochastic precipitation generation model, *Journal of Hydrology*, *210*, 178–191.

Wilks, D. S., and R. L. Wilby (1999), The weather generation game: a review of stochastic weather models, *Progress in Physical Geography*, *23*(3), 329–357.

Willems, P. (2001), A spatial rainfall generator for small spatial scales, *Journal of Hydrology*, *252*(1-4), 126–144.

Willems, P., and J. Berlamont (1999), Probabilistic modelling of sewer system overflow emissions, *Water Science and Technology*, *39*(9), 47–54.

Wood, S. J., D. A. Jones, and R. J. Moore (2000), Accuracy of rainfall measurement for scales of hydrological interest, *Hydrology and Earth System Sciences*, *4*(4), 531–543.

Zawadzki, I. (1987), Fractal structure and exponential decorrelation in rain, *Journal of Geophysical Research-Atmospheres*, *92*(D8), 9586–9590.

Zhang, L., and V. Singh (2006), Bivariate flood frequency analysis using the copula method, *Journal of Hydrologic Engineering*, *11*(2), 150–164, doi:10.1061/(ASCE) 1084-0699(2006)11:2(150).

Zimmer, D., and P. Trivedi (2006), Using trivariate copulas to model sample selection and treatment effects: Application to family health care demand, *Journal of Business & Economic Statistics*, *24*(1), 63–76, doi:10.1198/073500105000000153.

Zucchini, W., and P. Guttorp (1991), A hidden markov model for space-time precipitation, *Water Resources Research*, *27*(8), 1917–1923.

Appendices

Appendix A
Spatial Storm Extent

A.1 List of rainfall gauges

The following two tables respectively show the pluviograph gauges and daily rainfall gauges used in the case study. The same order of gauges is preserved when comparing the simulated statistics to observed statistics.

Table A.1 List of pluviograph gauges from Sydney Water Observation Network

Gauge ID	Latitude	Longitude	Description
563059	-33.69	150.301	KATOOMBA (CASCADE CK DAM No.1)
563070	-33.7	150.485	LINDEN (WOODFORD CK DAM)
566017	-33.803	151.18	CHATSWOOD
566018	-34.033	151.163	CRONULLA STP
566020	-33.891	151.094	ENFIELD (COMPOSITE SITE)
566025	-33.783	151.257	MANLY DAM
566026	-33.921	151.157	MARRICKVILLE SPS
566028	-33.937	151.198	MASCOT BOWLING CLUB
566032	-33.89	151.224	PADDINGTON (COMPOSITE SITE)
566033	-33.939	151.026	PADSTOW
566036	-33.895	151.034	POTTS HILL RESERVOIR
566038	-33.862	151.278	VAUCLUSE BOWLING CLUB
566040	-33.771	151.064	WEST EPPING BOWLING CLUB
566047	-33.975	151.076	MORTDALE BOWLING CLUB
566051	-33.691	151.3	WARRIEWOOD STP
567076	-33.714	150.983	CASTLE HILL STP
567077	-33.883	150.951	FAIRFIELD STP
567078	-33.986	150.907	GLENFIELD STP
567087	-33.734	150.767	ST MARYS STP
567100	-33.653	150.847	RIVERSTONE STP

567102	-33.699	151.025	DURAL (WPS14)
568045	-33.891	150.592	WARRAGAMBA MET. STATION
568130	-34.06	150.679	WEST CAMDEN STP
563059	-33.69	150.301	KATOOMBA

Table A.2 List of Bureau of Meteorology daily rainfall gauges

Gauge ID	Latitude	Longitude	Description
66062	-33.86	151.2	SYDNEY (OBSERVATORY HILL)
067015	-33.97	150.72	BRINGELLY (MARYLAND)
068045	-34.55	150.38	MOSS VALE HOSKINS STREET
063043	-33.54	150.63	KURRAJONG HEIGHTS (BELLS LINE OF ROAD)
066046	-33.82	151	PARRAMATTA
063056	-33.59	150.25	MOUNT VICTORIA (MT VICTORIA (SELSDON STR
067021	-33.62	150.75	RICHMOND - UWS HAWKESBURY
061023	-33.43	151.34	GOSFORD (GERTRUDE PLACE)
063077	-33.7	150.56	SPRINGWOOD POST OFFICE
068007	-34.03	150.64	CAMDEN (BROWNLOW HILL)
068014	-34.07	150.8	CAMPBELLTOWN 1
068052	-34.17	150.61	PICTON BOWLING CLUB
063039	-33.72	150.3	KATOOMBA COMPOSITE
066006	-33.87	151.22	SYDNEY BOTANIC GARDENS
068013	-34.13	150.74	MENANGLE JMAI
066020	-33.77	151.08	EPPING CHESTER STREET
068044	-34.45	150.46	MITTAGONG BEATRICE STREET
067019	-33.82	150.91	PROSPECT DAM
066052	-33.91	151.24	RANDWICK BOWLING CLUB
068028	-34.2	150.97	HELENSBURGH (PARKES STREET)
066007	-33.93	151.22	BOTANY NO.1 DAM
068009	-34.59	150.52	BURRAWANG (RANGE STREET)
068000	-34.57	150.78	ALBION PARK POST OFFICE
066000	-33.89	151.13	ASHFIELD BOWLING CLUB
067018	-33.75	150.68	PENRITH LADBURY AVENUE
068024	-34.23	150.91	DARKES FOREST (KINTYRE)
063044	-33.72	150.43	LAWSON (WILSON STREET)
063118	-33.52	150.49	BILPIN (FERN GROVE)
066042	-33.82	151.24	MOSMAN BAPAUME ROAD
066050	-33.89	151.03	POTTS HILL

063057	-33.5	150.37	MOUNT WILSON (NOOROO)
067031	-33.61	150.82	WINDSOR FITZGERALD STREET
063009	-33.62	150.3	BLACKHEATH (GODSON AVE)
066044	-33.73	151.27	CROMER GOLF CLUB
066058	-34	151.13	SANS SOUCI (THE BOULEVARDE)
068043	-34.03	150.84	MINTO SURREY STREET
068054	-34.58	150.62	ROBERTSON POST OFFICE
067009	-33.97	150.9	GLENFIELD (MACQUARIE)
068033	-34.46	150.49	MITTAGONG (KIA ORA)
061119	-33.39	150.98	WISEMANS FERRY (OLD PO)
066010	-33.8	151.19	CHATSWOOD COUNCIL DEPOT
067052	-33.63	151.15	BEROWRA GOODWYN ROAD
066160	-33.9	151.23	CENTENNIAL PARK
068016	-34.27	150.81	CATARACT DAM
066131	-33.83	151.15	RIVERVIEW OBSERVATORY
068011	-34.05	150.72	CAMDEN BOWLING CLUB
066040	-34.04	151.1	MIRANDA BLACKWOOD ST
066120	-33.76	151.15	GORDON BOWLING CLUB
067004	-33.75	150.67	EMU PLAINS
066153	-33.78	151.25	MANLY VALE (MANLY DAM)
068022	-34.5	150.78	DAPTO BOWLING CLUB
068001	-34.21	150.79	APPIN CHURCH ST

A.2 SIMULATED ANNUAL TOTALS

The following plots show the simulated distribution of annual totals compared to the observed distribution at each of the 52 daily rainfall sites. The plots correspond to the same order of sites as listed in Table A.2 when read from left to right, top to bottom. The distributions are plotted against a normal probability-axis. The lines correspond to 0.05, 0.5, 0.95 simulated order statistics at each quantile. The mean of this distribution is matched exactly for each site owing to the scaling methodology. Reasons for undersimulating the variance of this distribution are discussed in Chapter 7

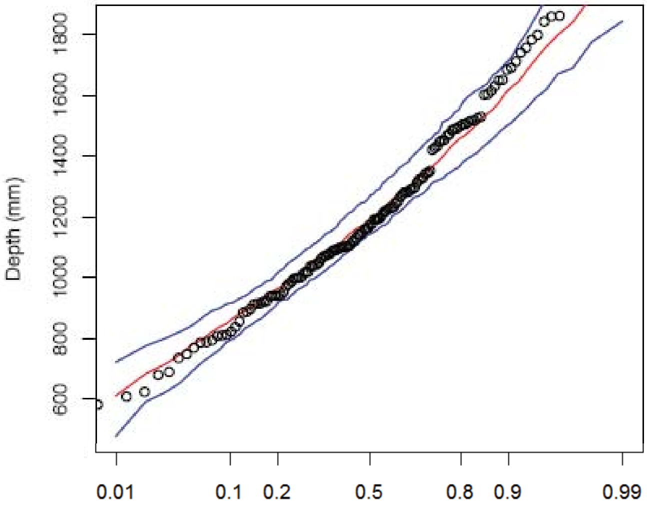
Depth (mm)
600
800
1000
1200
1400
1600
1800
0.01
0.1
0.2
0.5
0.8
0.9
0.99

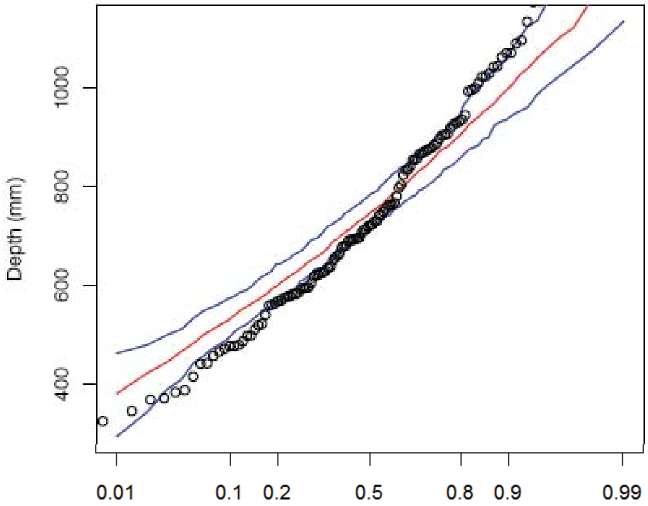
Depth (mm)
400
600
800
1000
0.01
0.1
0.2
0.5
0.8
0.9
0.99

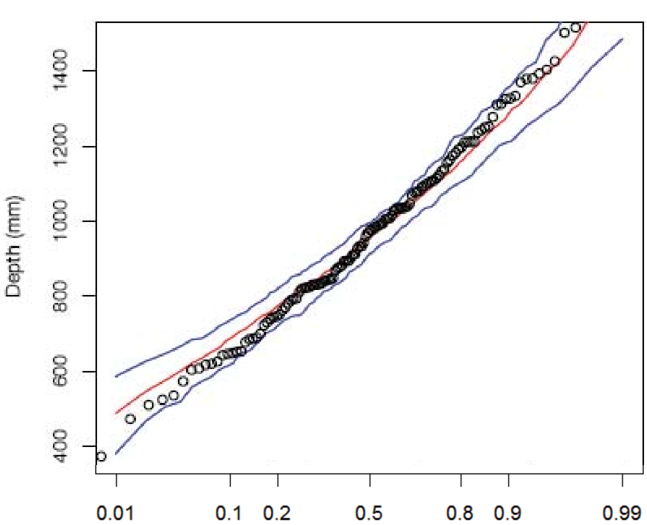
Depth (mm)
400
600
800
1000
1200
1400
0.01
0.1
0.2
0.5
0.8
0.9
0.99

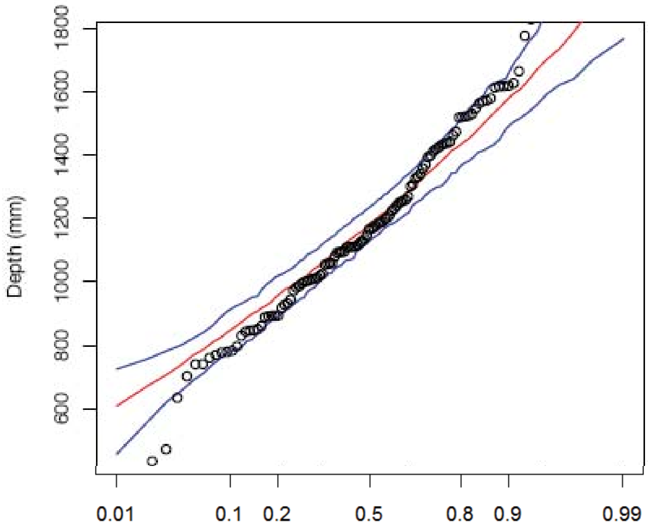
Depth (mm)
600
800
1000
1200
1400
1600
1800
0.01
0.1
0.2
0.5
0.8
0.9
0.99

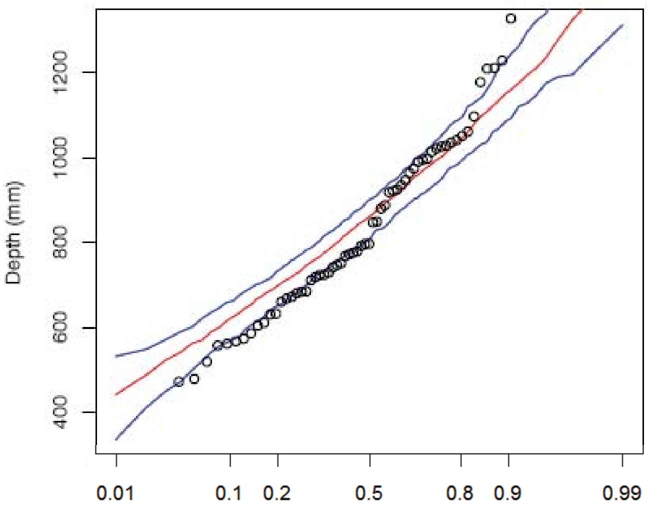
Depth (mm)
400
600
800
1000
1200
0.01
0.1
0.2
0.5
0.8
0.9
0.99

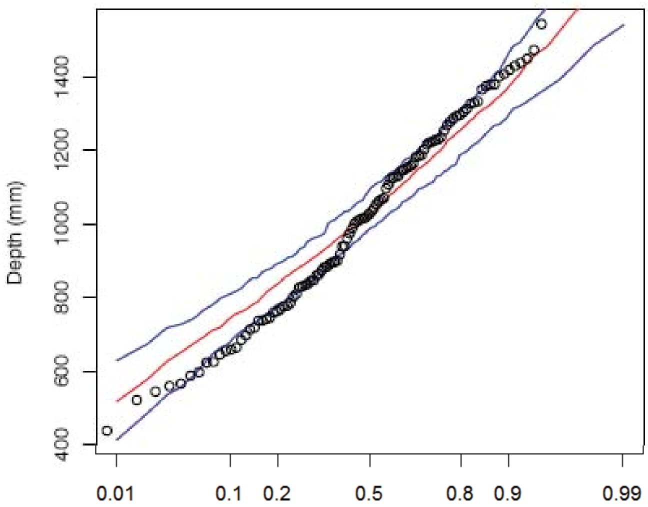
Depth (mm)
400
600
800
1000
1200
1400
0.01
0.1
0.2
0.5
0.8
0.9
0.99

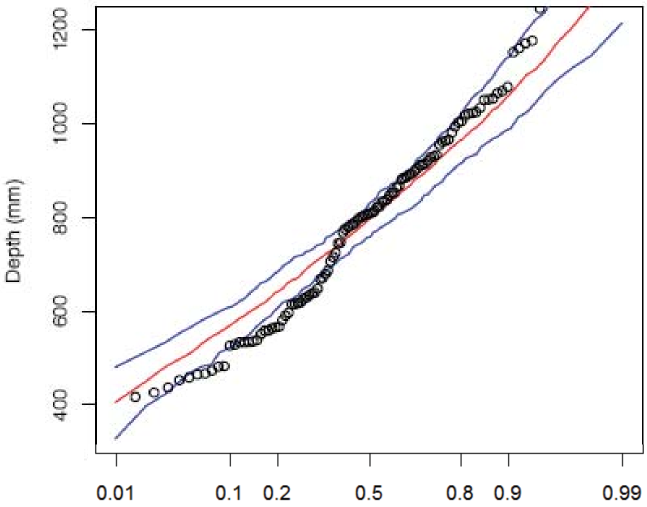
Depth (mm)
400
600
800
1000
1200
0.01
0.1
0.2
0.5
0.8
0.9
0.99

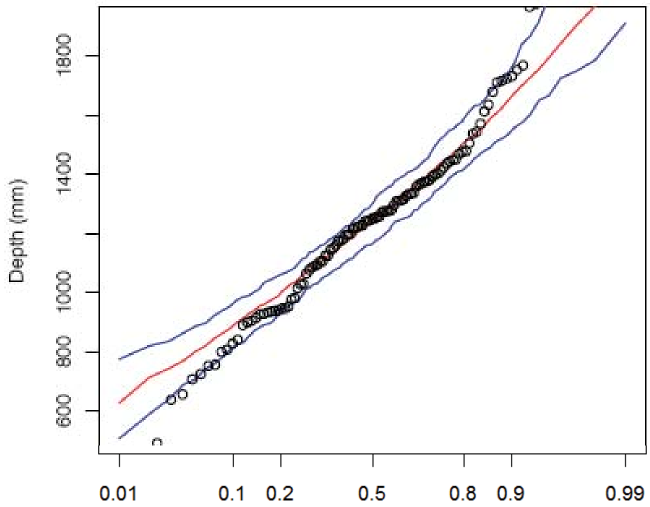
Depth (mm)
600
800
1000
1400
1800
0.01
0.1
0.2
0.5
0.8
0.9
0.99

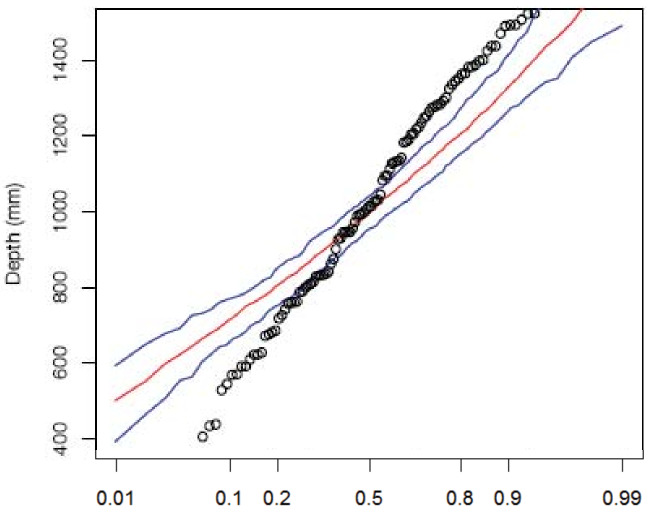
Depth (mm)
400
600
800
1000
1200
1400
0.01
0.1
0.2
0.5
0.8
0.9
0.99

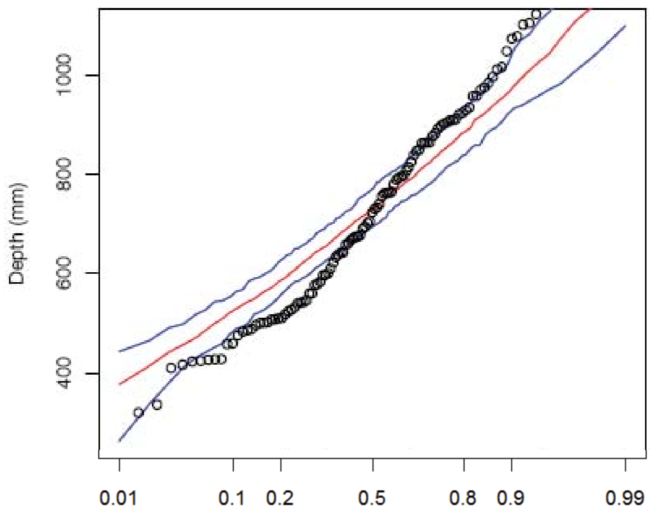
Depth (mm)
400
600
800
1000
0.01
0.1
0.2
0.5
0.8
0.9
0.99

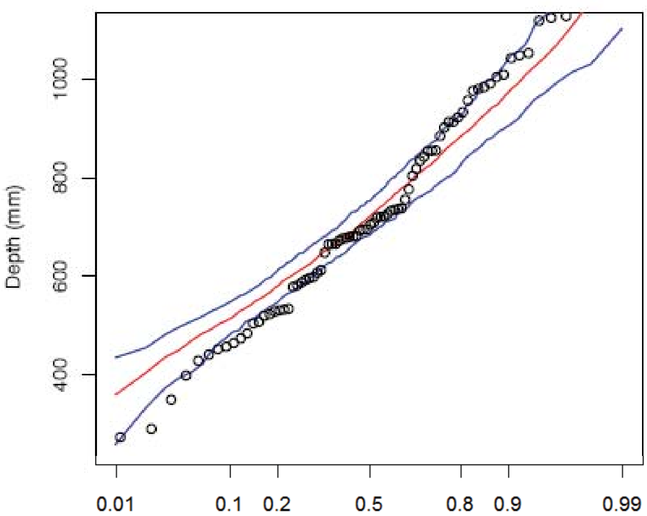
Depth (mm)
400
600
800
1000
0.01
0.1
0.2
0.5
0.8
0.9
0.99

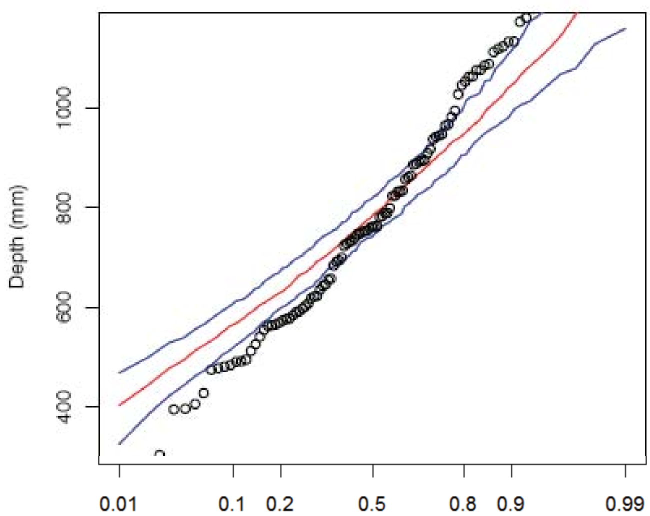
Depth (mm)
400
600
800
1000
0.01
0.1
0.2
0.5
0.8
0.9
0.99

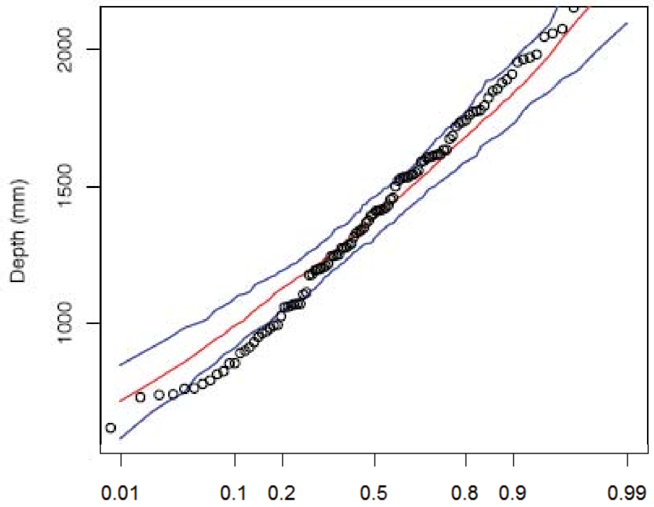
Depth (mm)
1000
1500
2000
0.01
0.1
0.2
0.5
0.8
0.9
0.99

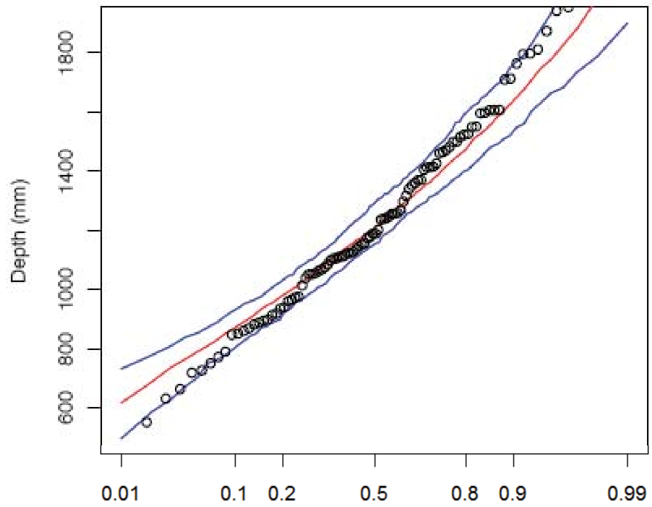
Depth (mm)
600
800
1000
1400
1800
0.01
0.1
0.2
0.5
0.8
0.9
0.99

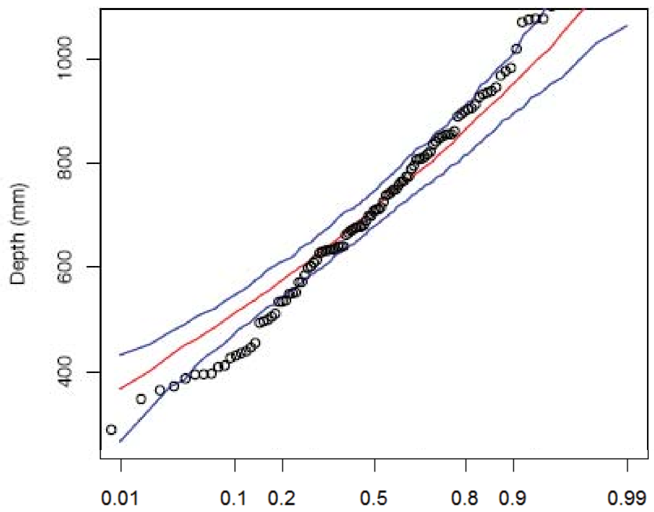
Depth (mm)
400
600
800
1000
0.01
0.1
0.2
0.5
0.8
0.9
0.99

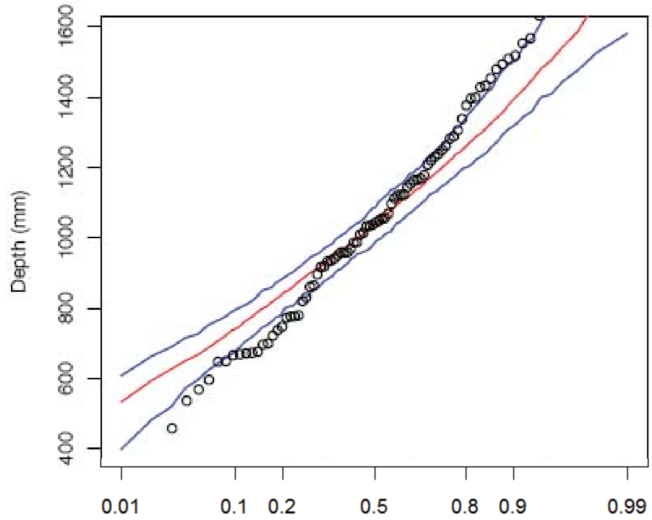
Depth (mm)
400
600
800
1000
1200
1400
1600
0.01
0.1
0.2
0.5
0.8
0.9
0.99

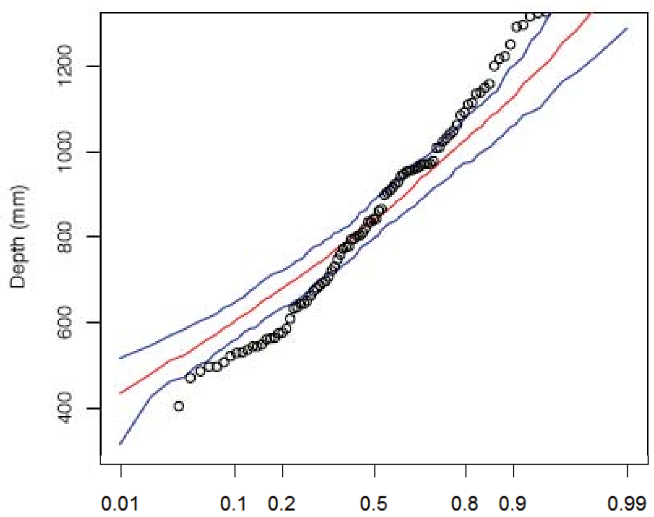
Depth (mm)
400
600
800
1000
1200
0.01
0.1
0.2
0.5
0.8
0.9
0.99

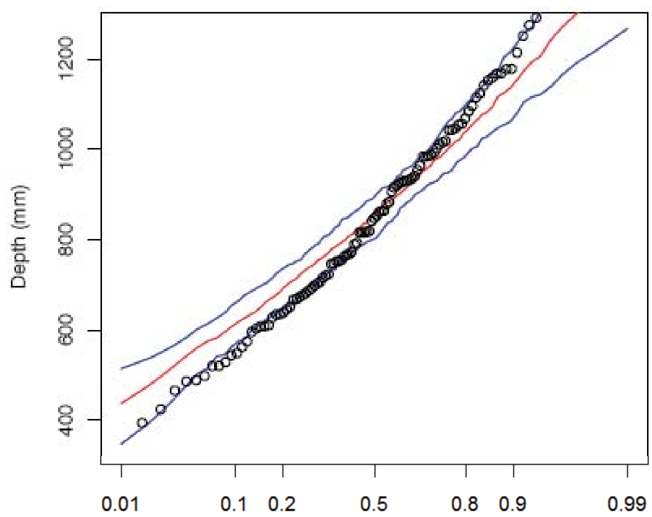
Depth (mm)
400
600
800
1000
1200
0.01
0.1
0.2
0.5
0.8
0.9
0.99

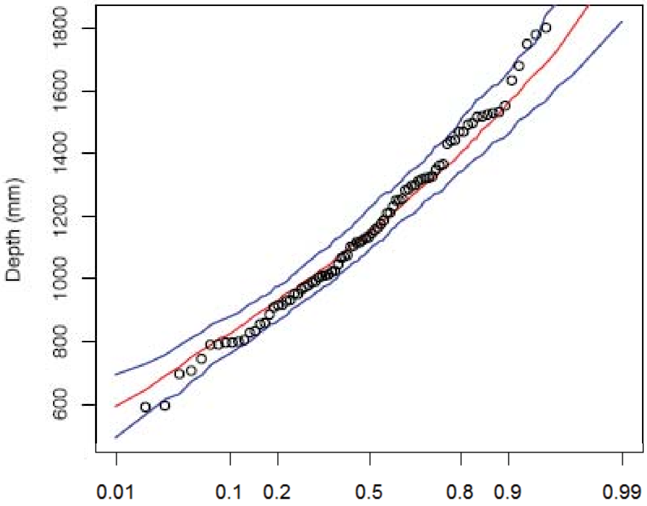
Depth (mm)
600
800
1000
1200
1400
1600
1800
0.01
0.1
0.2
0.5
0.8
0.9
0.99

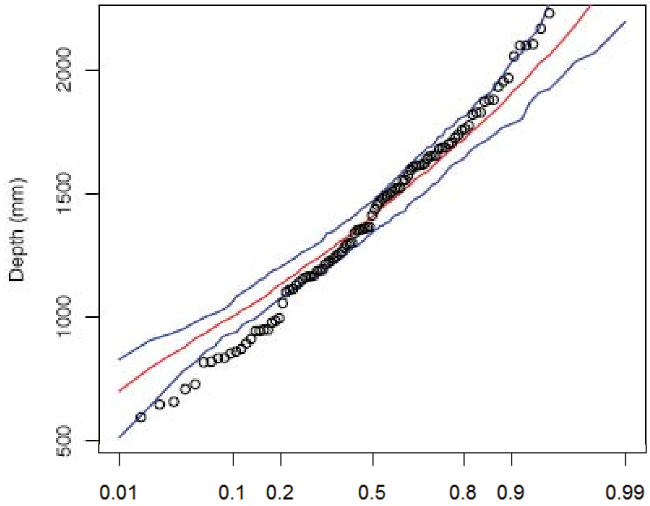
Depth (mm)
500
1000
1500
2000
0.01
0.1
0.2
0.5
0.8
0.9
0.99

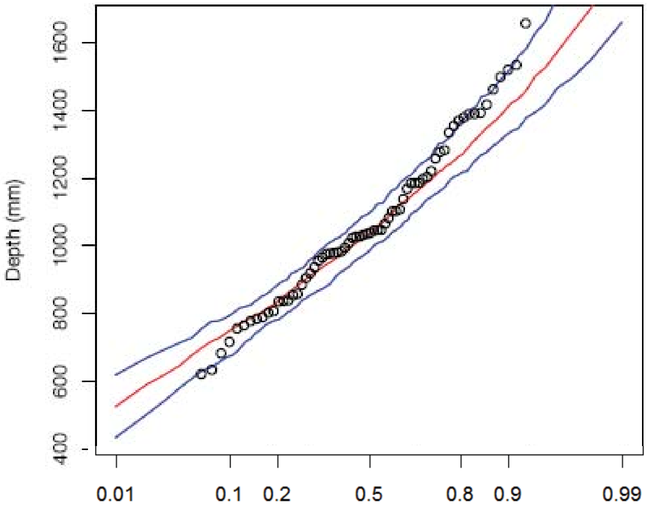
Depth (mm)
400
600
800
1000
1200
1400
1600
0.01
0.1
0.2
0.5
0.8
0.9
0.99

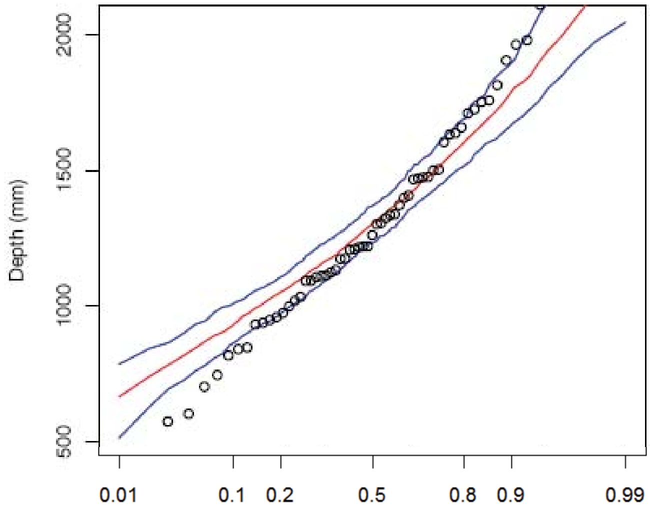
Depth (mm)
500
1000
1500
2000
0.01
0.1
0.2
0.5
0.8
0.9
0.99

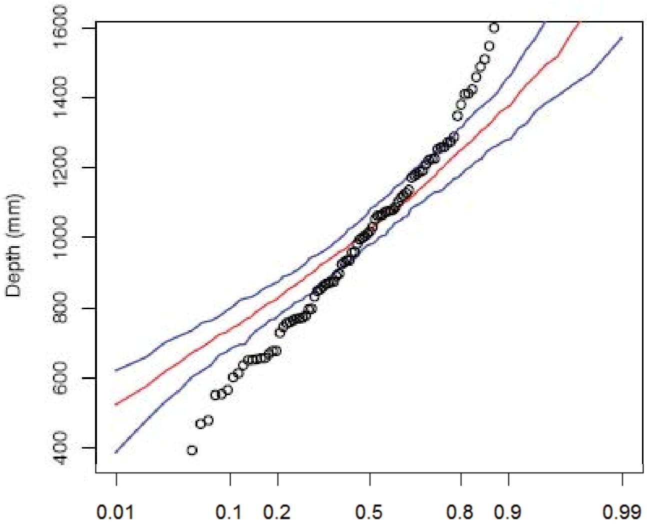
Depth (mm)
400
600
800
1000
1200
1400
1600
0.01
0.1
0.2
0.5
0.8
0.9
0.99

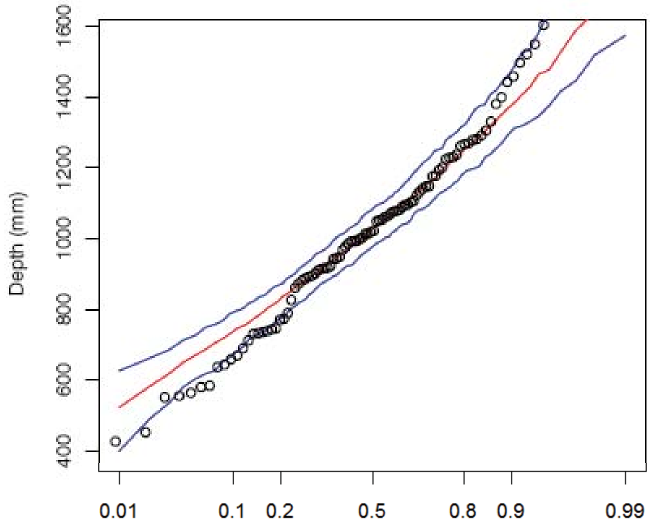
Depth (mm)
400
600
800
1000
1200
1400
1600
0.01
0.1
0.2
0.5
0.8
0.9
0.99

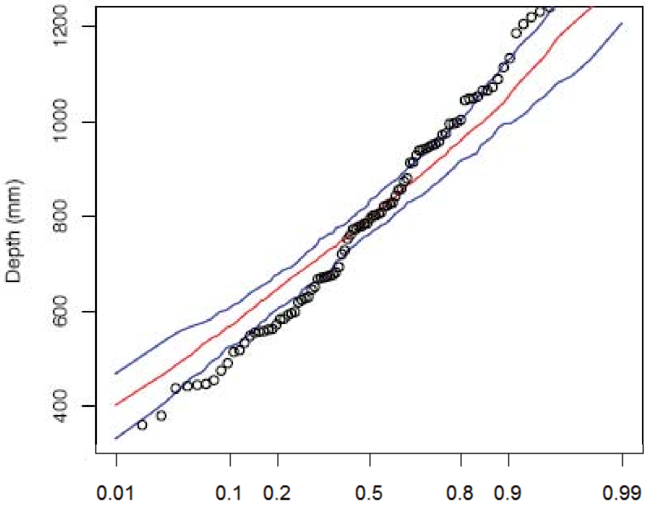
Depth (mm)
400 600 800 1000 1200
0.01 0.1 0.2 0.5 0.8 0.9 0.99

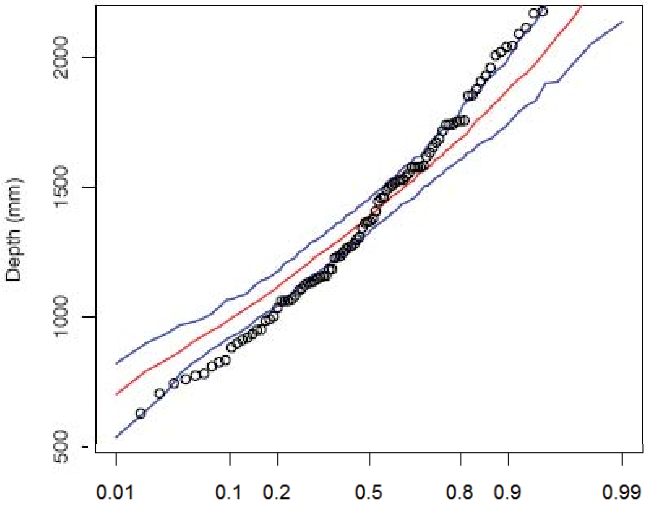
Depth (mm)
500 1000 1500 2000
0.01 0.1 0.2 0.5 0.8 0.9 0.99

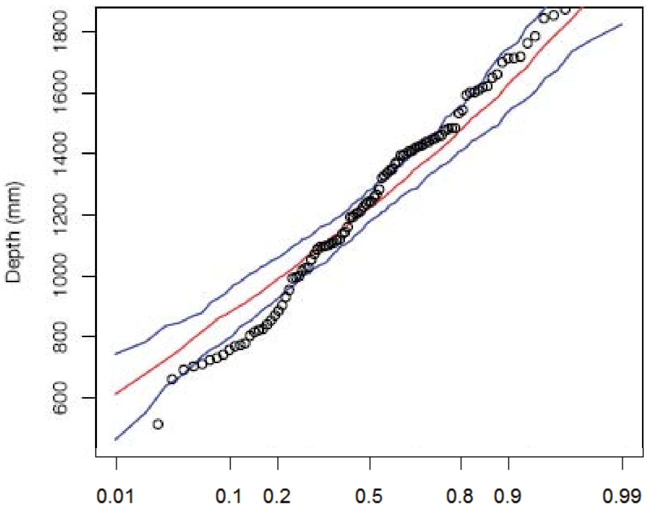
Depth (mm)
600 800 1000 1200 1400 1600 1800
0.01 0.1 0.2 0.5 0.8 0.9 0.99

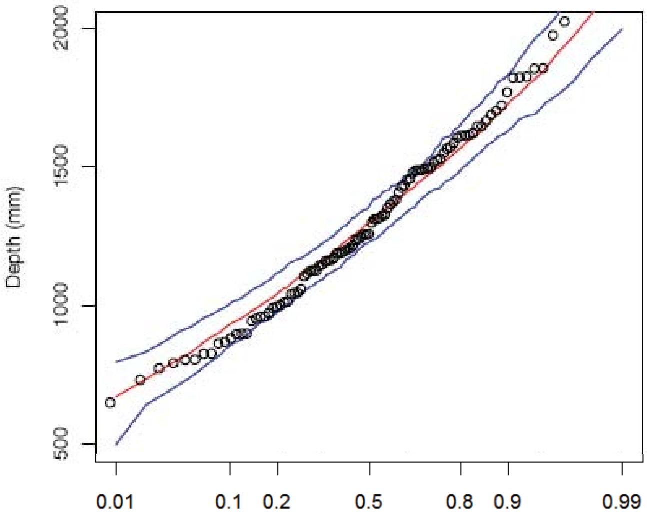
Depth (mm)
500 1000 1500 2000
0.01 0.1 0.2 0.5 0.8 0.9 0.99

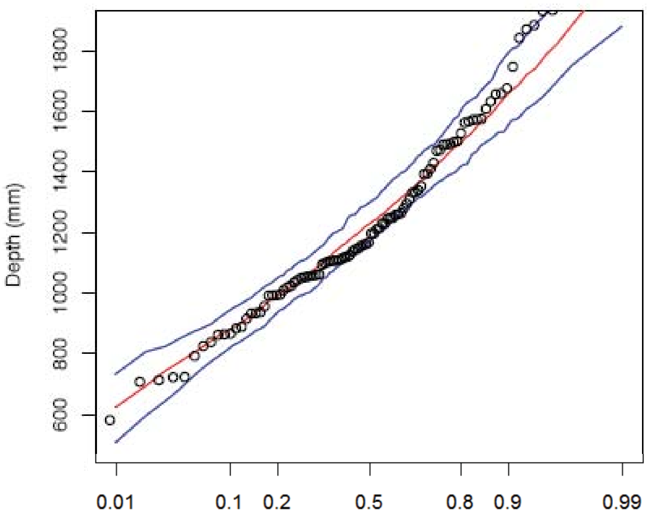
Depth (mm)
600 800 1000 1200 1400 1600 1800
0.01 0.1 0.2 0.5 0.8 0.9 0.99

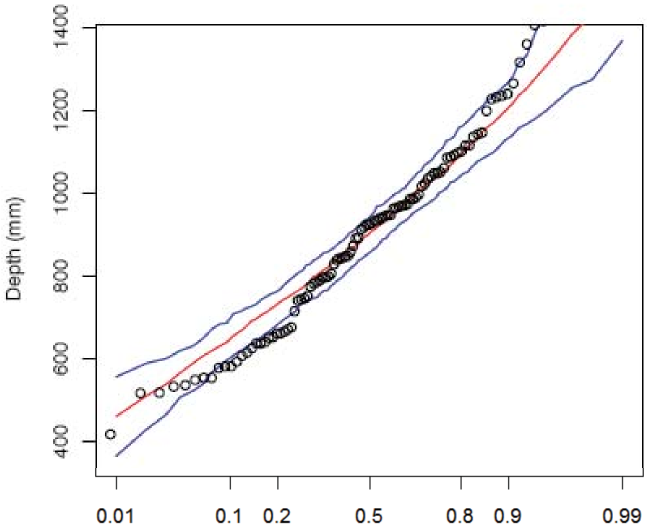
Depth (mm)
400 600 800 1000 1200 1400
0.01 0.1 0.2 0.5 0.8 0.9 0.99

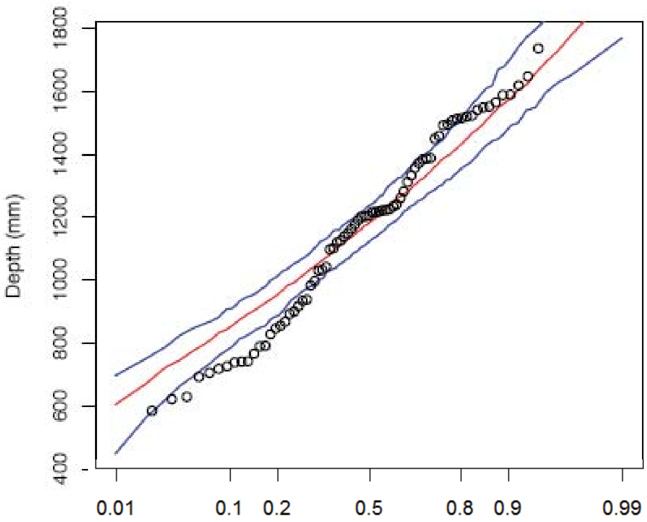
Depth (mm)
400
600
800
1000
1200
1400
1600
1800
0.01
0.1
0.2
0.5
0.8
0.9
0.99

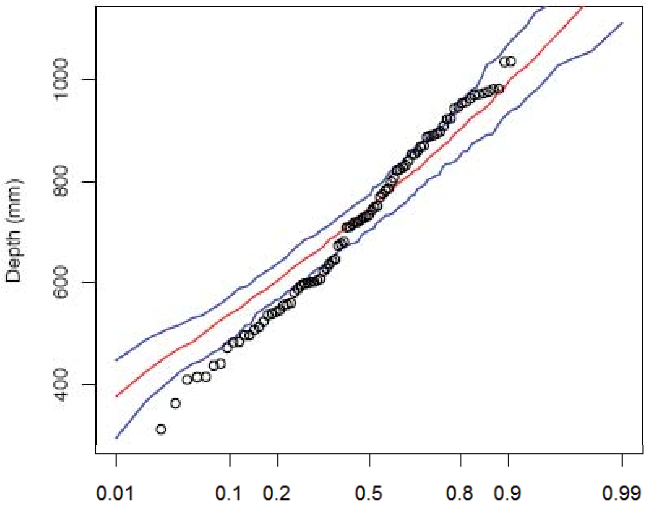
Depth (mm)
400
600
800
1000
0.01
0.1
0.2
0.5
0.8
0.9
0.99

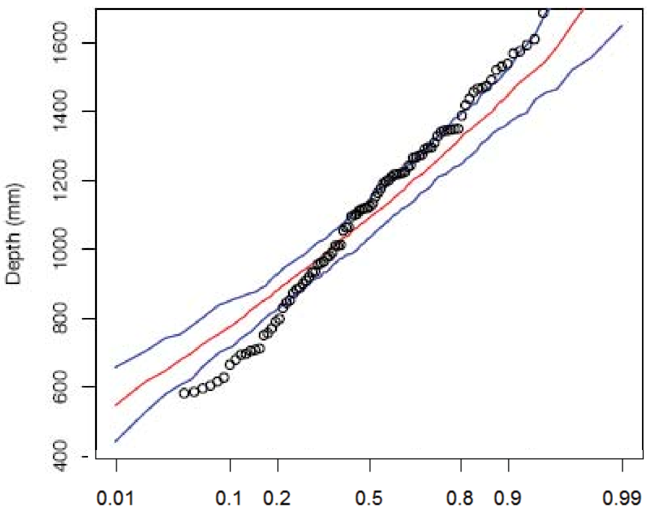
Depth (mm)
400
600
800
1000
1200
1400
1600
0.01
0.1
0.2
0.5
0.8
0.9
0.99

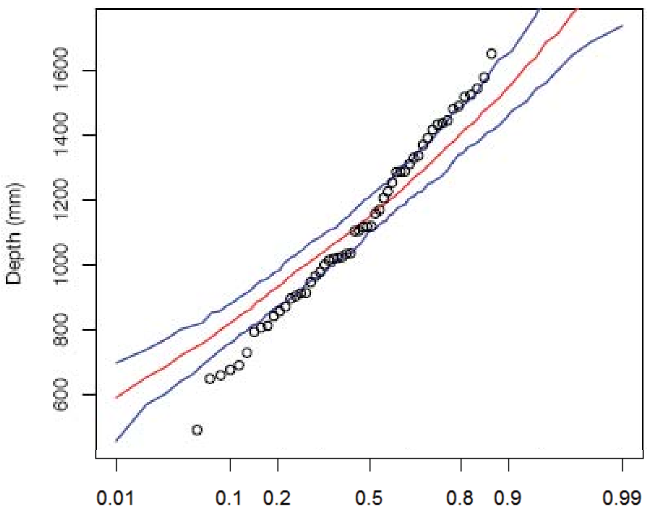
Depth (mm)
600
800
1000
1200
1400
1600
0.01
0.1
0.2
0.5
0.8
0.9
0.99

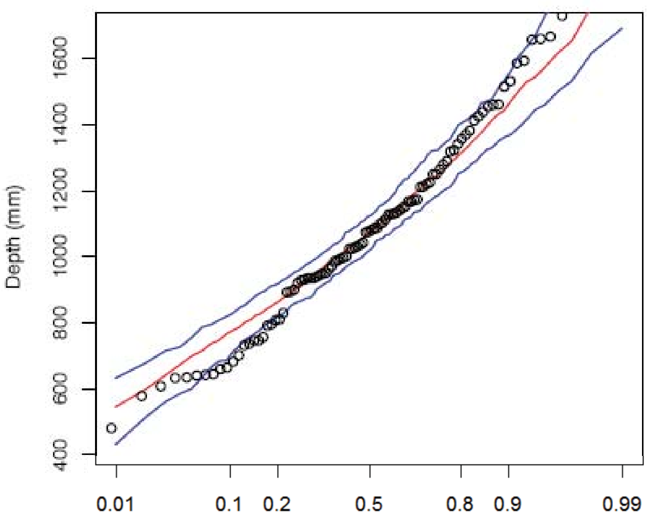
Depth (mm)
400
600
800
1000
1200
1400
1600
0.01
0.1
0.2
0.5
0.8
0.9
0.99

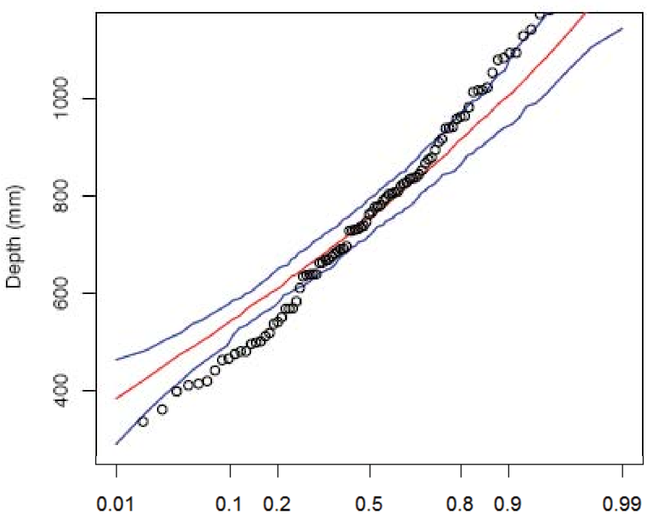
Depth (mm)
400
600
800
1000
0.01
0.1
0.2
0.5
0.8
0.9
0.99

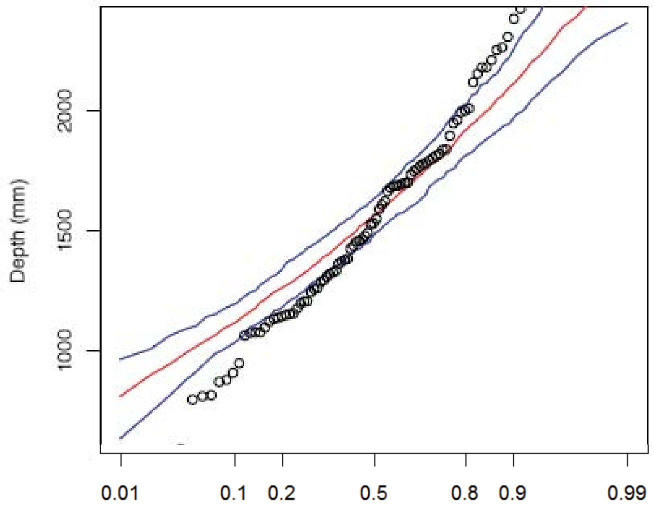
Depth (mm)
1000
1500
2000
0.01
0.1
0.2
0.5
0.8
0.9
0.99

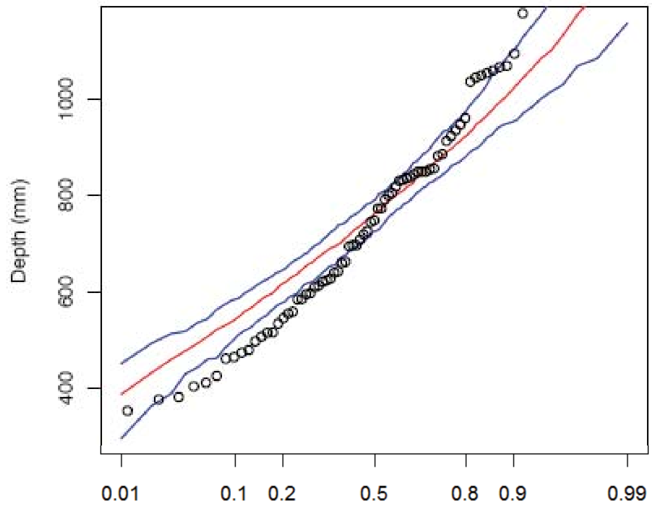
Depth (mm)
400
600
800
1000
0.01
0.1
0.2
0.5
0.8
0.9
0.99

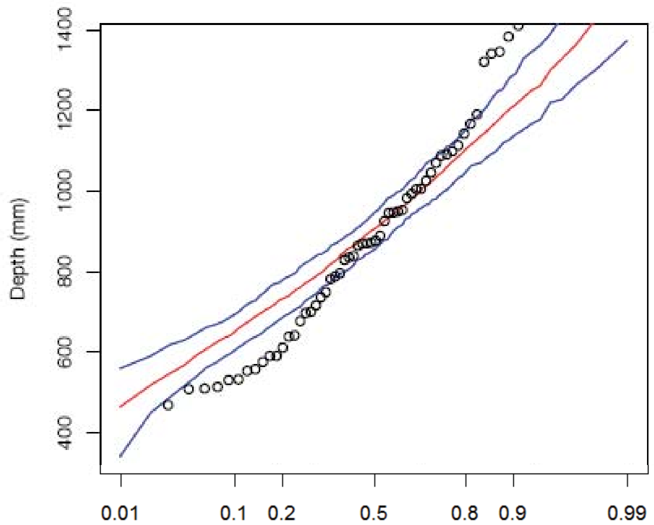
Depth (mm)
400
600
800
1000
1200
1400
0.01
0.1
0.2
0.5
0.8
0.9
0.99

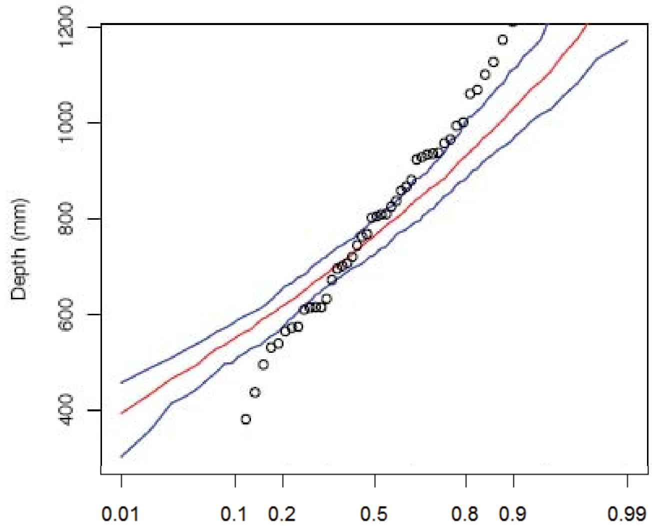
Depth (mm)
400
600
800
1000
1200
0.01
0.1
0.2
0.5
0.8
0.9
0.99

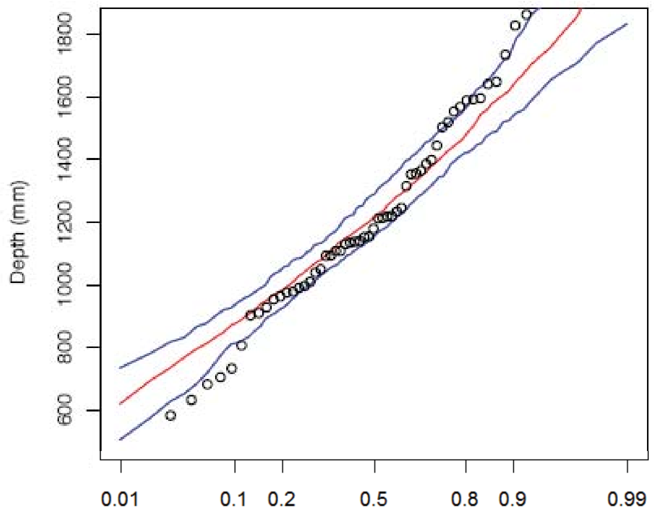
Depth (mm)
600
800
1000
1200
1400
1600
1800
0.01
0.1
0.2
0.5
0.8
0.9
0.99

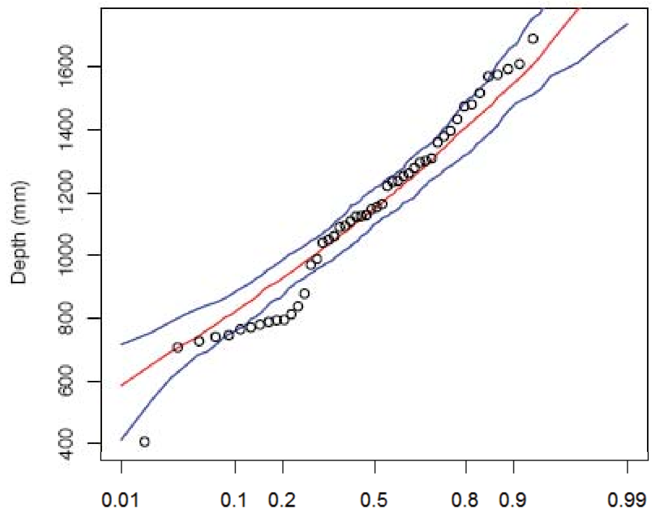
Depth (mm)
400
600
800
1000
1200
1400
1600
0.01
0.1
0.2
0.5
0.8
0.9
0.99

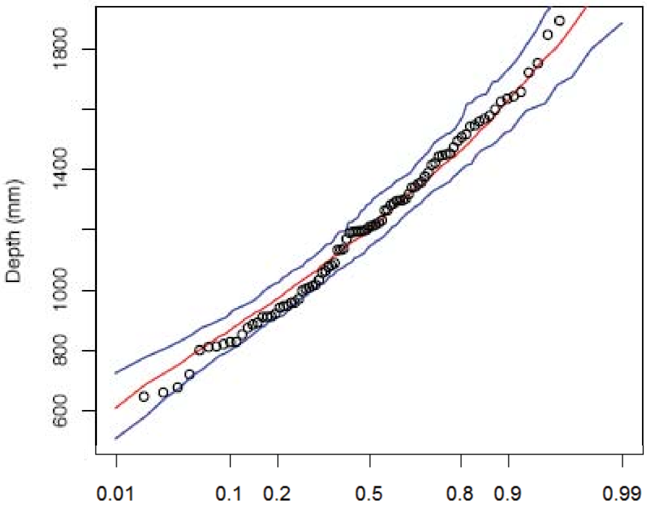
Depth (mm)
600 800 1000 1400 1800
0.01 0.1 0.2 0.5 0.8 0.9 0.99

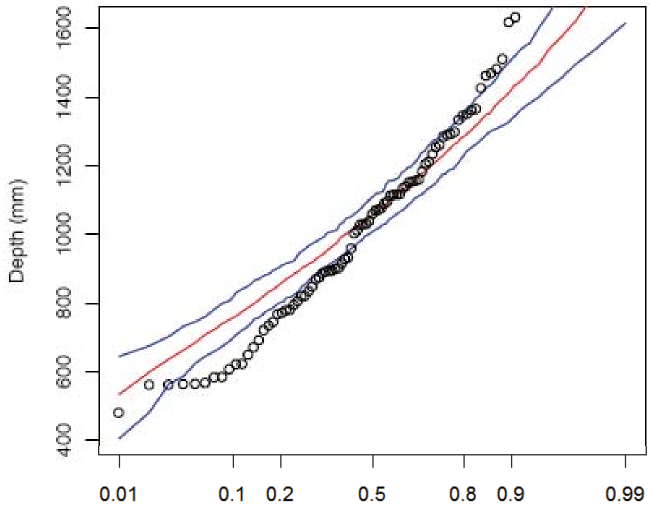
Depth (mm)
400 600 800 1000 1200 1400 1600
0.01 0.1 0.2 0.5 0.8 0.9 0.99

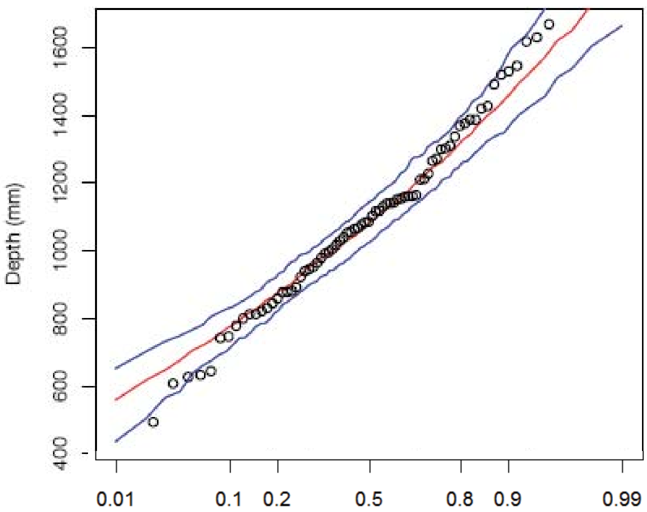
Depth (mm)
400 600 800 1000 1200 1400 1600
0.01 0.1 0.2 0.5 0.8 0.9 0.99

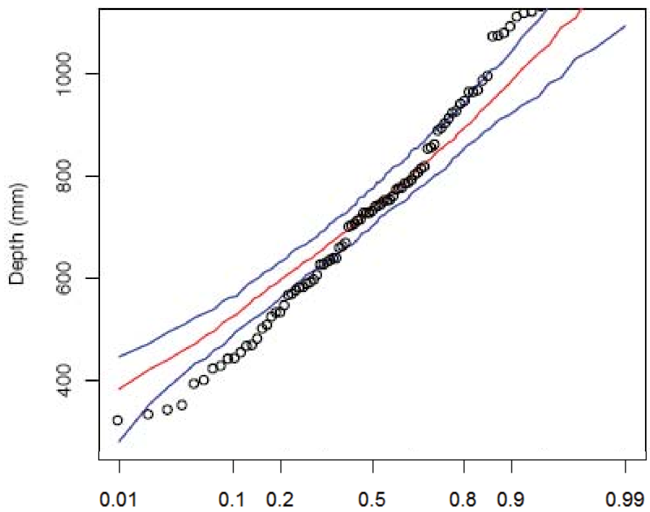
Depth (mm)
400 600 800 1000
0.01 0.1 0.2 0.5 0.8 0.9 0.99

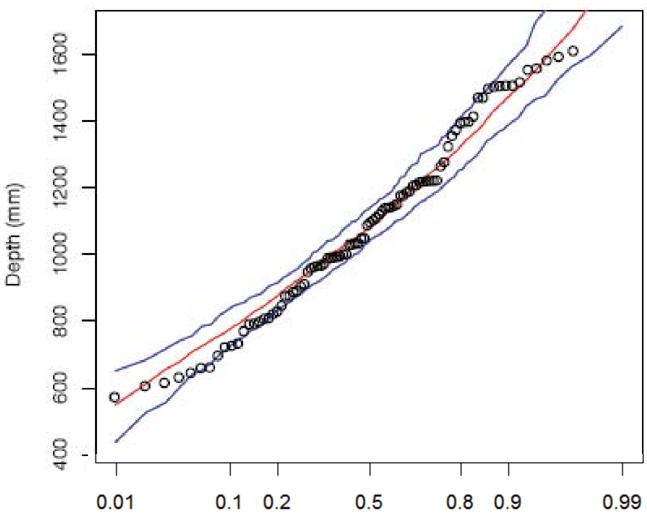
Depth (mm)
400 600 800 1000 1200 1400 1600
0.01 0.1 0.2 0.5 0.8 0.9 0.99

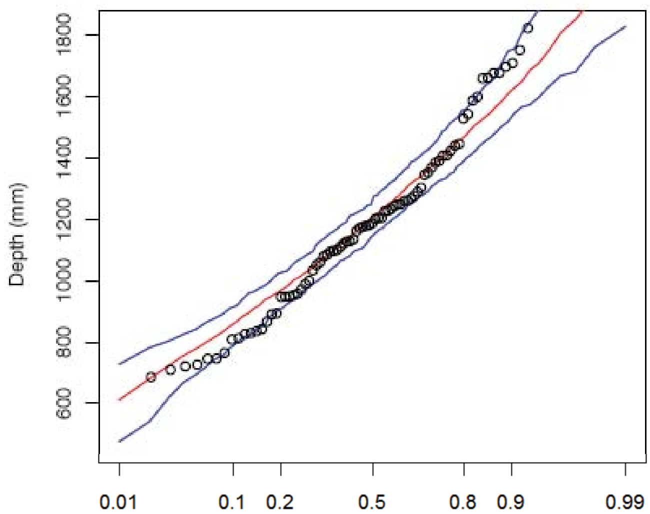
Depth (mm)
600 800 1000 1200 1400 1600 1800
0.01 0.1 0.2 0.5 0.8 0.9 0.99

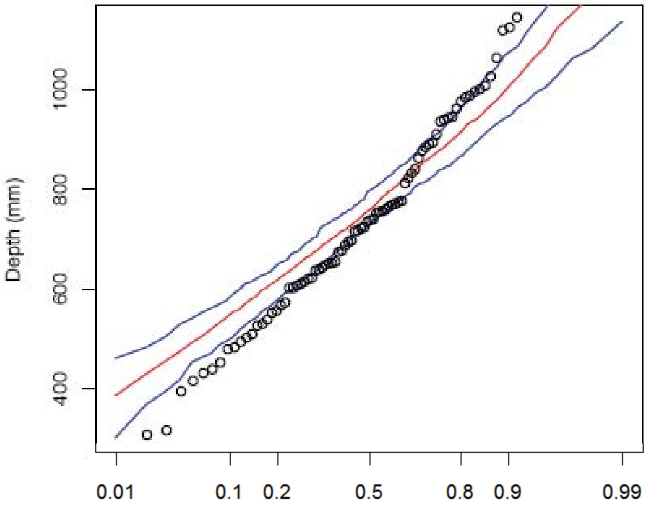
Depth (mm)
0.01
0.1
0.2
0.5
0.8
0.9
0.99

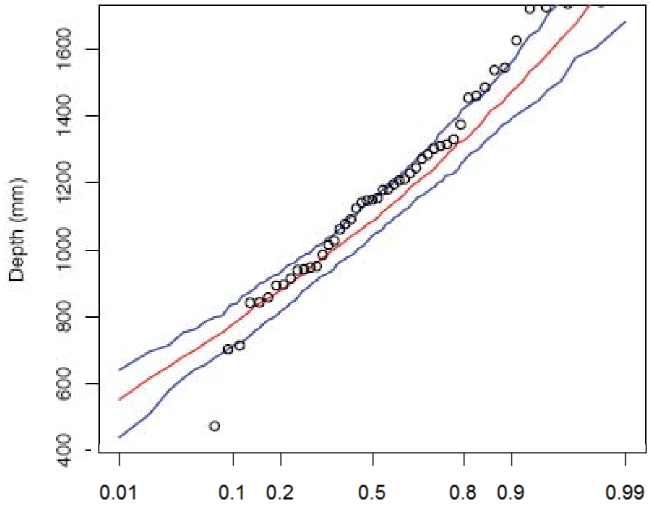
Depth (mm)
0.01
0.1
0.2
0.5
0.8
0.9
0.99

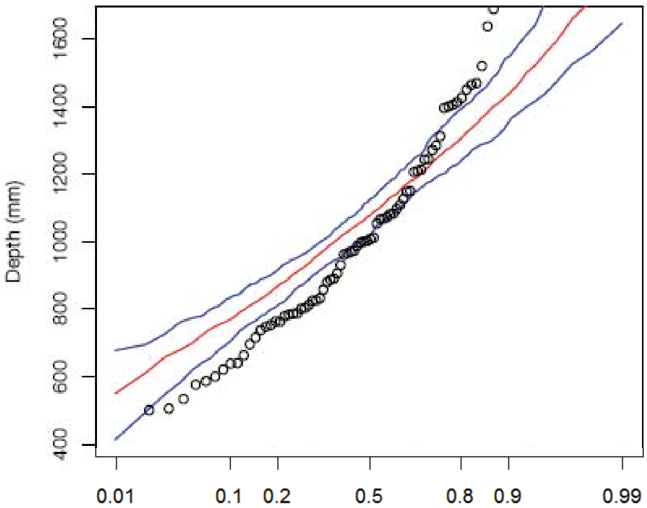
Depth (mm)
0.01
0.1
0.2
0.5
0.8
0.9
0.99

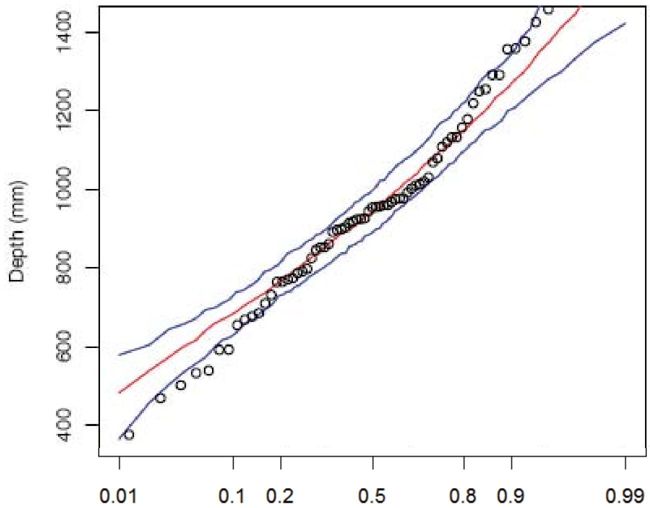
Depth (mm)
0.01
0.1
0.2
0.5
0.8
0.9
0.99

A.3 SIMULATED EXTREME VALUES

The following plots show the simulated distribution of extreme values compared to observed values, first for the 24 pluviograph gauges and secondly for the 52 daily rainfall sites. The plots correspond to the same order of sites as listed in Table A.1 and Table A.2 when read from left to right, top to bottom. The distributions are plotted against a Gumbel probability-axis. The lines correspond to 0.05, 0.5, 0.95 simulated order statistics at each quantile. For the pluviograph gauges the 1-hour and 6-hour extreme values are compared and for the daily sites the 24 hours extreme values are compared. To ensure a comparison of like-with-like, the simulated data was binned into 24-hour aggregates before extracting maxima.

Extreme value distributions provide a good test of the model because they are not used in the calibration, and there is no parameter that directly 'fixes' an aspect of these distributions. The pluviograph gauges show a reasonable comparison for most, but not all gauges. At least three gauges consistently oversimulate the distribution of 1-hour and 6-hour extremes. The daily gauges are better in this regard, but the observed extremes exhibit a skewness that is not reproduced by the model (i.e. the mid-region of the simulated distribution is too low). There is considerable difficulty in improving these fit to these statistics, as gains in one statistic or at one site can yield poorer comparisons when inspecting other statistics or other sites.

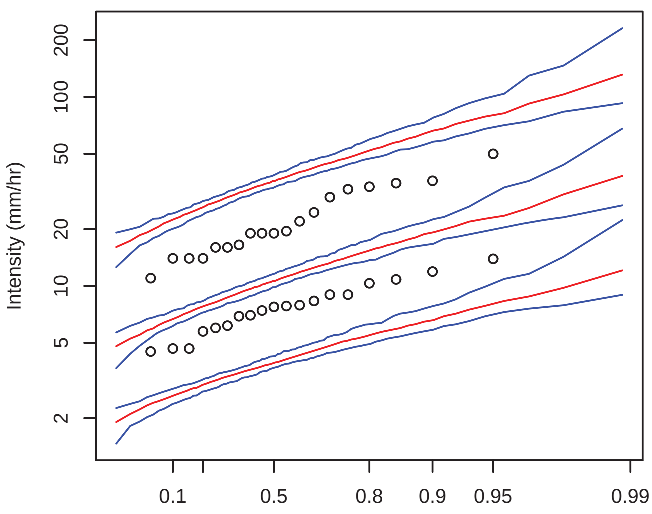
Intensity (mm/hr)
2 5 10 20 50 100 200
0.1 0.5 0.8 0.9 0.95 0.99

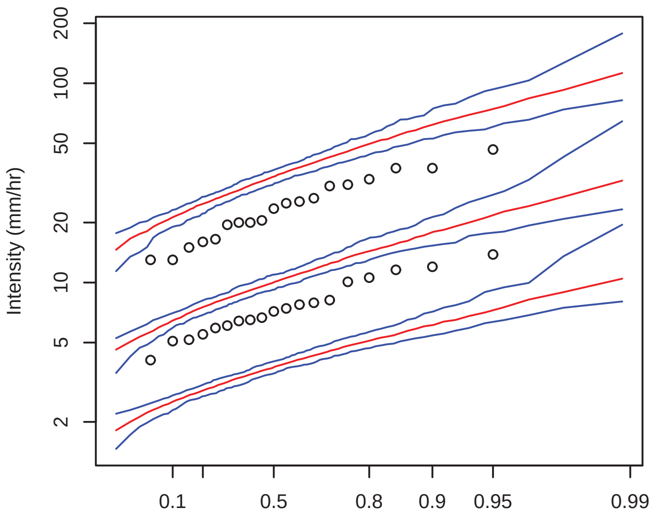
Intensity (mm/hr)
2 5 10 20 50 100 200
0.1 0.5 0.8 0.9 0.95 0.99

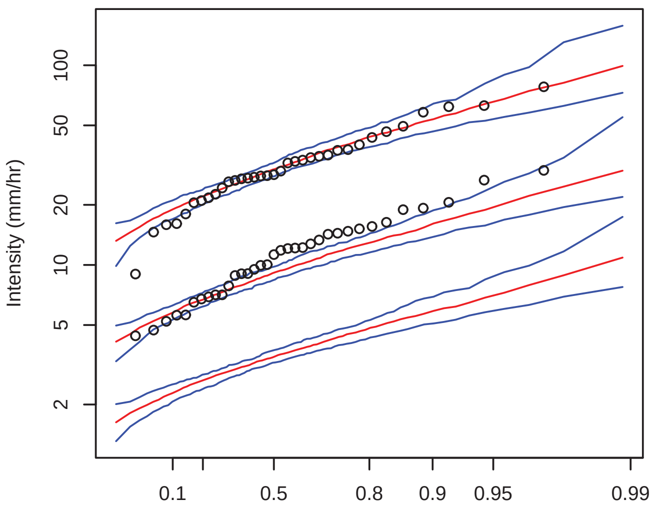
Intensity (mm/hr)
2 5 10 20 50 100
0.1 0.5 0.8 0.9 0.95 0.99

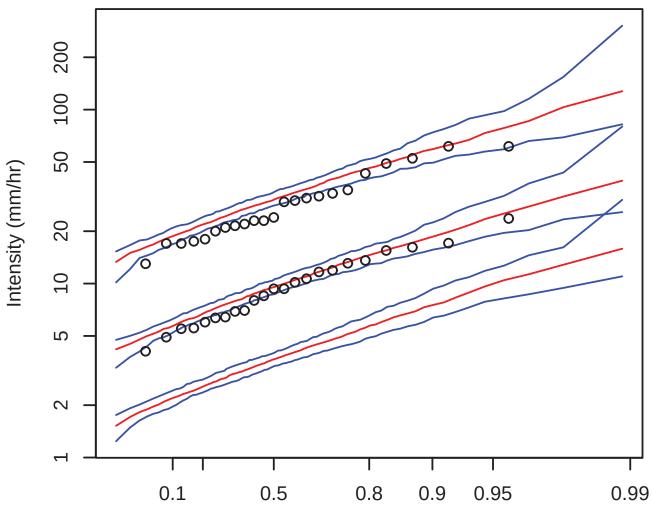
Intensity (mm/hr)
1 2 5 10 20 50 100 200
0.1 0.5 0.8 0.9 0.95 0.99

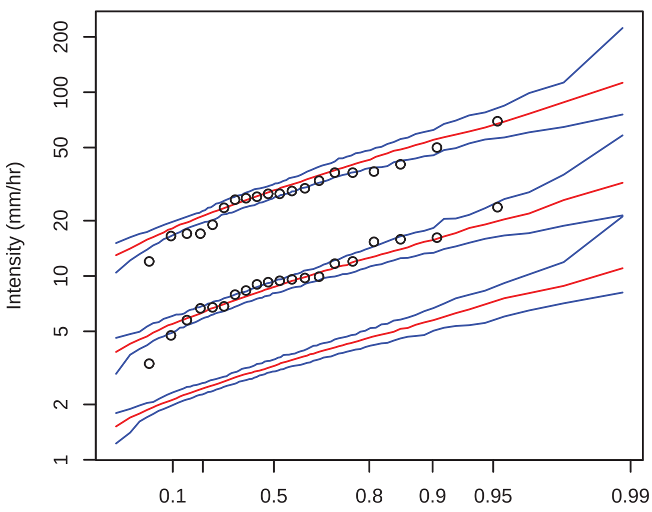
Intensity (mm/hr)
1 2 5 10 20 50 100 200
0.1 0.5 0.8 0.9 0.95 0.99

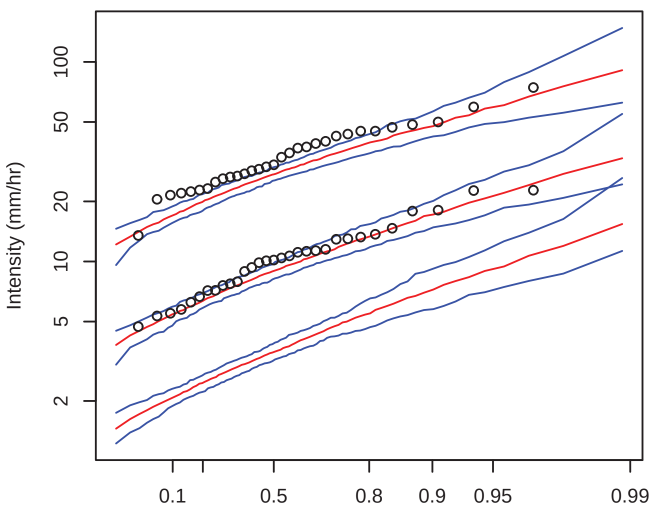
Intensity (mm/hr)
2 5 10 20 50 100
0.1 0.5 0.8 0.9 0.95 0.99

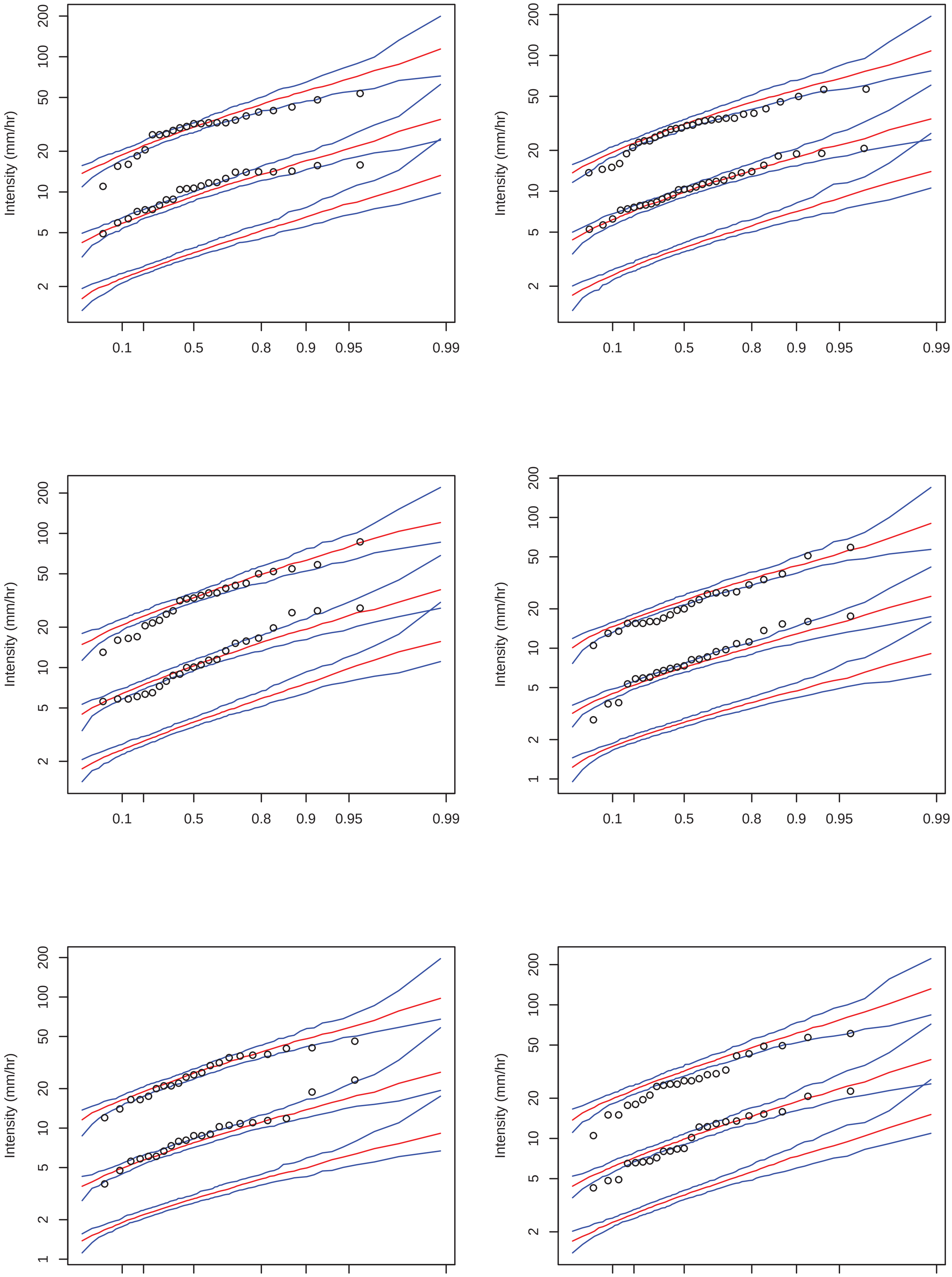
Intensity (mm/hr)
200
100
50
20
10
5
2
1
0.1
0.5
0.8
0.9
0.95
0.99

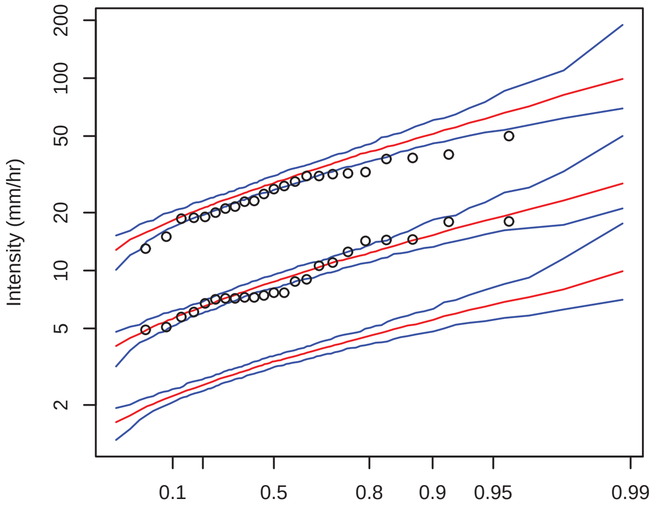
Intensity (mm/hr)
2 5 10 20 50 100 200
0.1 0.5 0.8 0.9 0.95 0.99

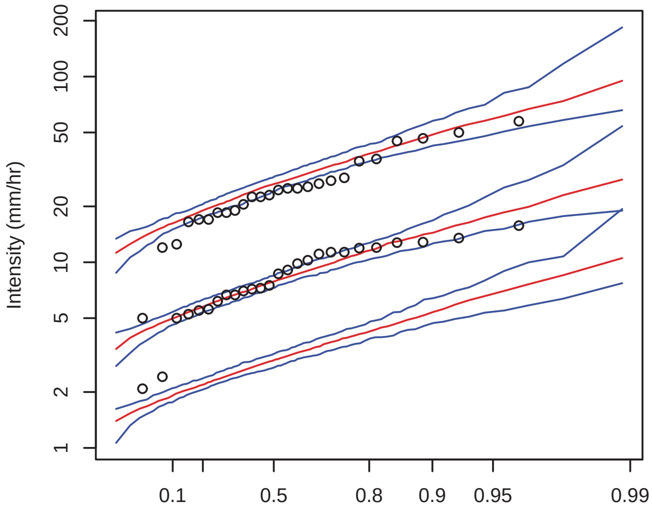
Intensity (mm/hr)
1 2 5 10 20 50 100 200
0.1 0.5 0.8 0.9 0.95 0.99

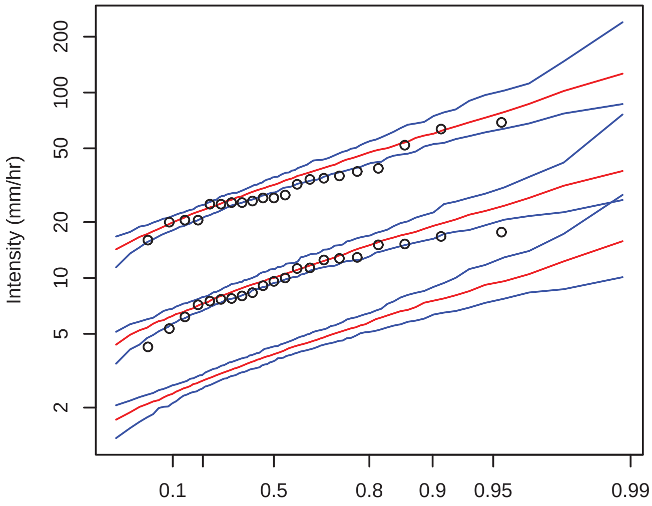
Intensity (mm/hr)
2 5 10 20 50 100 200
0.1 0.5 0.8 0.9 0.95 0.99

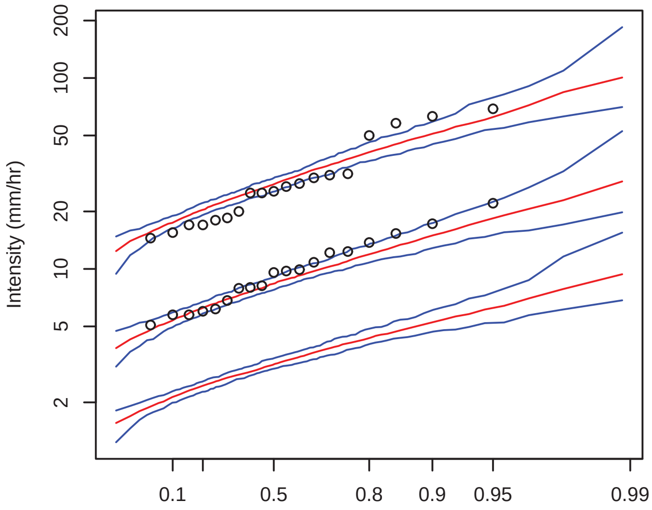
Intensity (mm/hr)
2 5 10 20 50 100 200
0.1 0.5 0.8 0.9 0.95 0.99

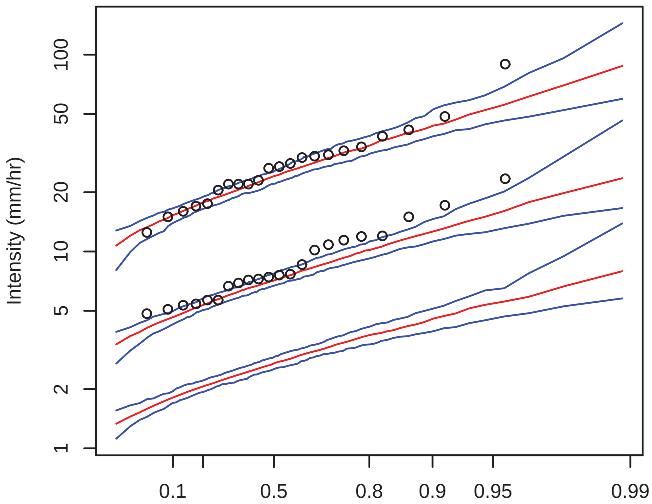
Intensity (mm/hr)
1 2 5 10 20 50 100
0.1 0.5 0.8 0.9 0.95 0.99

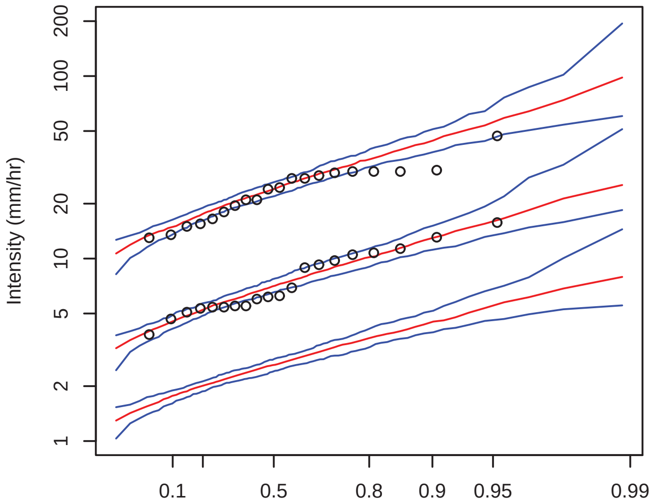
Intensity (mm/hr)
1 2 5 10 20 50 100 200
0.1 0.5 0.8 0.9 0.95 0.99

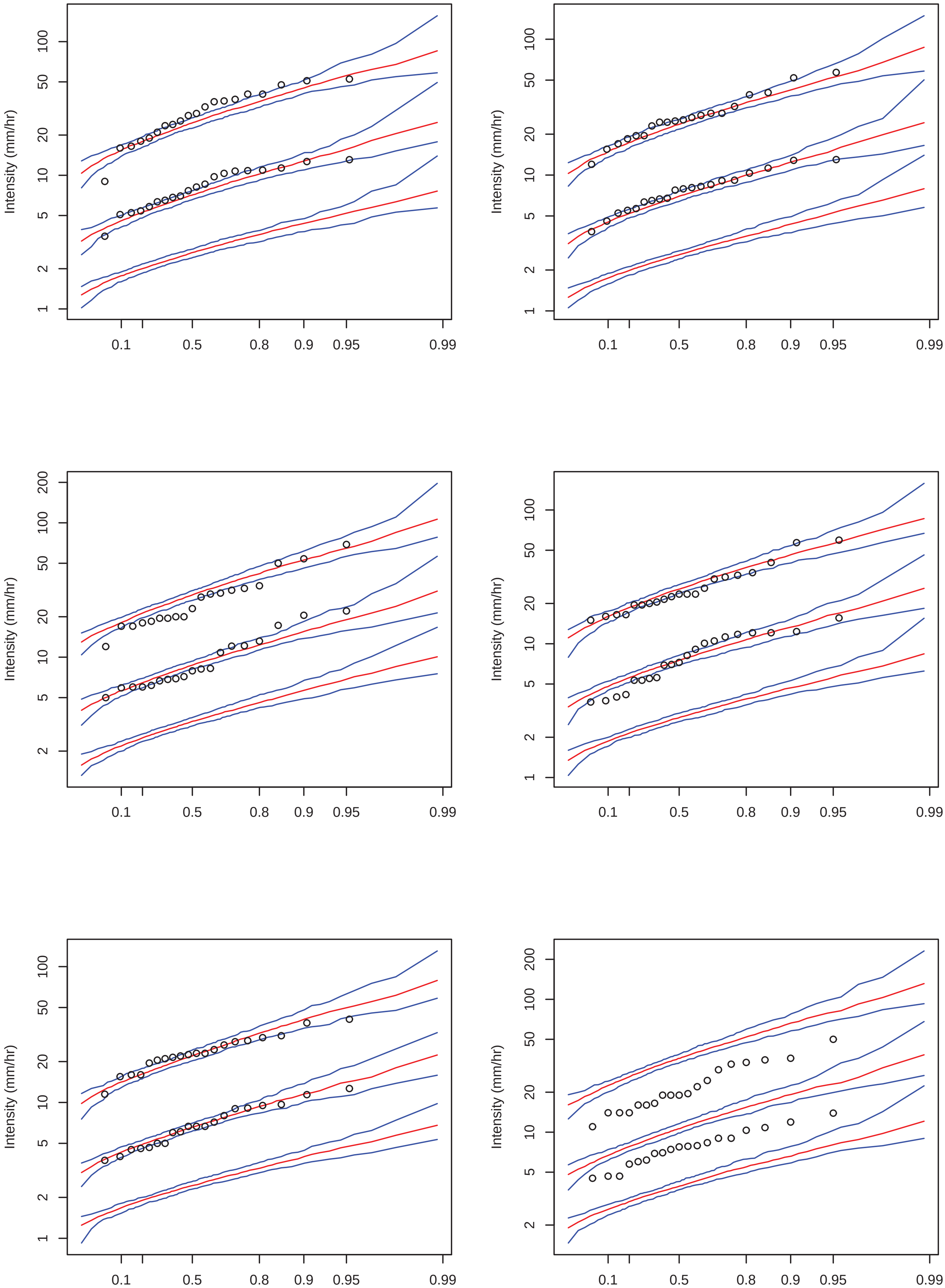
Intensity (mm/hr)
1
2
5
10
20
50
100
200
0.1
0.5
0.8
0.9
0.95
0.99

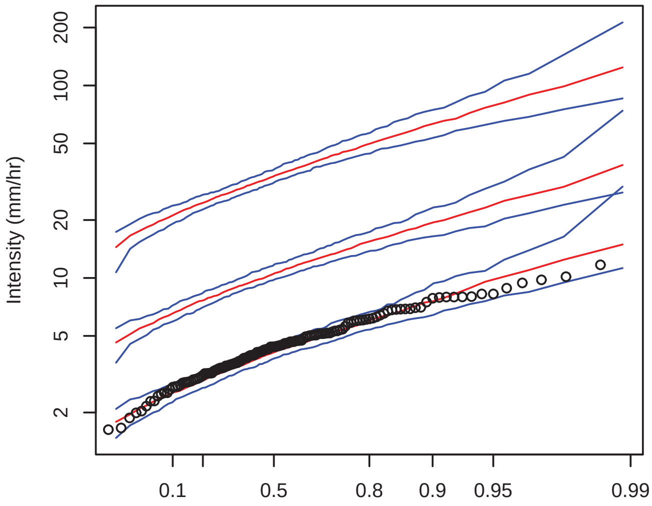
Intensity (mm/hr)
2
5
10
20
50
100
200
0.1
0.5
0.8
0.9
0.95
0.99

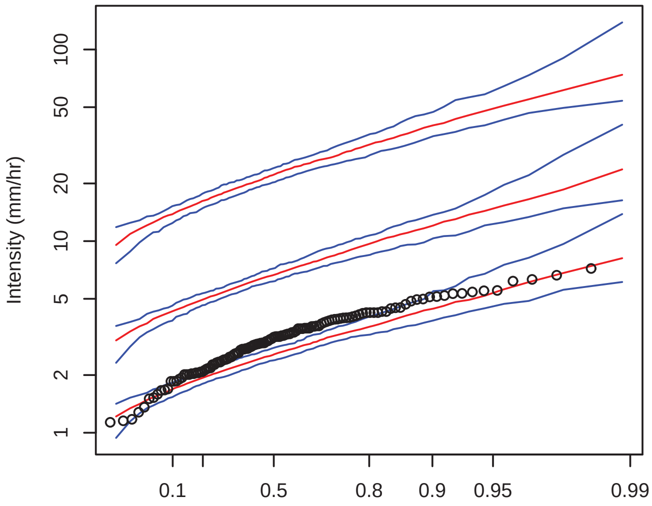
Intensity (mm/hr)
1
2
5
10
20
50
100
0.1
0.5
0.8
0.9
0.95
0.99

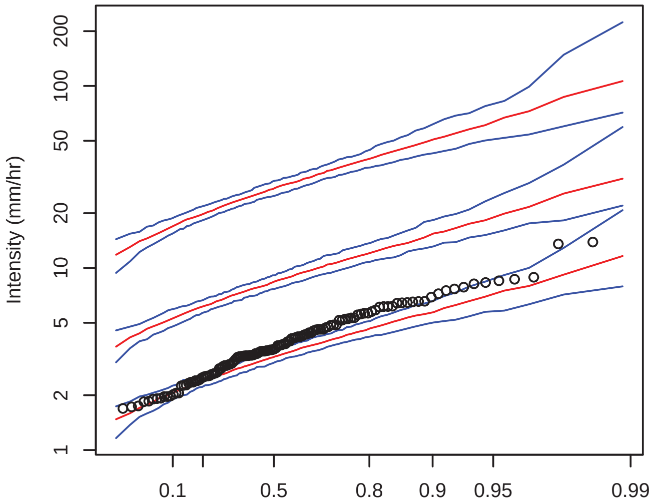
Intensity (mm/hr)
1
2
5
10
20
50
100
200
0.1
0.5
0.8
0.9
0.95
0.99

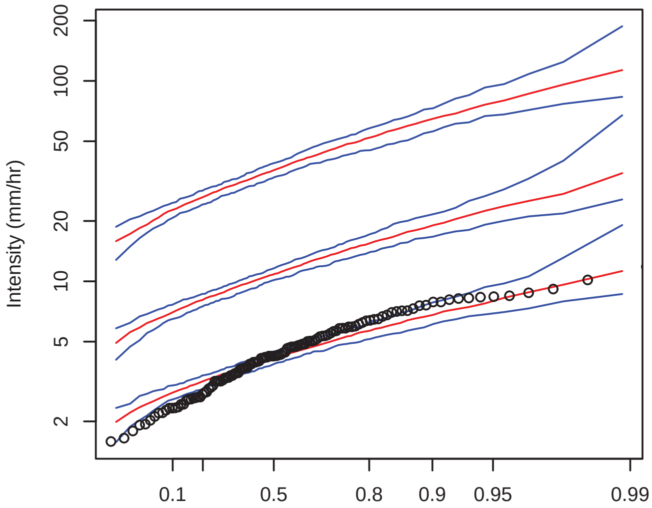
Intensity (mm/hr)
2
5
10
20
50
100
200
0.1
0.5
0.8
0.9
0.95
0.99

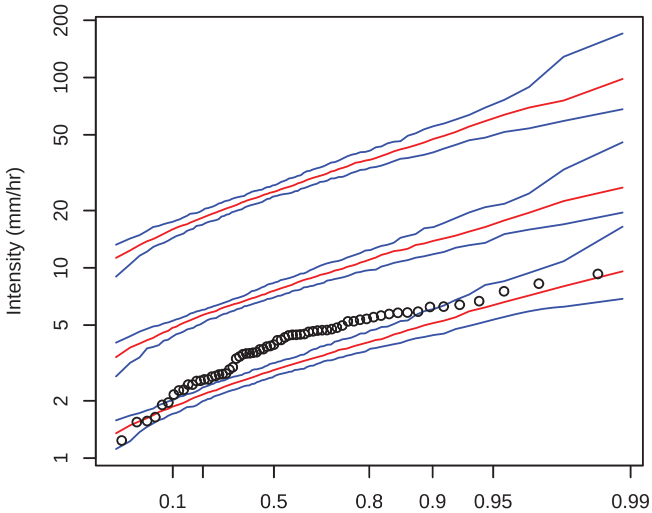
Intensity (mm/hr)
1
2
5
10
20
50
100
200
0.1
0.5
0.8
0.9
0.95
0.99

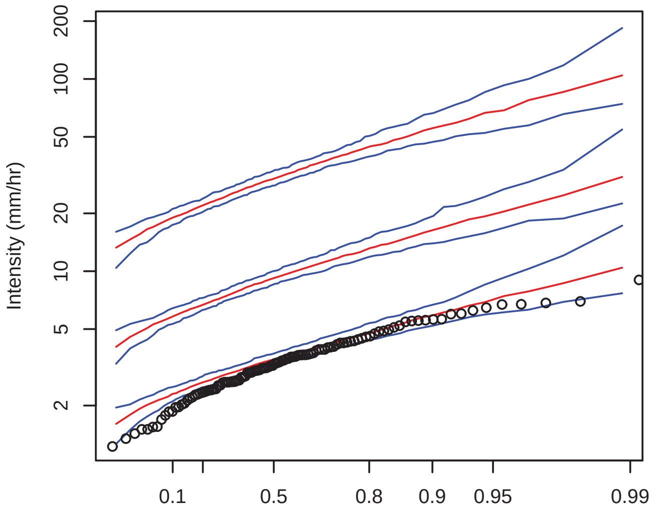
Intensity (mm/hr)
2
5
10
20
50
100
200
0.1
0.5
0.8
0.9
0.95
0.99

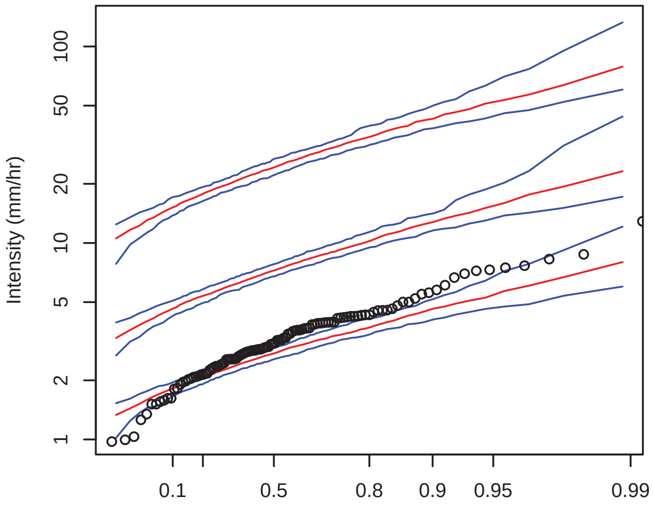
Intensity (mm/hr)
1
2
5
10
20
50
100
0.1
0.5
0.8
0.9
0.95
0.99

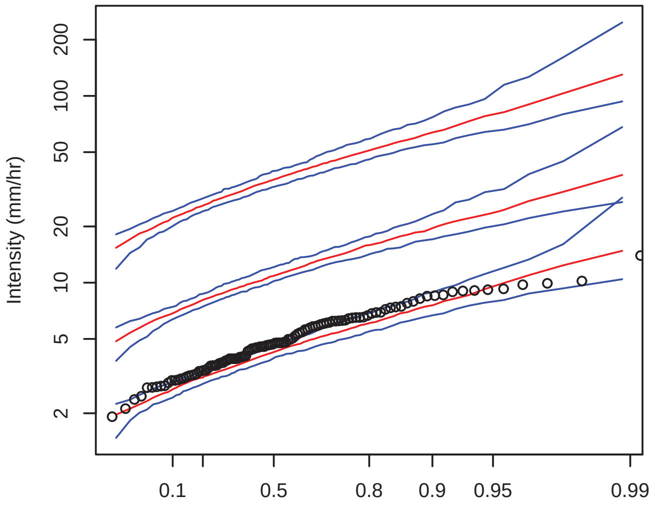
Intensity (mm/hr)
2
5
10
20
50
100
200
0.1
0.5
0.8
0.9
0.95
0.99

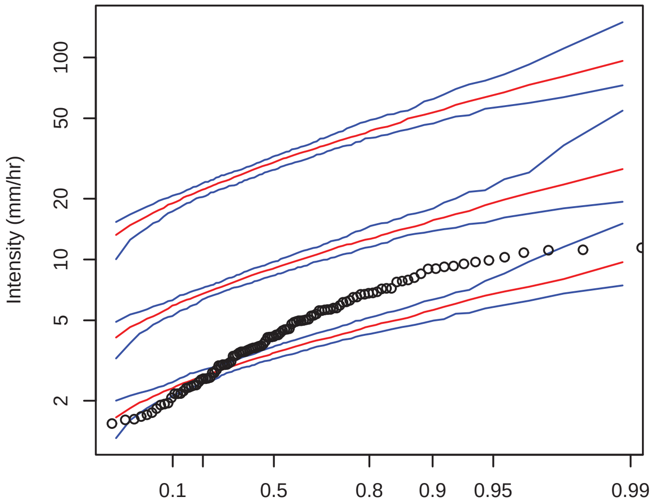
Intensity (mm/hr)
2
5
10
20
50
100
0.1
0.5
0.8
0.9
0.95
0.99

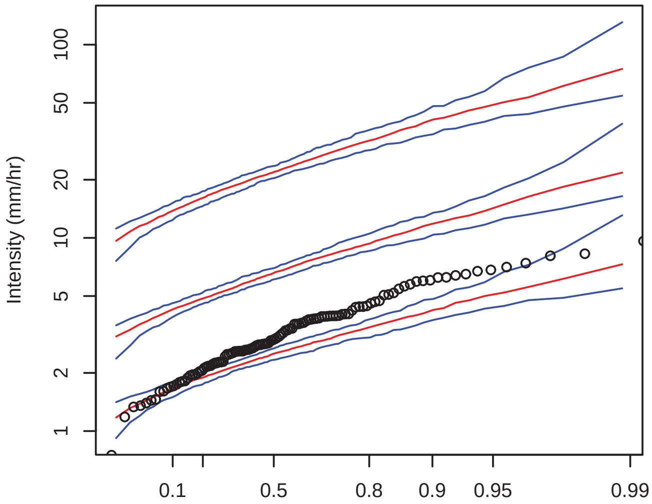
Intensity (mm/hr)
1
2
5
10
20
50
100
0.1
0.5
0.8
0.9
0.95
0.99

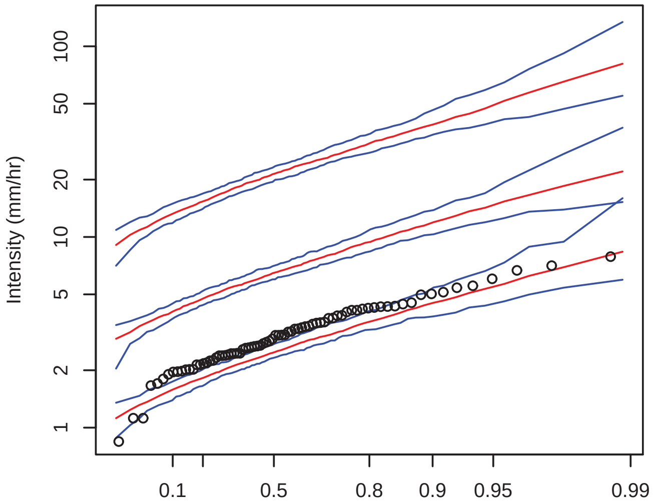
Intensity (mm/hr)
1
2
5
10
20
50
100
0.1
0.5
0.8
0.9
0.95
0.99

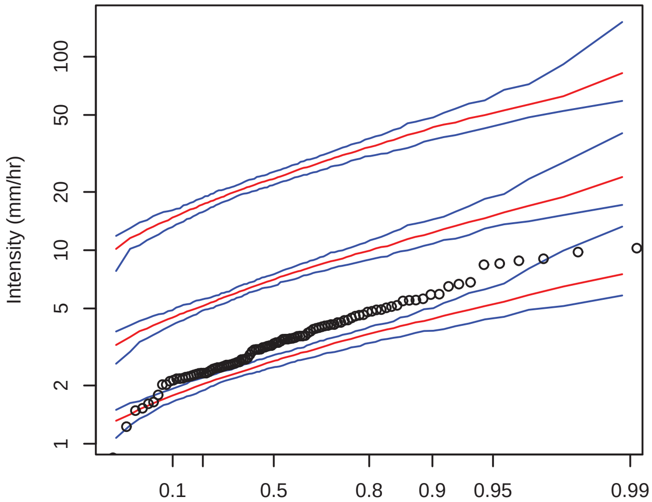
Intensity (mm/hr)
1
2
5
10
20
50
100
0.1
0.5
0.8
0.9
0.95
0.99

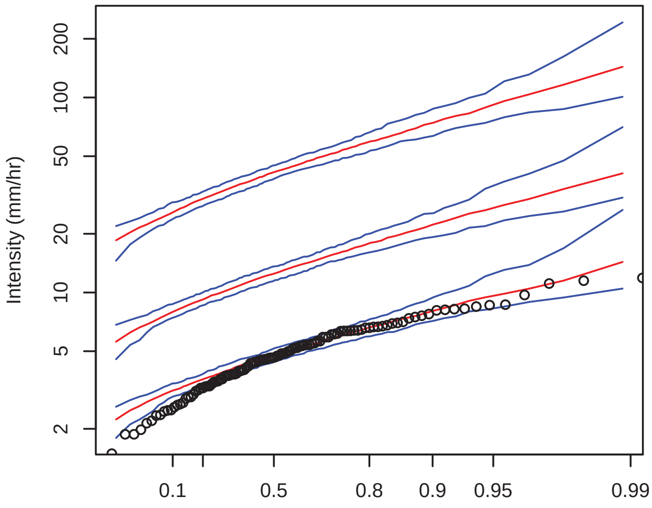
Intensity (mm/hr)
2 5 10 20 50 100 200
0.1 0.5 0.8 0.9 0.95 0.99

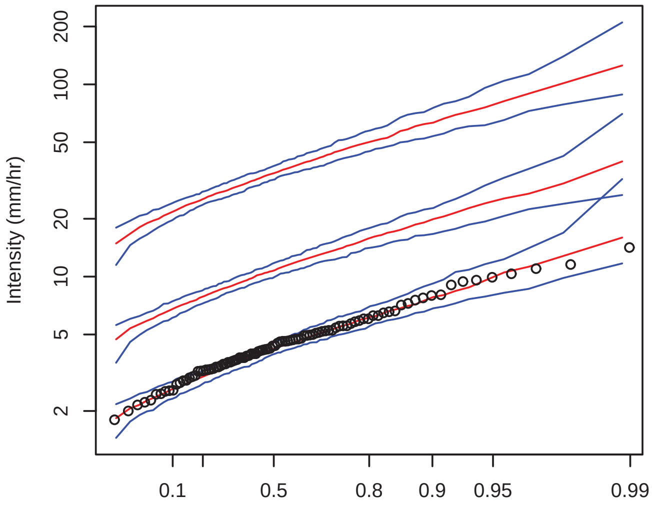
Intensity (mm/hr)
2 5 10 20 50 100 200
0.1 0.5 0.8 0.9 0.95 0.99

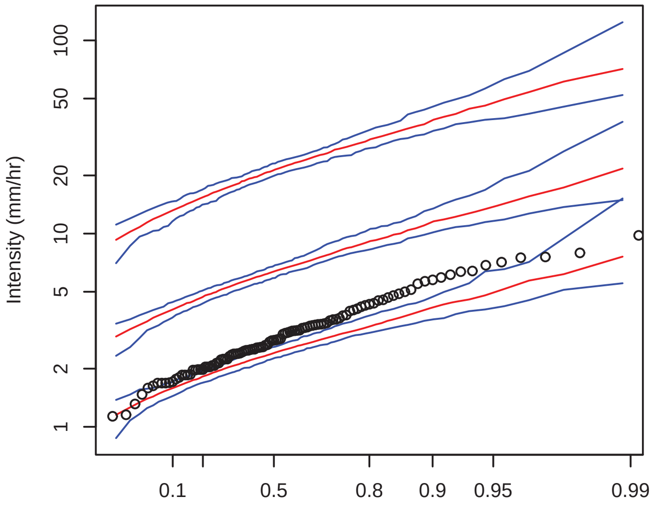
Intensity (mm/hr)
1 2 5 10 20 50 100
0.1 0.5 0.8 0.9 0.95 0.99

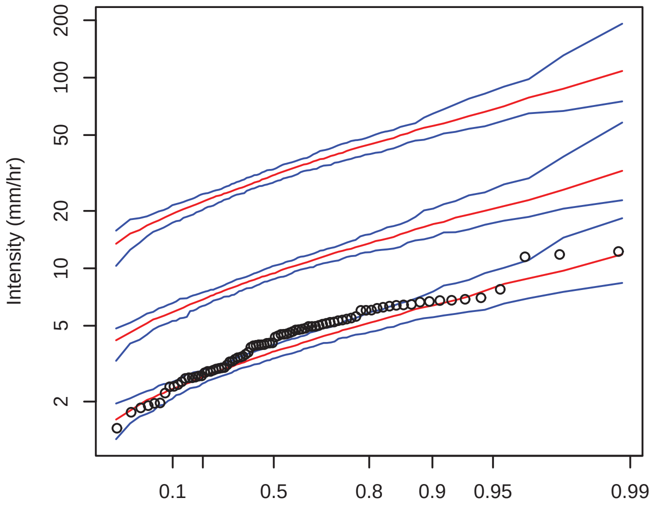
Intensity (mm/hr)
2 5 10 20 50 100 200
0.1 0.5 0.8 0.9 0.95 0.99

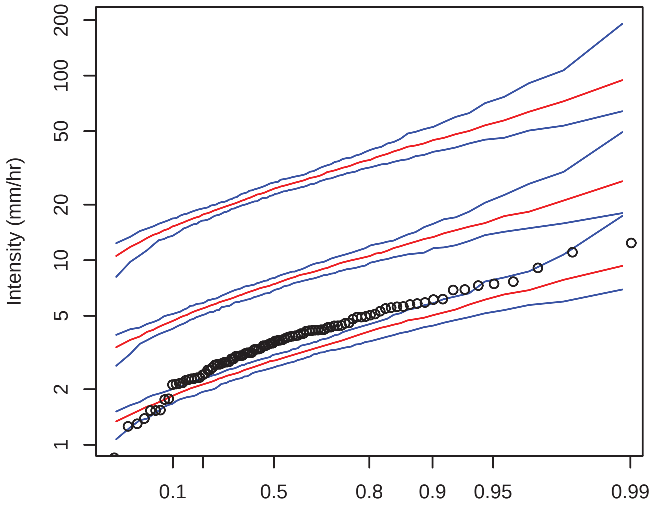
Intensity (mm/hr)
1 2 5 10 20 50 100 200
0.1 0.5 0.8 0.9 0.95 0.99

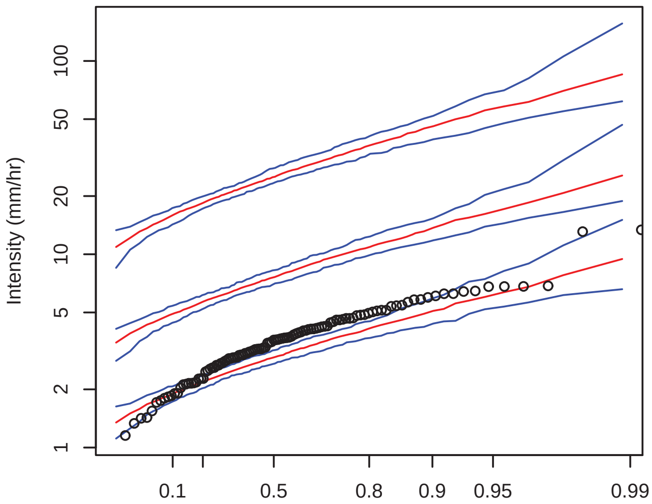
Intensity (mm/hr)
1 2 5 10 20 50 100
0.1 0.5 0.8 0.9 0.95 0.99

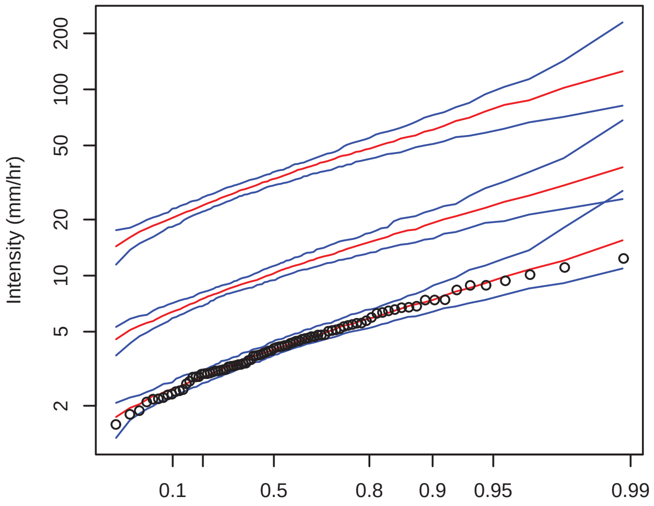
Intensity (mm/hr)
200
100
50
20
10
5
2
0.1
0.5
0.8
0.9
0.95
0.99

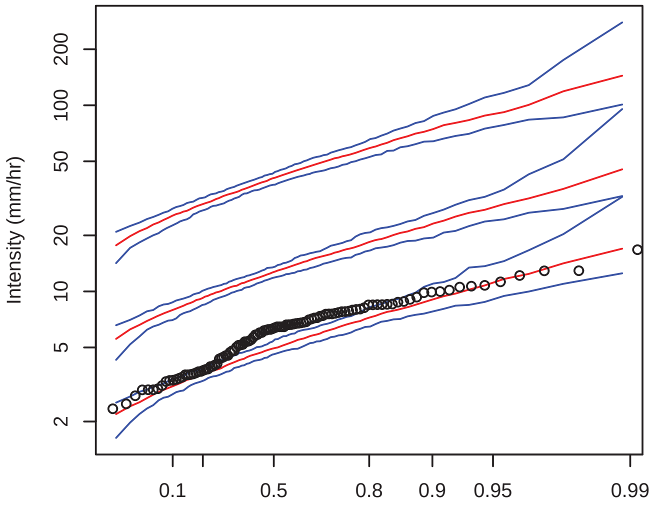
Intensity (mm/hr)
200
100
50
20
10
5
2
0.1
0.5
0.8
0.9
0.95
0.99

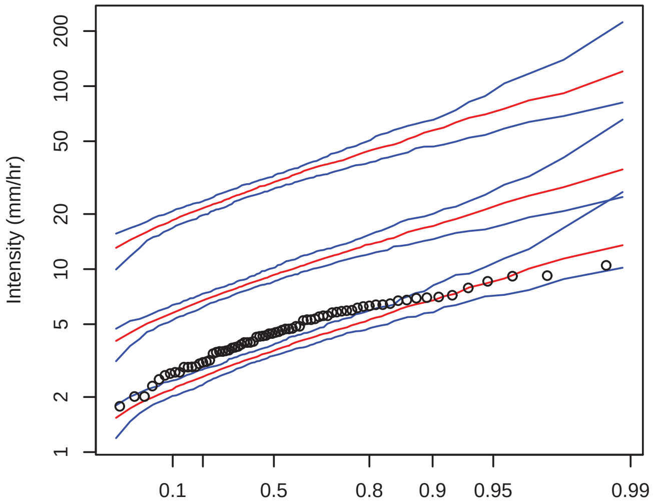
Intensity (mm/hr)
200
100
50
20
10
5
2
1
0.1
0.5
0.8
0.9
0.95
0.99

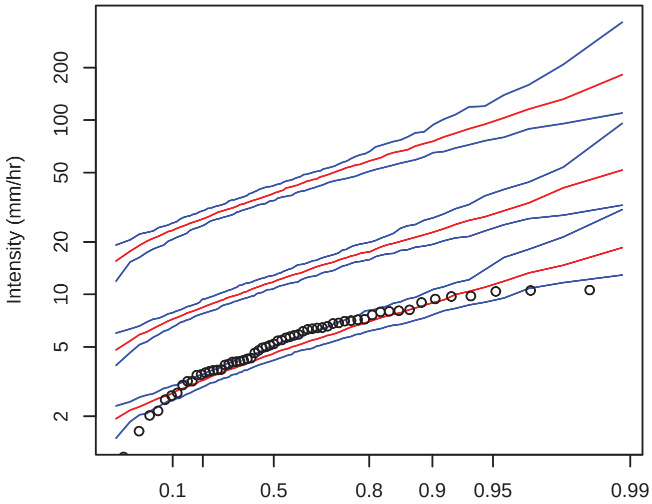
Intensity (mm/hr)
200
100
50
20
10
5
2
0.1
0.5
0.8
0.9
0.95
0.99

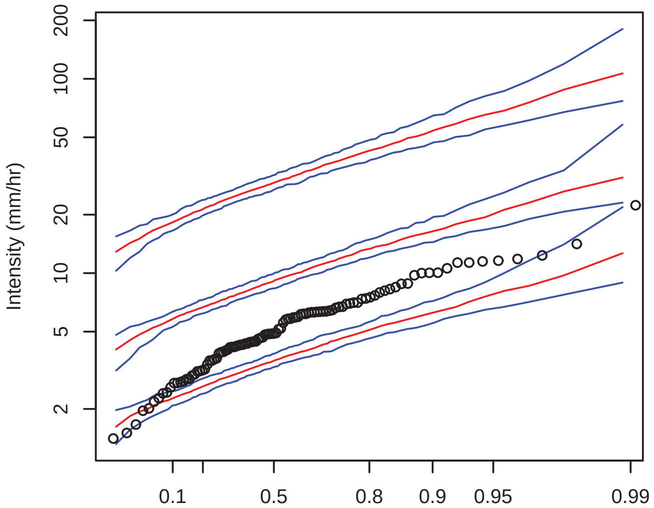
Intensity (mm/hr)
200
100
50
20
10
5
2
0.1
0.5
0.8
0.9
0.95
0.99

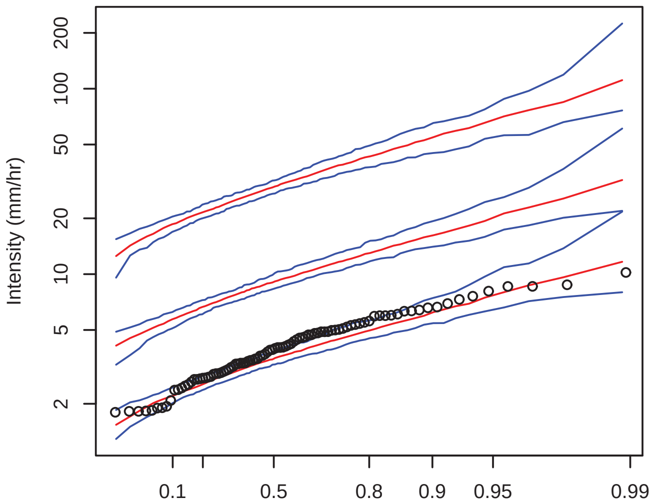
Intensity (mm/hr)
200
100
50
20
10
5
2
0.1
0.5
0.8
0.9
0.95
0.99

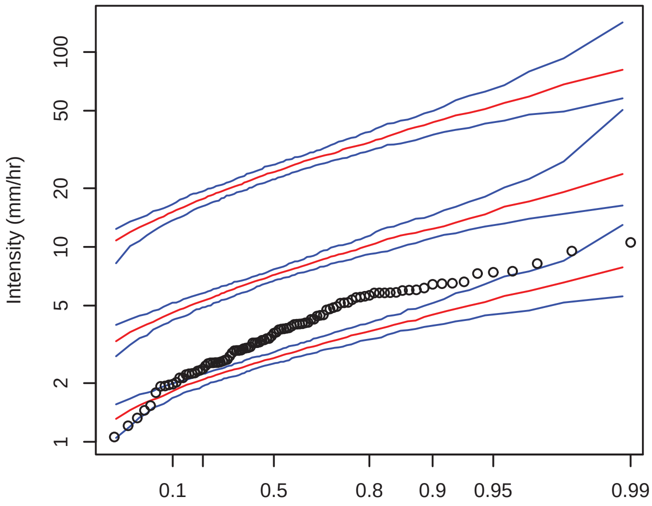
Intensity (mm/hr)
1
2
5
10
20
50
100
0.1
0.5
0.8
0.9
0.95
0.99

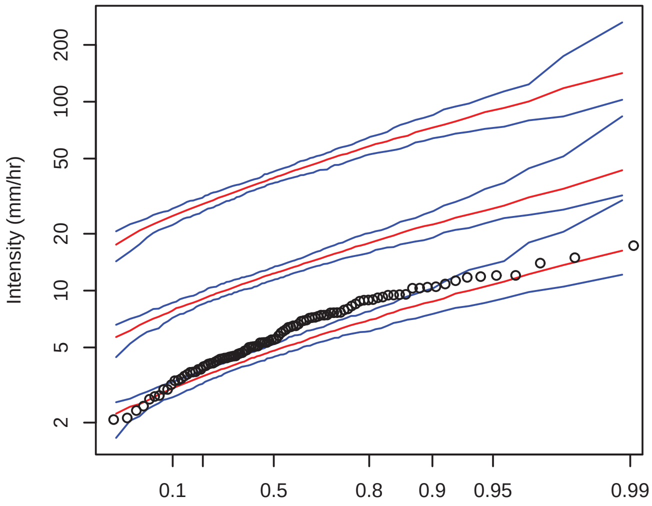
Intensity (mm/hr)
2
5
10
20
50
100
200
0.1
0.5
0.8
0.9
0.95
0.99

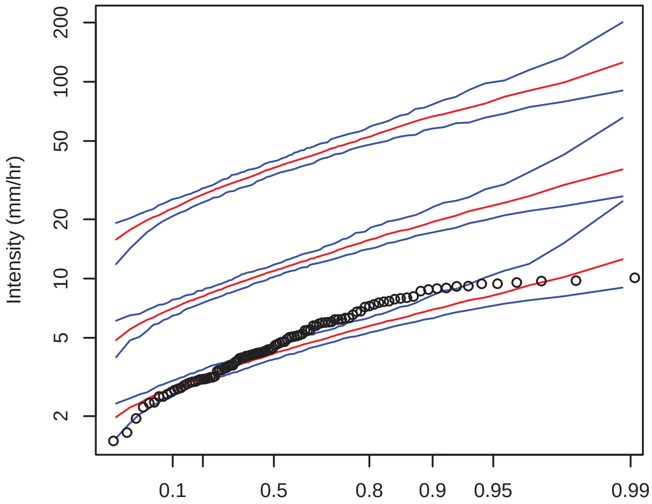
Intensity (mm/hr)
2
5
10
20
50
100
200
0.1
0.5
0.8
0.9
0.95
0.99

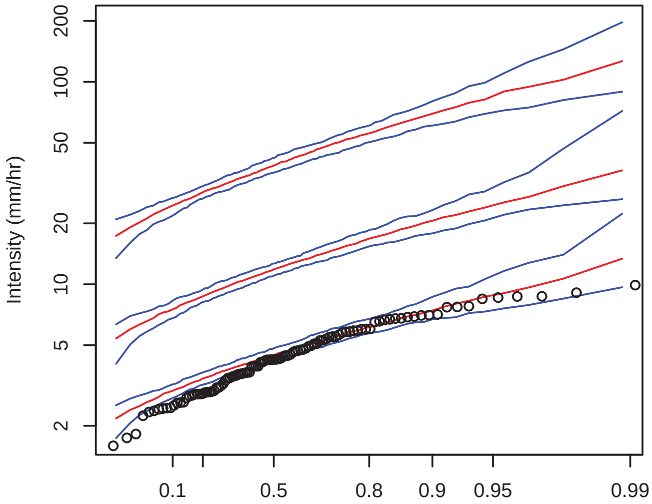
Intensity (mm/hr)
2
5
10
20
50
100
200
0.1
0.5
0.8
0.9
0.95
0.99

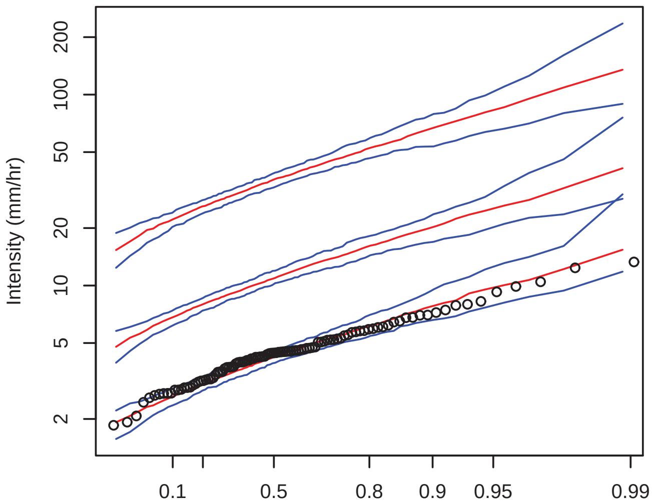
Intensity (mm/hr)
2
5
10
20
50
100
200
0.1
0.5
0.8
0.9
0.95
0.99

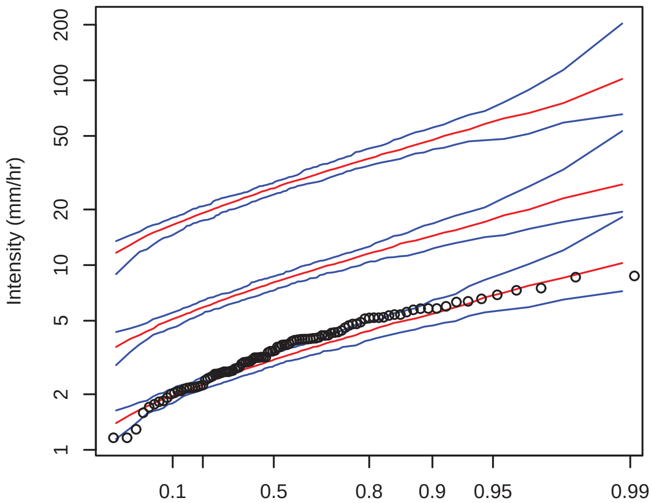
Intensity (mm/hr)
1
2
5
10
20
50
100
200
0.1
0.5
0.8
0.9
0.95
0.99

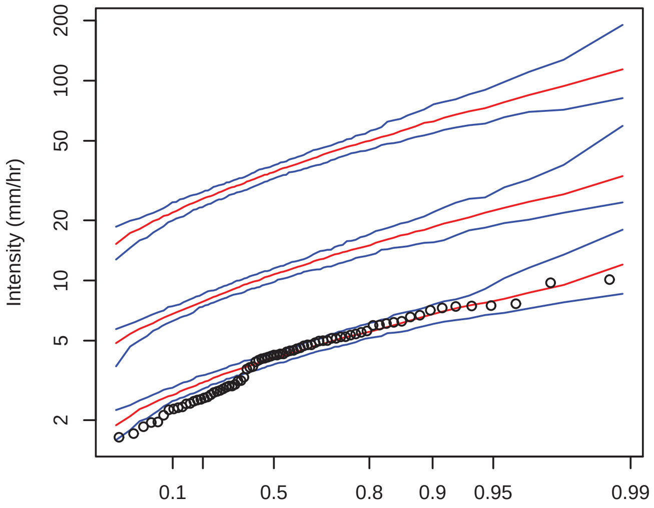
Intensity (mm/hr)
200
100
50
20
10
5
2
0.1
0.5
0.8
0.9
0.95
0.99

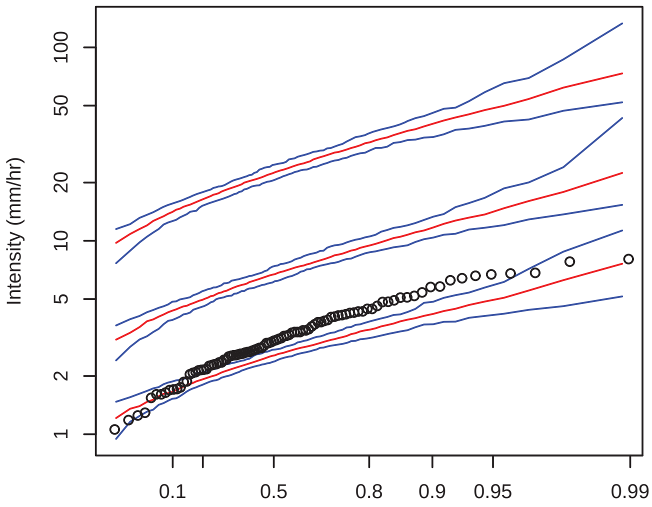
Intensity (mm/hr)
100
50
20
10
5
2
1
0.1
0.5
0.8
0.9
0.95
0.99

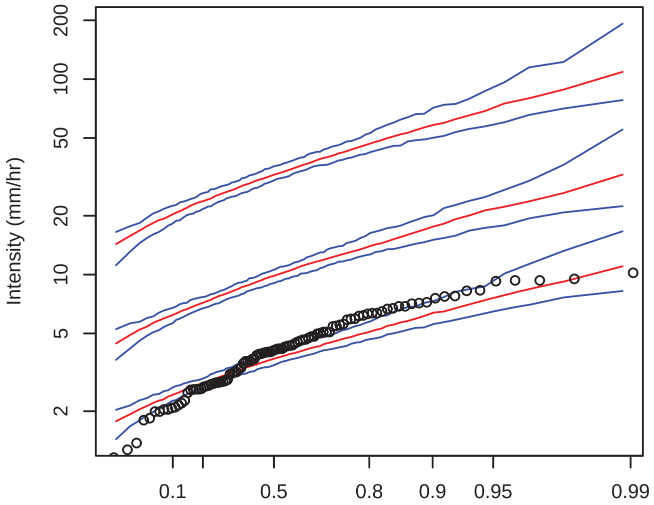
Intensity (mm/hr)
200
100
50
20
10
5
2
0.1
0.5
0.8
0.9
0.95
0.99

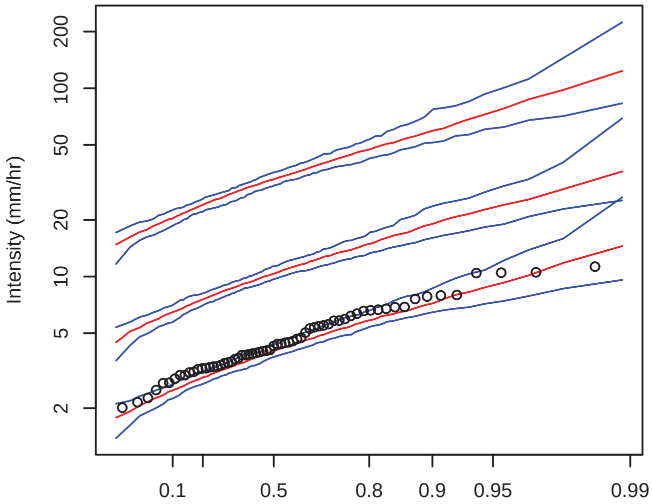
Intensity (mm/hr)
200
100
50
20
10
5
2
0.1
0.5
0.8
0.9
0.95
0.99

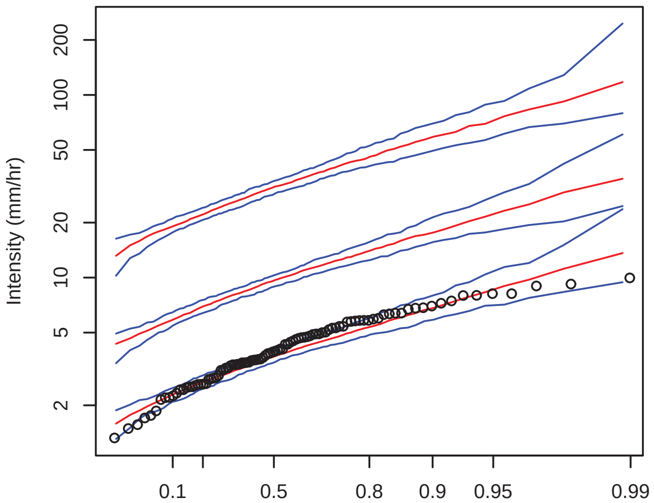
Intensity (mm/hr)
200
100
50
20
10
5
2
0.1
0.5
0.8
0.9
0.95
0.99

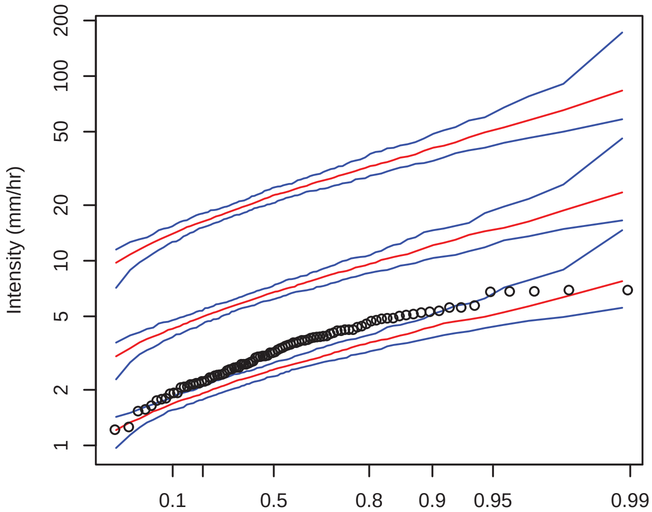
Intensity (mm/hr)
200
100
50
20
10
5
2
1
0.1
0.5
0.8
0.9
0.95
0.99

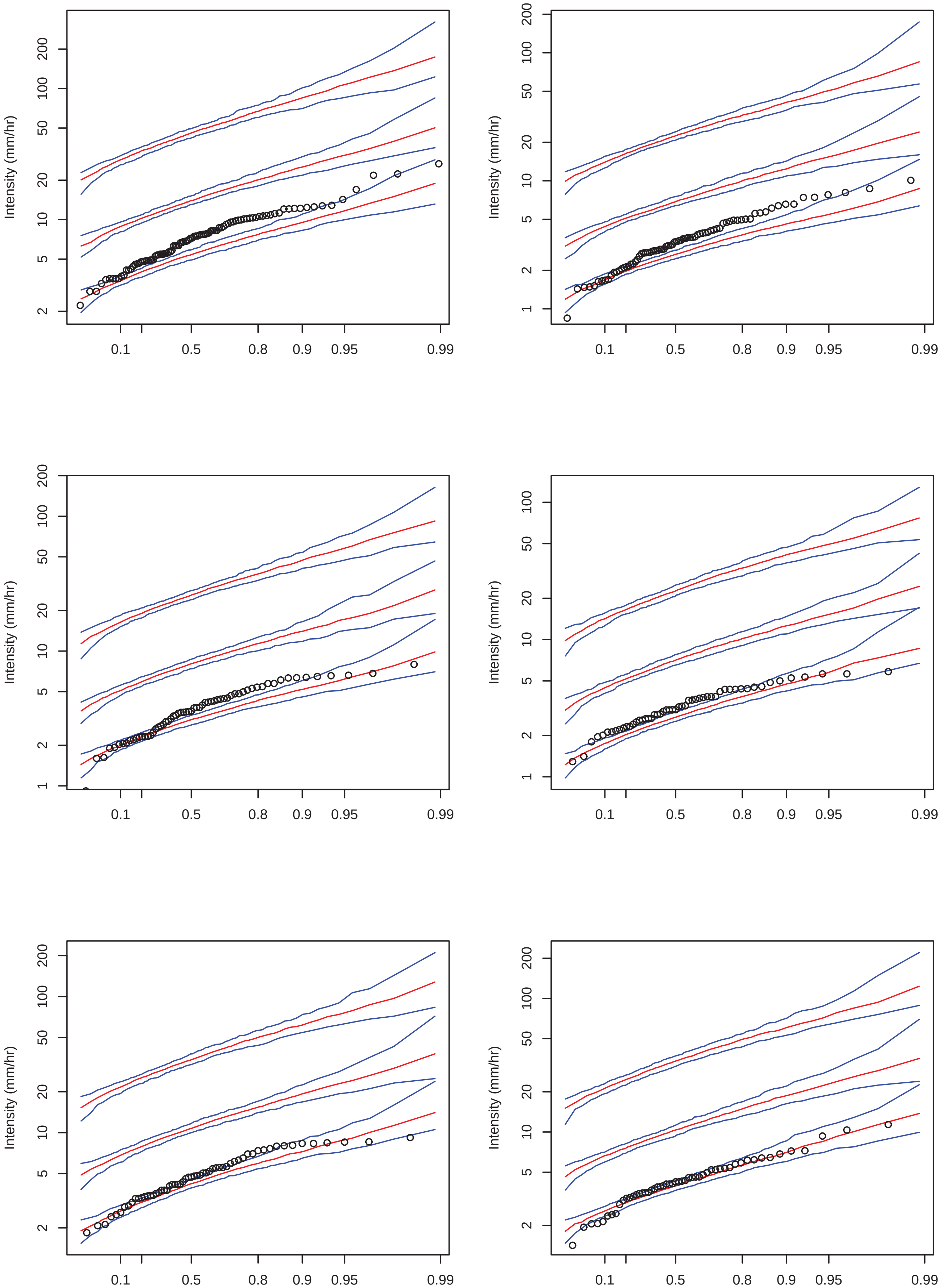
Intensity (mm/hr)
1
2
5
10
20
50
100
200
0.1
0.5
0.8
0.9
0.95
0.99

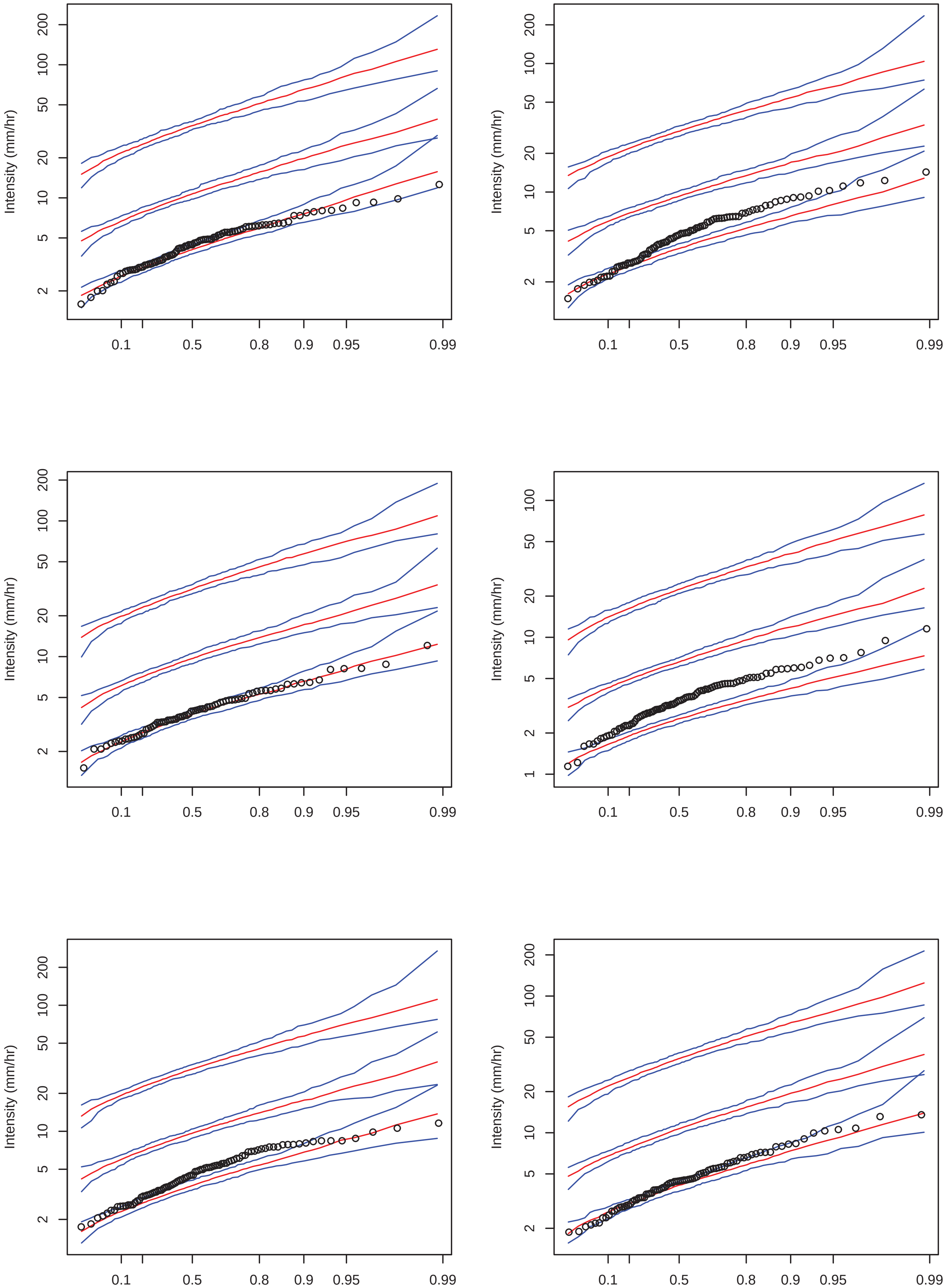
Intensity (mm/hr)
2
5
10
20
50
100
200
1
0.1
0.5
0.8
0.9
0.95
0.99

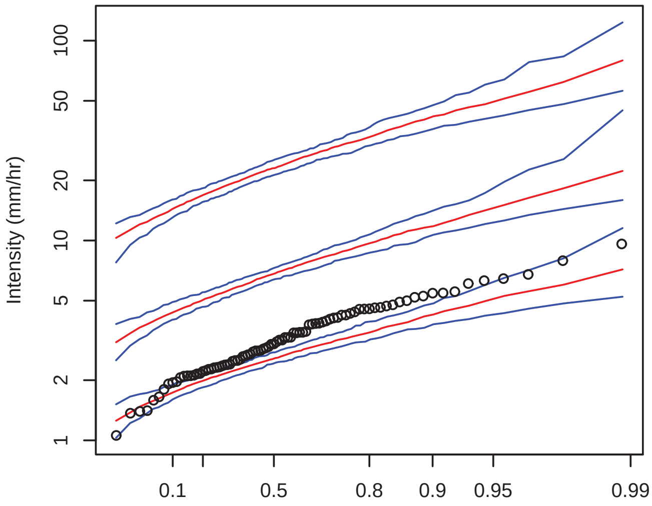

Intensity (mm/hr)
1
2
5
10
20
50
100
0.1
0.5
0.8
0.9
0.95
0.99

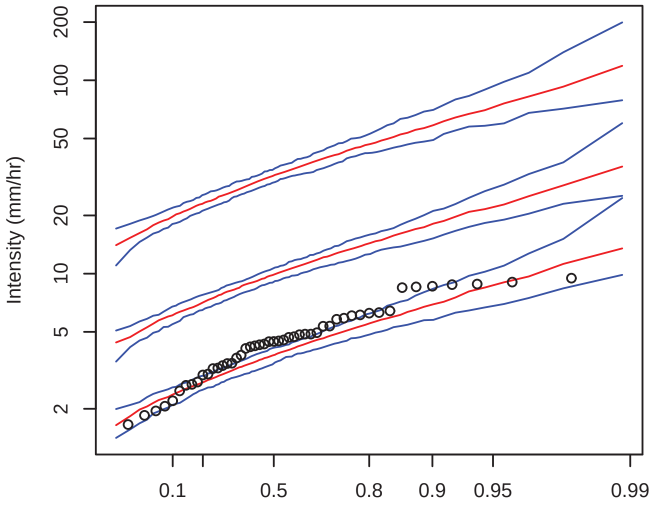

Intensity (mm/hr)
2
5
10
20
50
100
200
0.1
0.5
0.8
0.9
0.95
0.99

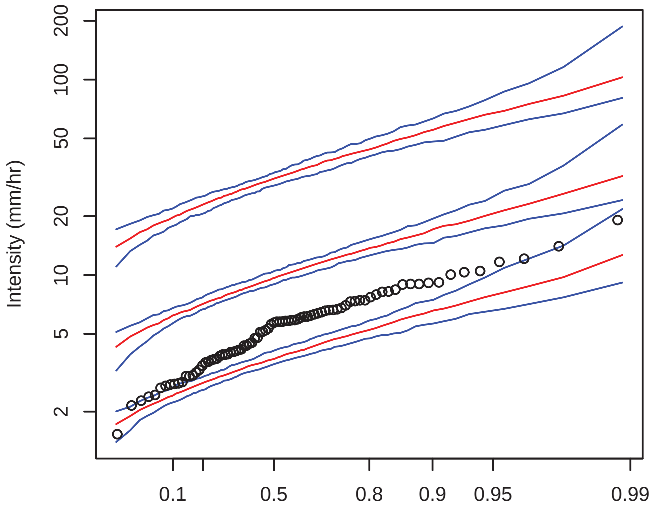

Intensity (mm/hr)
2
5
10
20
50
100
200
0.1
0.5
0.8
0.9
0.95
0.99

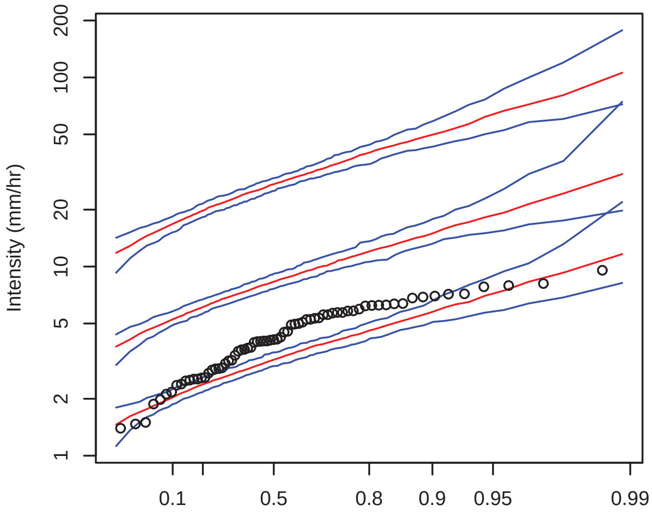

Intensity (mm/hr)
1
2
5
10
20
50
100
200
0.1
0.5
0.8
0.9
0.95
0.99

Appendix B
Bourke Case Study

B.1 Observed SOI Partitioned Annual Extremes

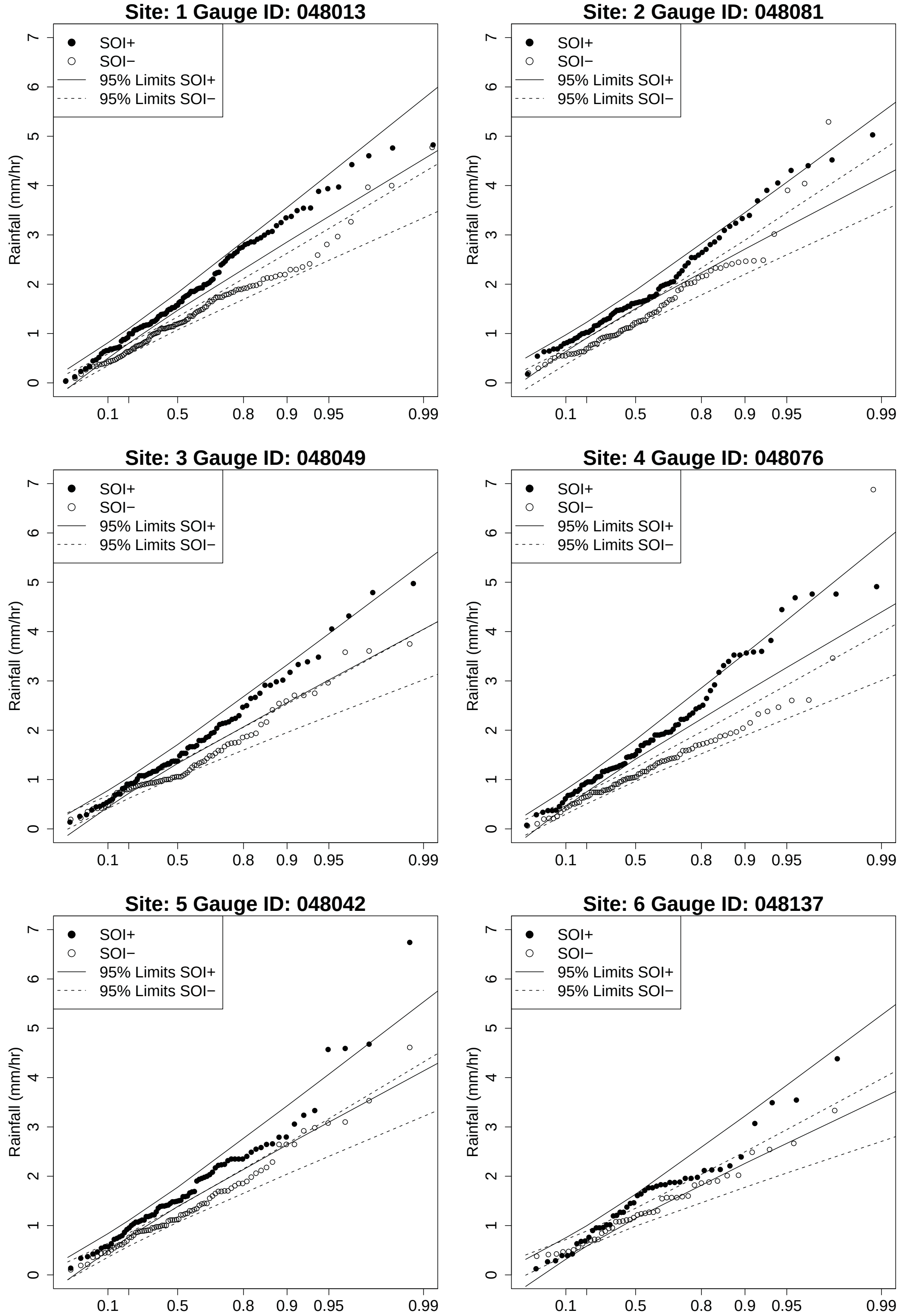

Figure B.1 Annual extremes of daily rainfall at Bourke partitioned by +ve/-ve phases of the SOI. Probabilities shown using a Gumbel axis. 95% Confidence intervals obtained from the distribution of estimates of the Gumbel parameters.

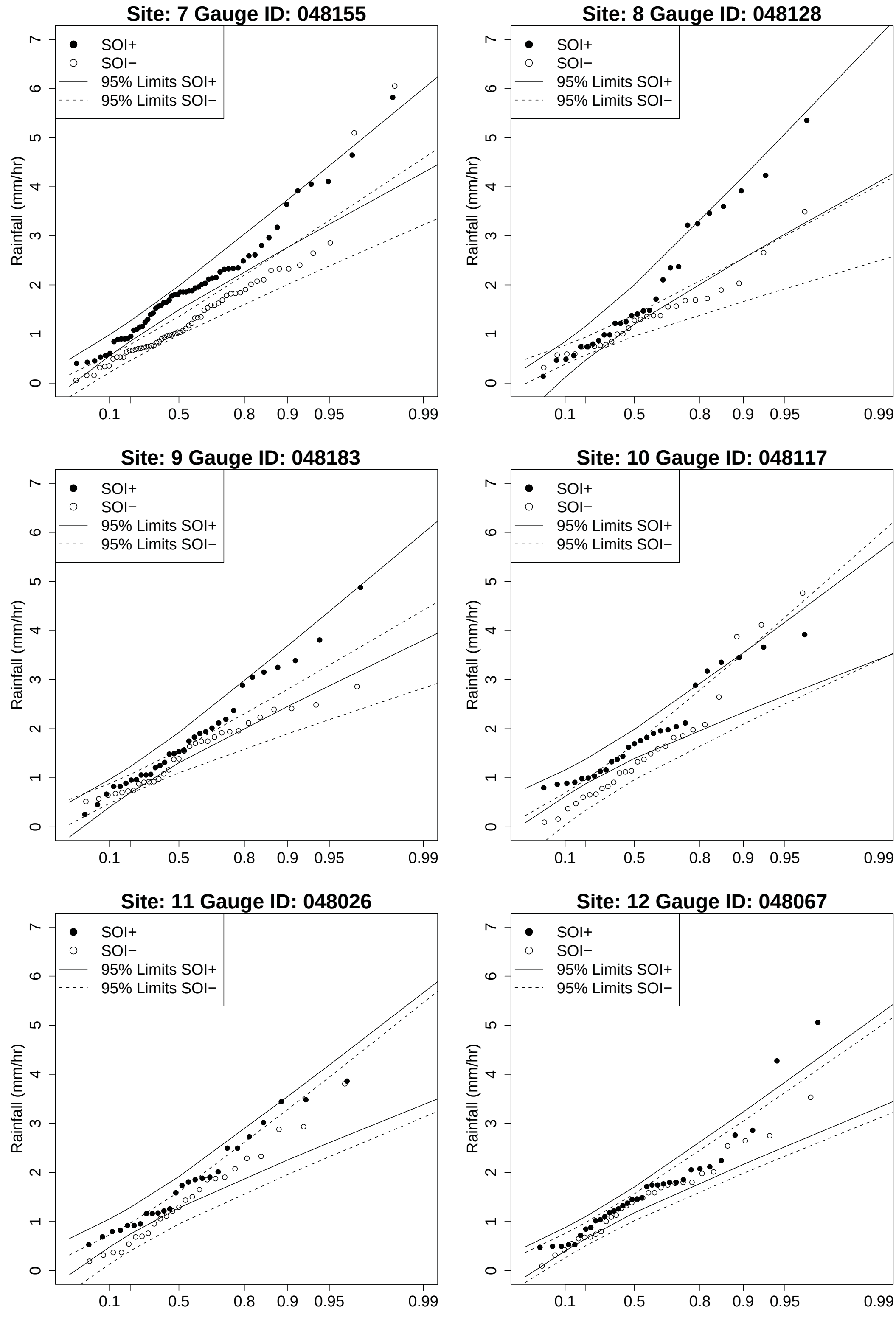

Figure B.2 Annual extremes of daily rainfall at Bourke partitioned by +ve/-ve phases of the SOI. Probabilities shown using a Gumbel axis. 95% Confidence intervals obtained from the distribution of estimates of the Gumbel parameters.

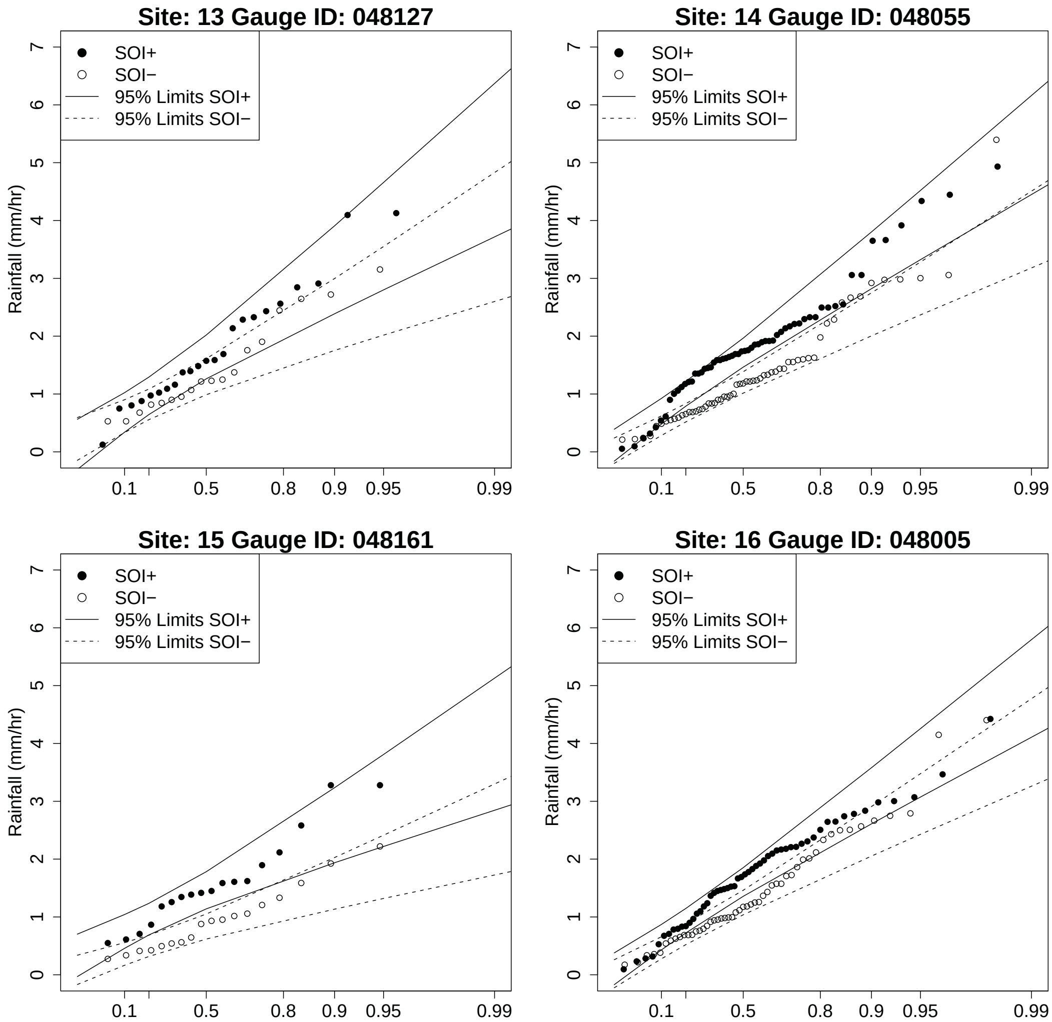

Figure B.3 Annual extremes of daily rainfall at Bourke partitioned by +ve/-ve phases of the SOI. Probabilities shown using a Gumbel axis. 95% Confidence intervals obtained from the distribution of estimates of the Gumbel parameters.

B.2 OBSERVED SOI PARTITIONED SUMMER EXTREMES

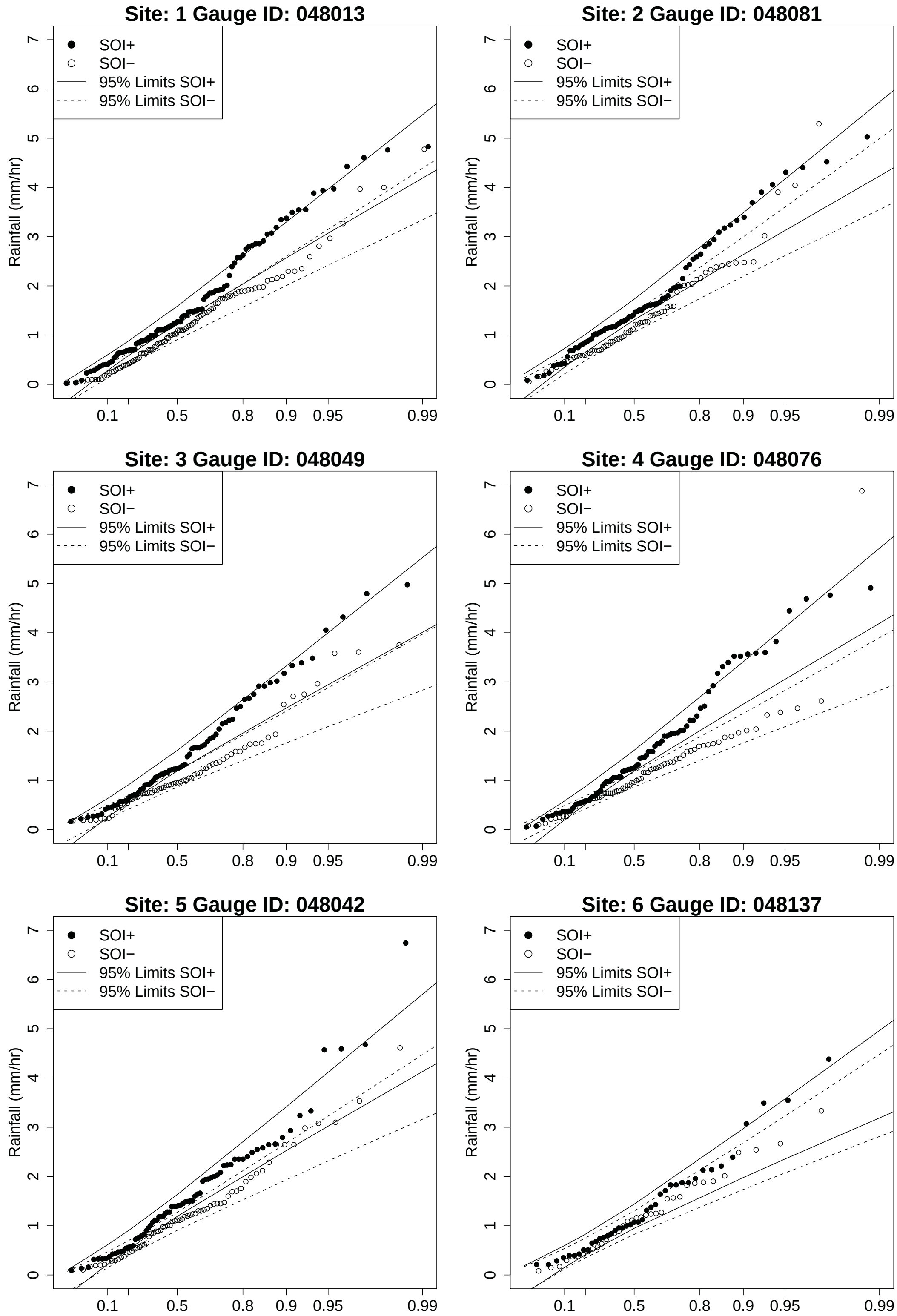

Figure B.4 Summer extremes of daily rainfall at Bourke partitioned by +ve/-ve phases of the SOI. Probabilities shown using a Gumbel axis. 95% Confidence intervals obtained from the distribution of estimates of the Gumbel parameters. Sites 1-6.

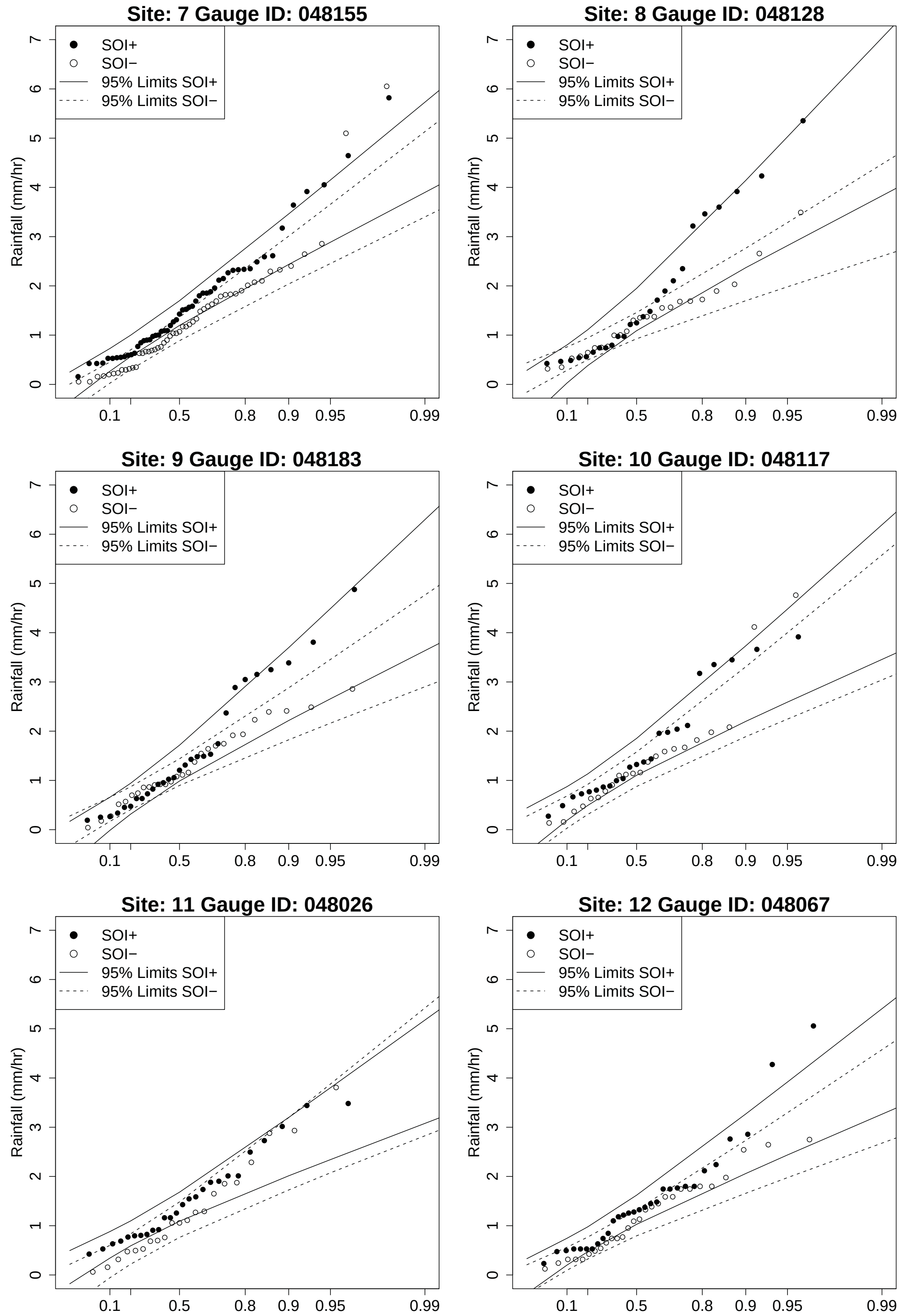

Figure B.5 Summer extremes of daily rainfall at Bourke partitioned by +ve/-ve phases of the SOI. Probabilities shown using a Gumbel axis. 95% Confidence intervals obtained from the distribution of estimates of the Gumbel parameters. Sites 7-12.

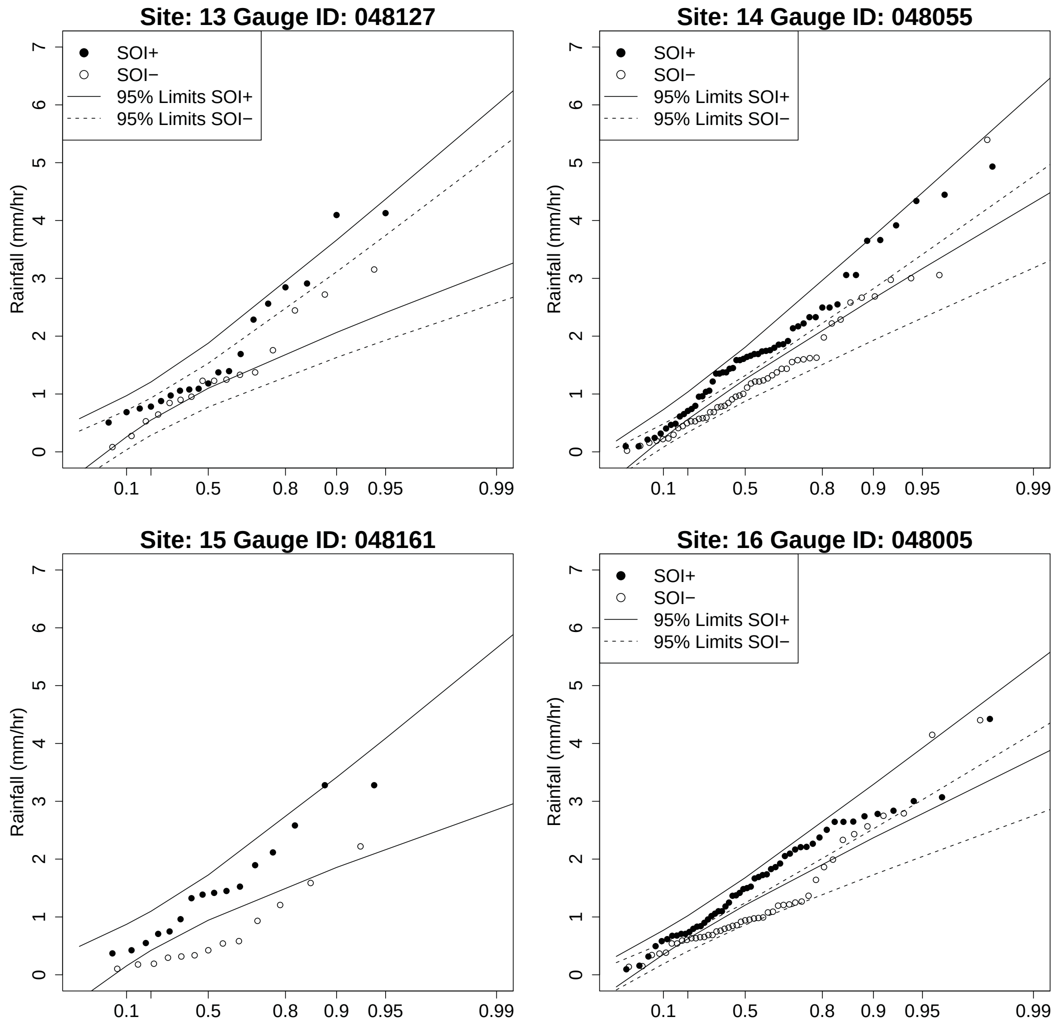

Figure B.6 Summer extremes of daily rainfall at Bourke partitioned by +ve/-ve phases of the SOI. Probabilities shown using a Gumbel axis. 95% Confidence intervals obtained from the distribution of estimates of the Gumbel parameters. Sites 13-16.

B.3 OBSERVED SOI PARTITIONED WINTER EXTREMES

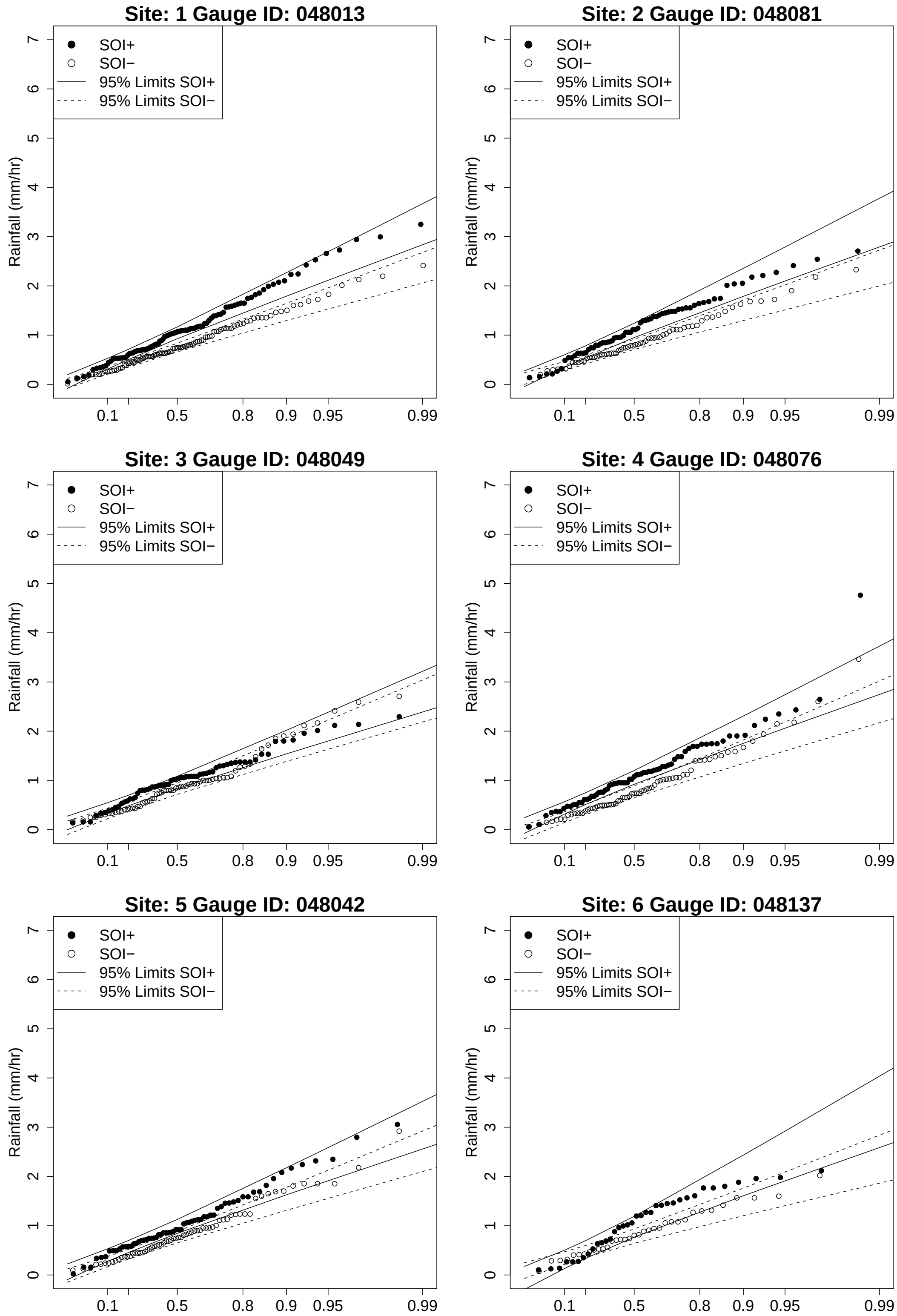

Figure B.7 Winter extremes of daily rainfall at Bourke partitioned by +ve/-ve phases of the SOI. Probabilities shown using a Gumbel axis. 95% Confidence intervals obtained from the distribution of estimates of the Gumbel parameters. Sites 1-6.

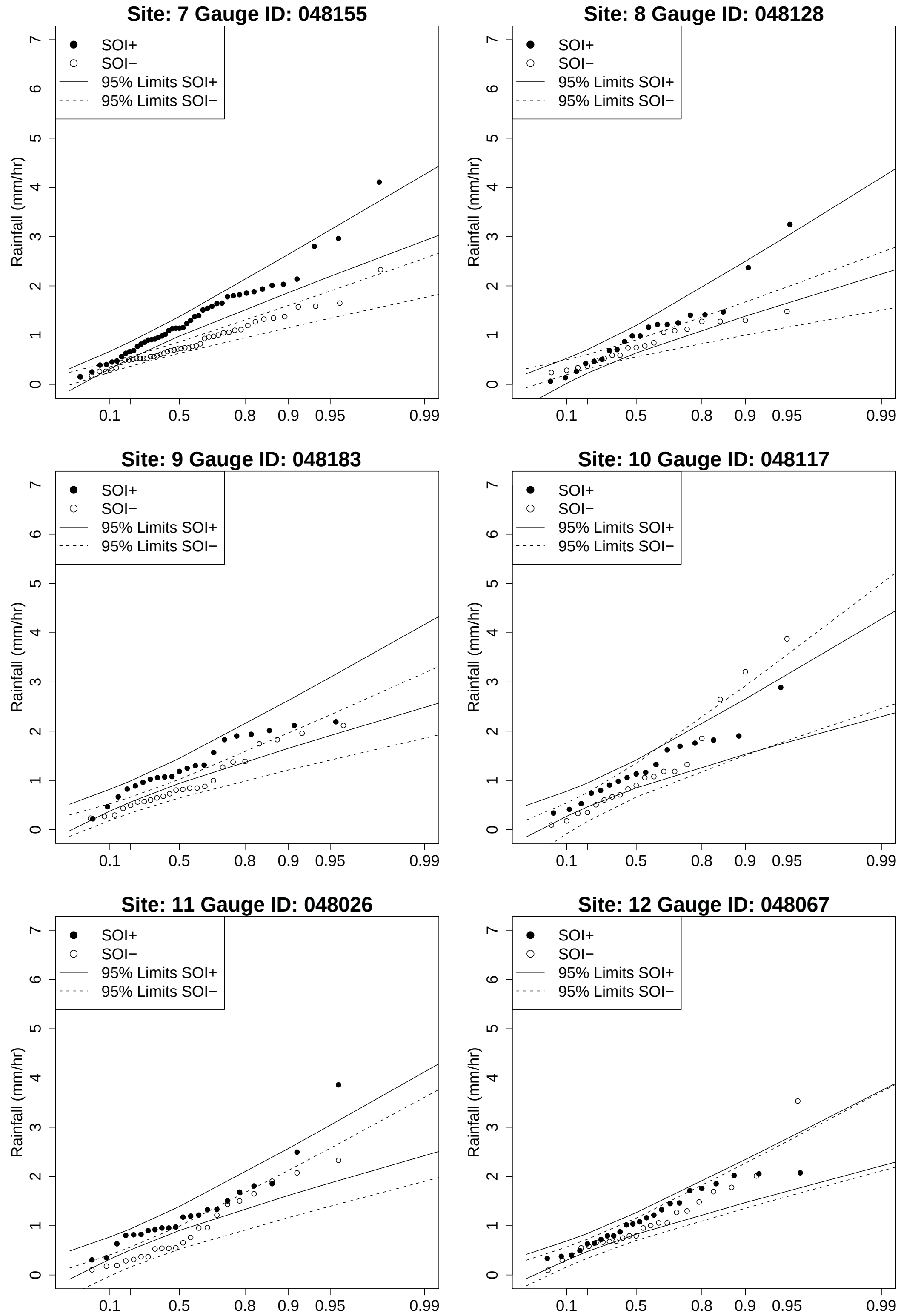

Figure B.8 Winter extremes of daily rainfall at Bourke partitioned by +ve/-ve phases of the SOI. Probabilities shown using a Gumbel axis. 95% Confidence intervals obtained from the distribution of estimates of the Gumbel parameters. Sites 7-12.

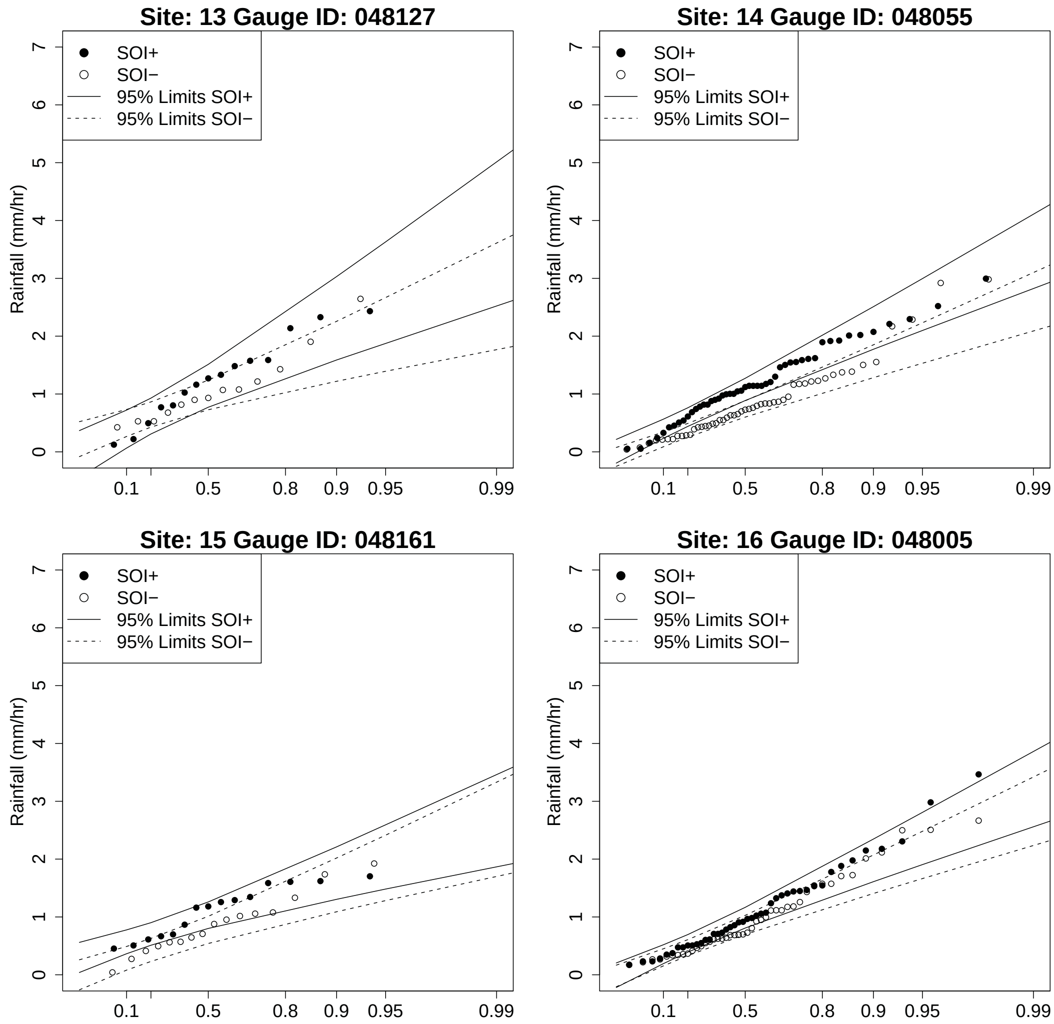

Figure B.9 Winter extremes of daily rainfall at Bourke partitioned by +ve/-ve phases of the SOI. Probabilities shown using a Gumbel axis. 95% Confidence intervals obtained from the distribution of estimates of the Gumbel parameters. Sites 13-16.

B.4 Observed Seasonally Partitioned SOI+ Extremes

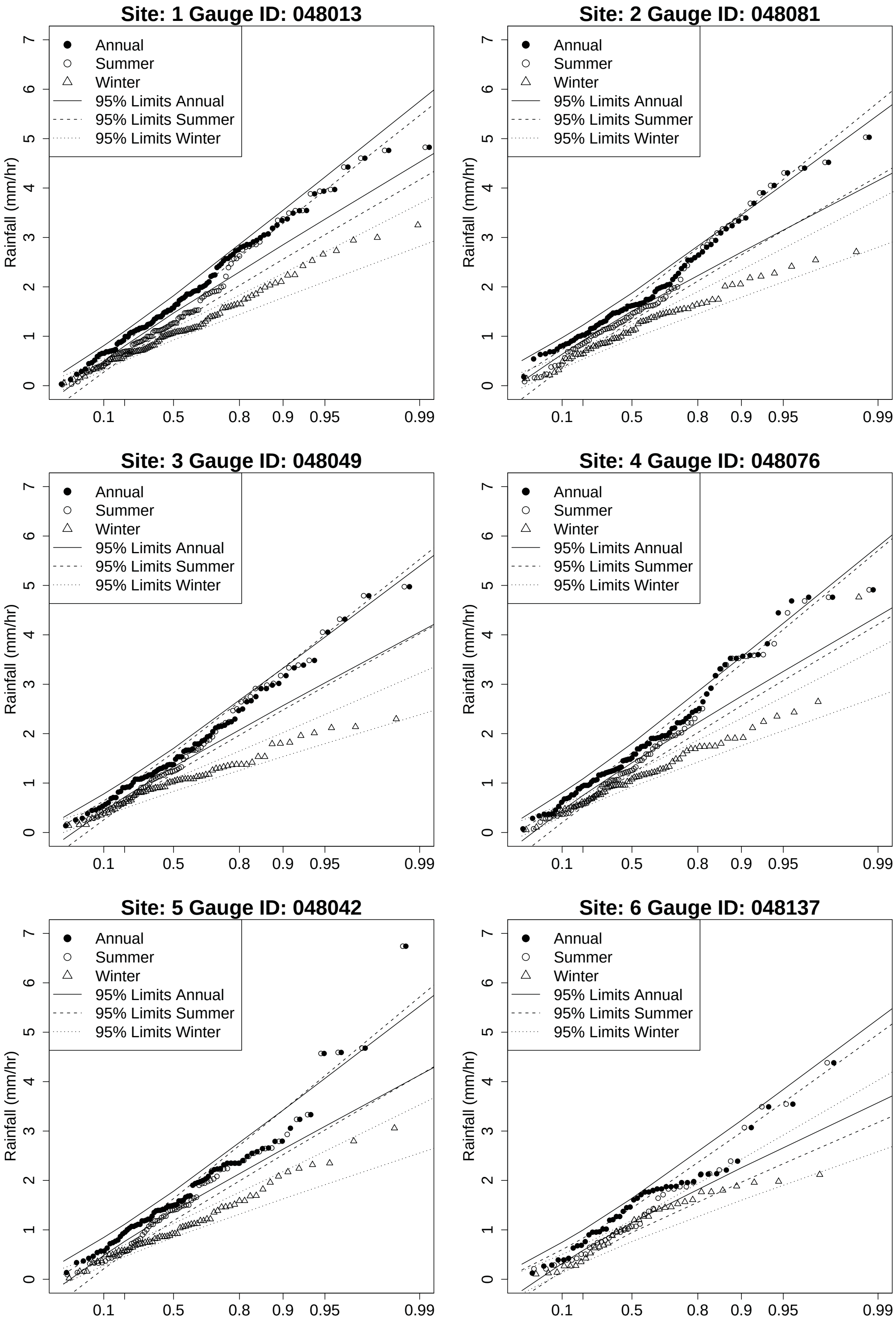

Figure B.10 Annual and 6-month seasonal extremes of daily rainfall at Bourke for +ve phase of the SOI. Probabilities shown using a Gumbel axis. 95% Confidence intervals obtained from the distribution of estimates of the Gumbel parameters. Sites 1-6.

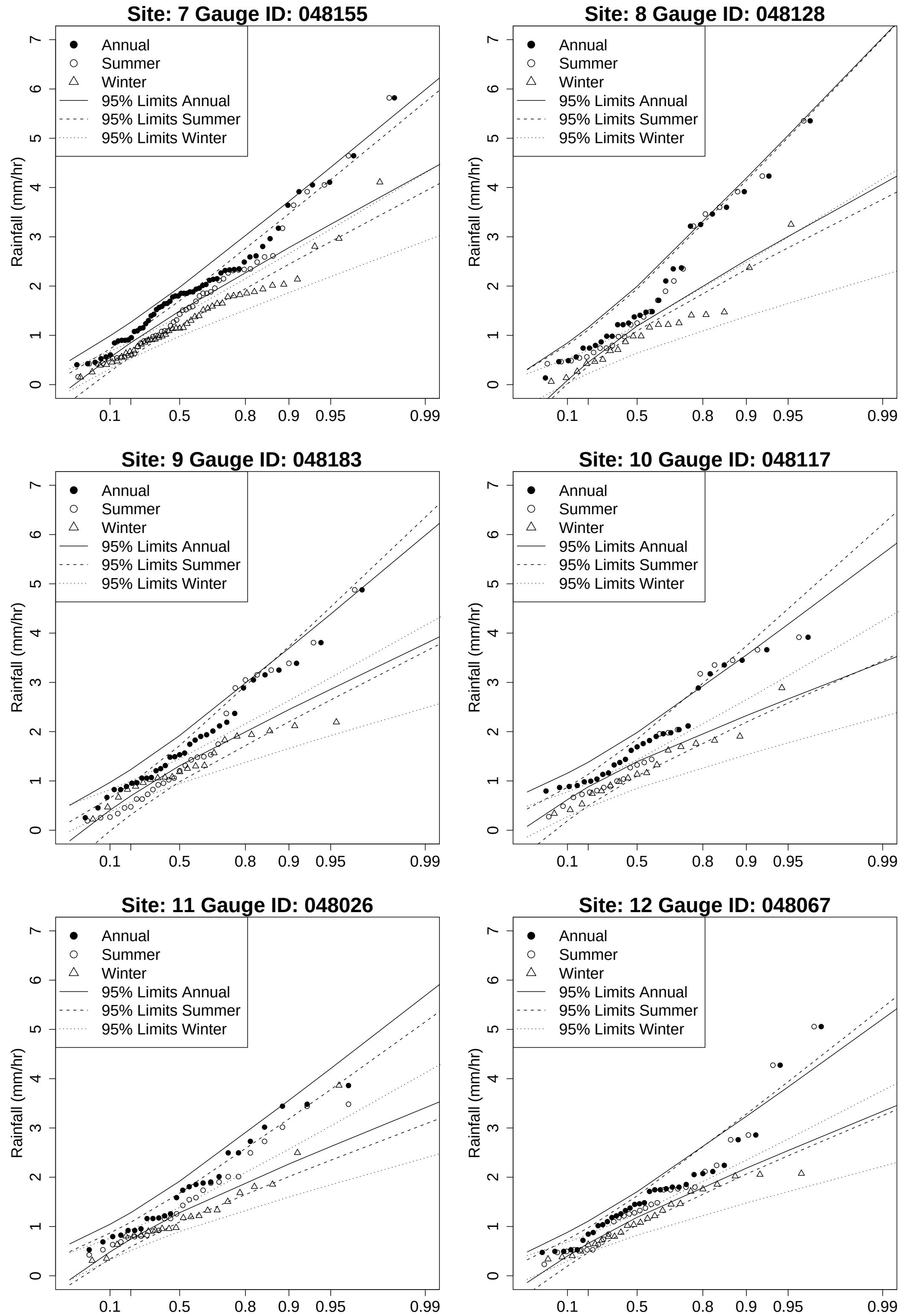

Figure B.11 Annual and 6-month seasonal extremes of daily rainfall at Bourke for +ve phase of the SOI. Probabilities shown using a Gumbel axis. 95% Confidence intervals obtained from the distribution of estimates of the Gumbel parameters. Sites 7-12.

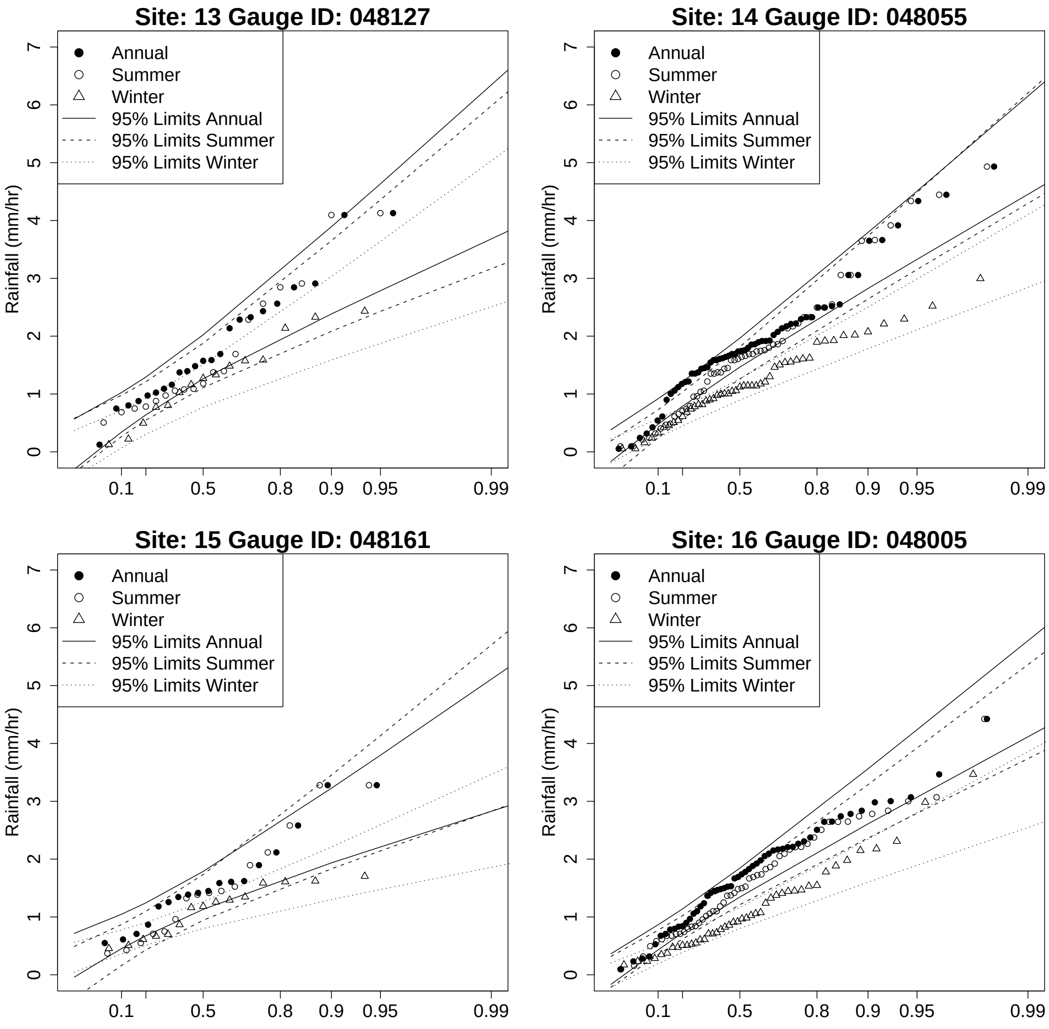

Figure B.12 Annual and 6-month seasonal extremes of daily rainfall at Bourke for +ve phase of the SOI. Probabilities shown using a Gumbel axis. 95% Confidence intervals obtained from the distribution of estimates of the Gumbel parameters. Sites 13-16.

B.5 OBSERVED SEASONALLY PARTITIONED SOI- EXTREMES

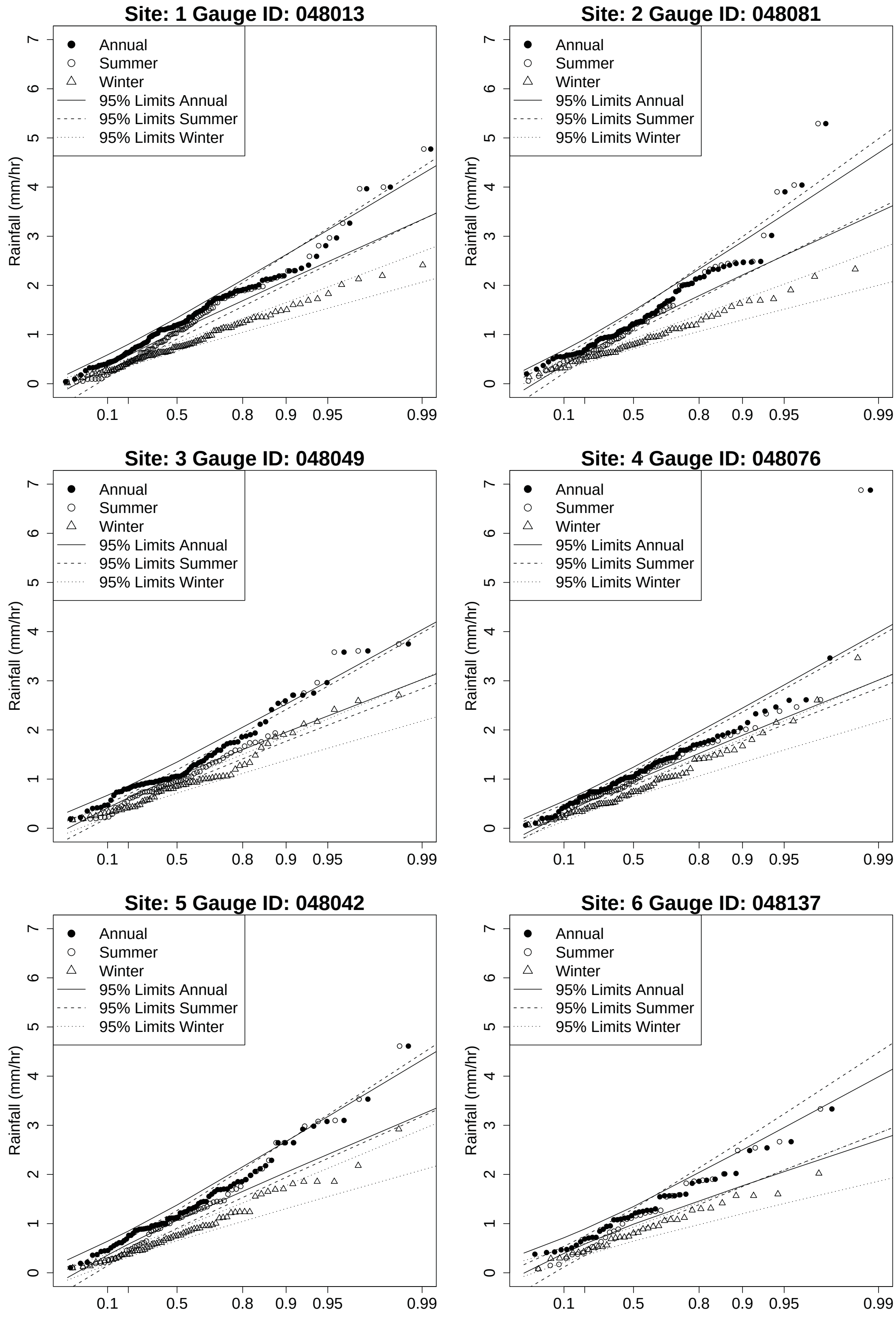

Figure B.13 Annual and 6-month seasonal extremes of daily rainfall at Bourke for -ve phase of the SOI. Probabilities shown using a Gumbel axis. 95% Confidence intervals obtained from the distribution of estimates of the Gumbel parameters. Sites 1-6.

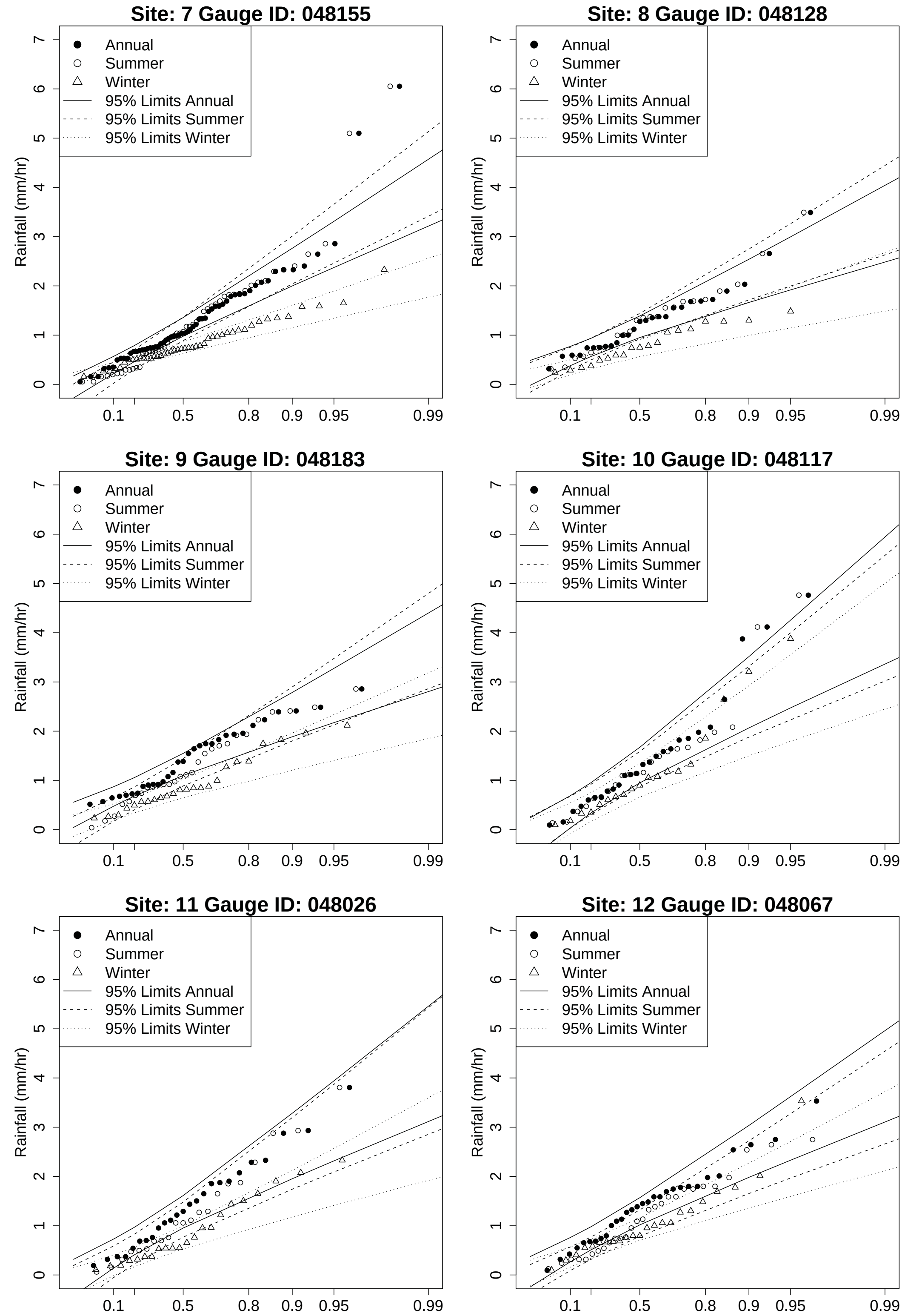

Figure B.14 Annual and 6-month seasonal extremes of daily rainfall at Bourke for -ve phase of the SOI. Probabilities shown using a Gumbel axis. 95% Confidence intervals obtained from the distribution of estimates of the Gumbel parameters. Sites 7-12.

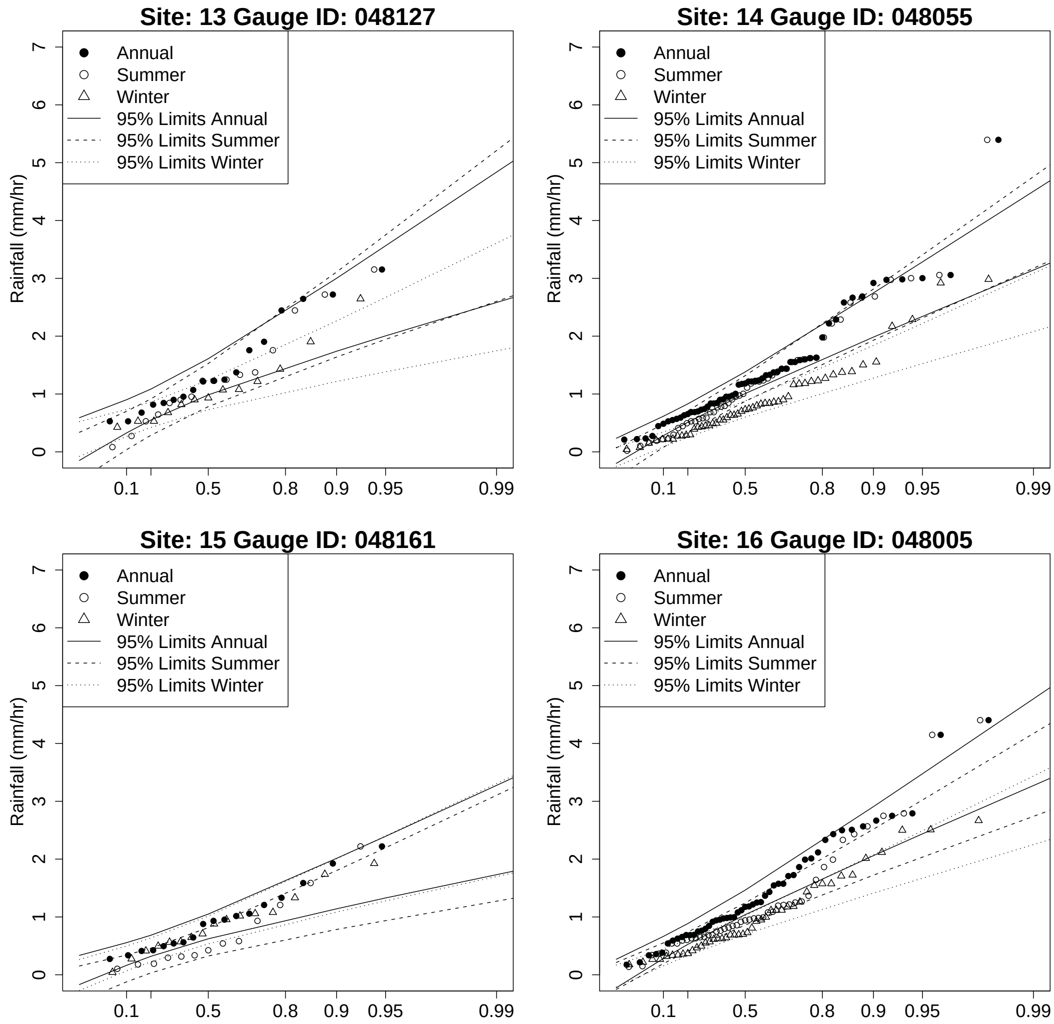

Figure B.15 Annual and 6-month seasonal extremes of daily rainfall at Bourke for -ve phase of the SOI. Probabilities shown using a Gumbel axis. 95% Confidence intervals obtained from the distribution of estimates of the Gumbel parameters. Sites 13-16.

B.6 Comparison of Observed and Simulated Extremes

The figures in this section compare extreme values irrespective of the phase of the SOI. Separate comparisons for SOI partitioned extremes have been omitted, but show a similar quality of fit.

The simulated confidence limits are from 1000 replicated series each having 100 years of 24 hour data. Note that the number of observed extremes is not in the vicinity of 100 at some of the sites, so the observed sampling variability will differ from the simulated sampling variability.

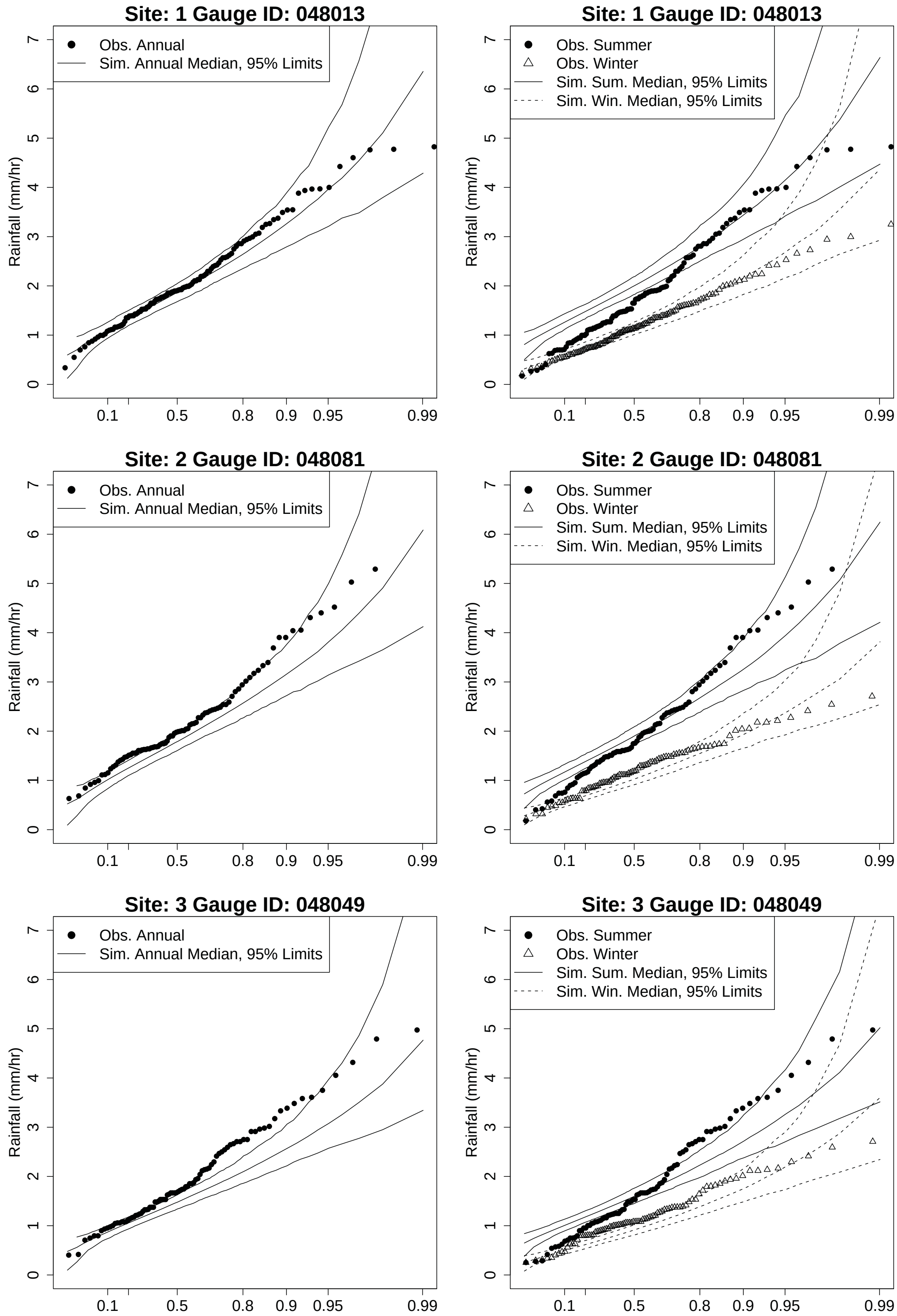

Figure B.16 L.H.S. compares observed annual extremes with the median and 95% limits of extremes from simulated daily records. R.H.S. figures compare observed 6-month seasonal extremes with simulated confidence limits. Simulated values from 1000 replicates of 100-year records. Probabilities shown using a Gumbel axis. Sites 1-3.

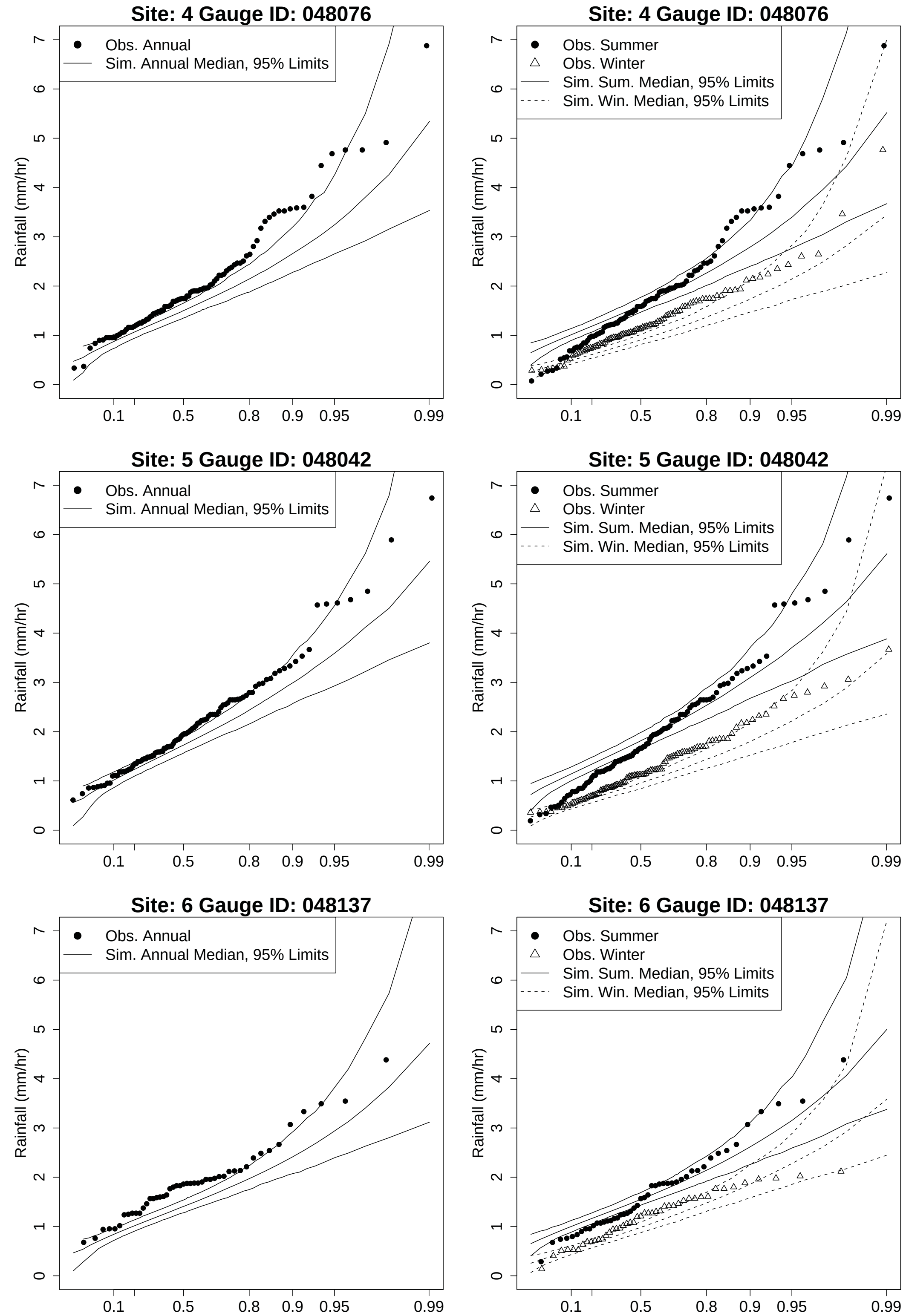

Figure B.17 L.H.S. compares observed annual extremes with the median and 95% limits of extremes from simulated daily records. R.H.S. figures compare observed 6-month seasonal extremes with simulated confidence limits. Simulated values from 1000 replicates of 100-year records. Probabilities shown using a Gumbel axis. Sites 4-6.

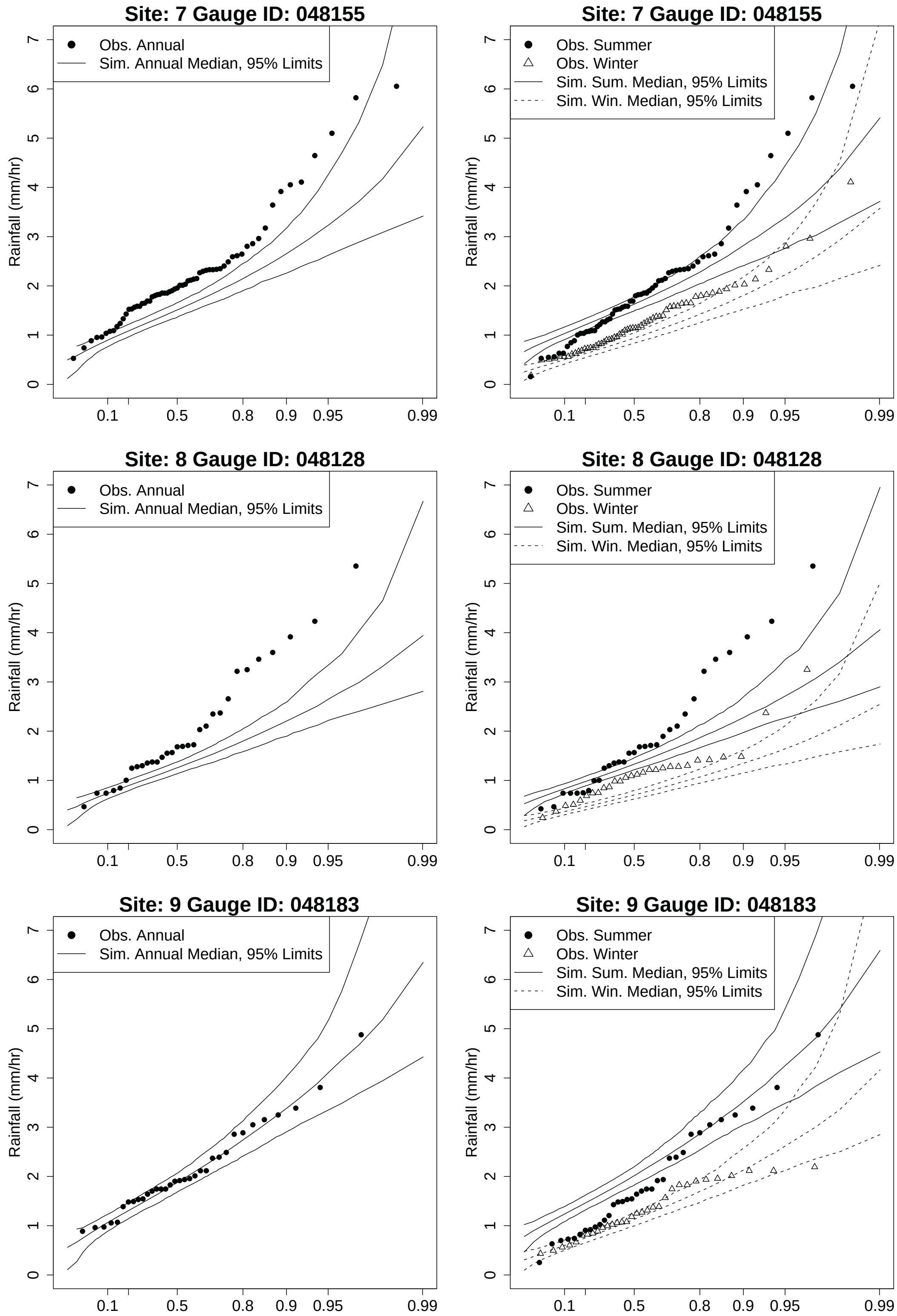

Figure B.18 L.H.S. compares observed annual extremes with the median and 95% limits of extremes from simulated daily records. R.H.S. figures compare observed 6-month seasonal extremes with simulated confidence limits. Simulated values from 1000 replicates of 100-year records. Probabilities shown using a Gumbel axis. Sites 7-9.

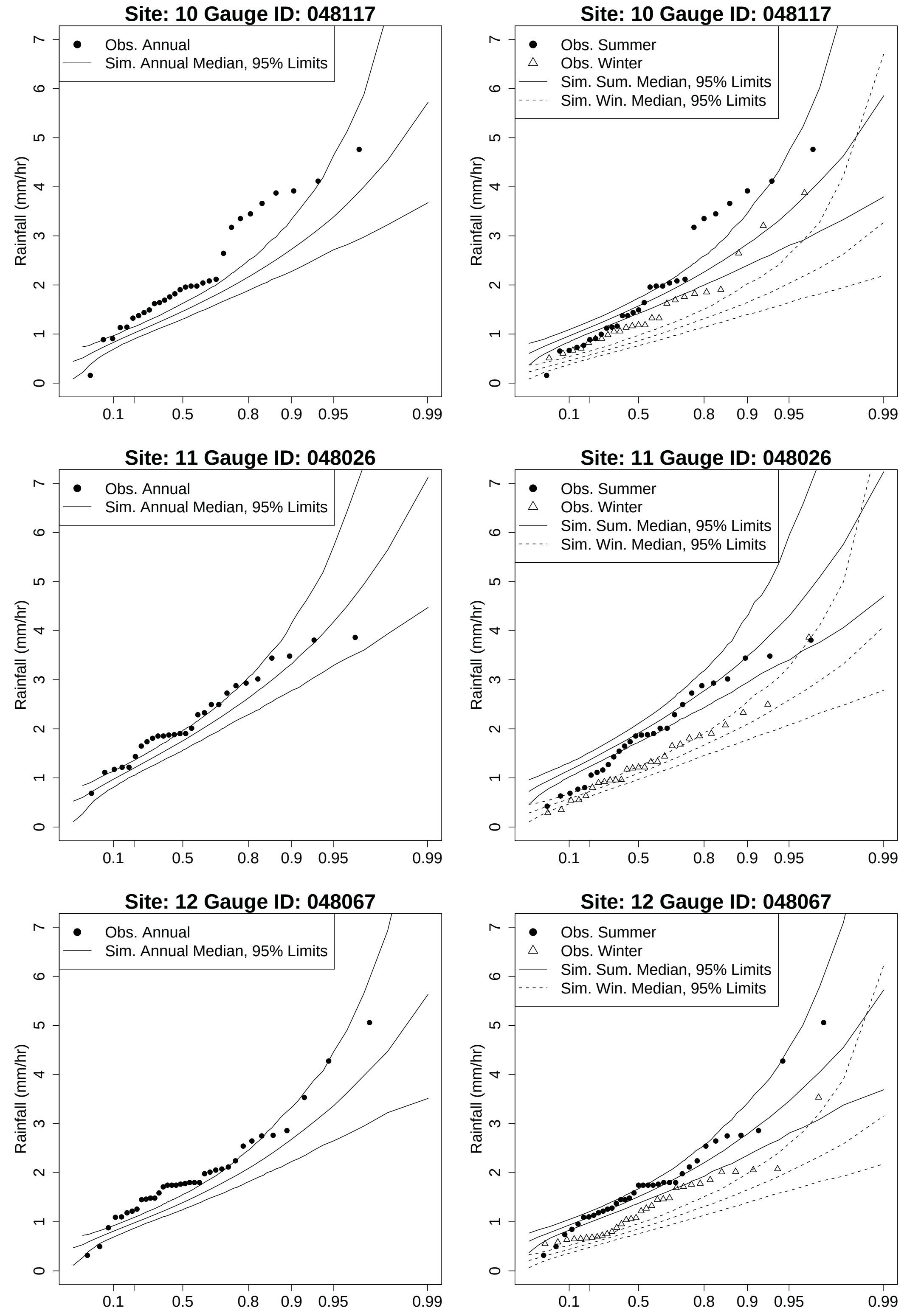

Figure B.19 L.H.S. compares observed annual extremes with the median and 95% limits of extremes from simulated daily records. R.H.S. figures compare observed 6-month seasonal extremes with simulated confidence limits. Simulated values from 1000 replicates of 100-year records. Probabilities shown using a Gumbel axis. Sites 10-12.

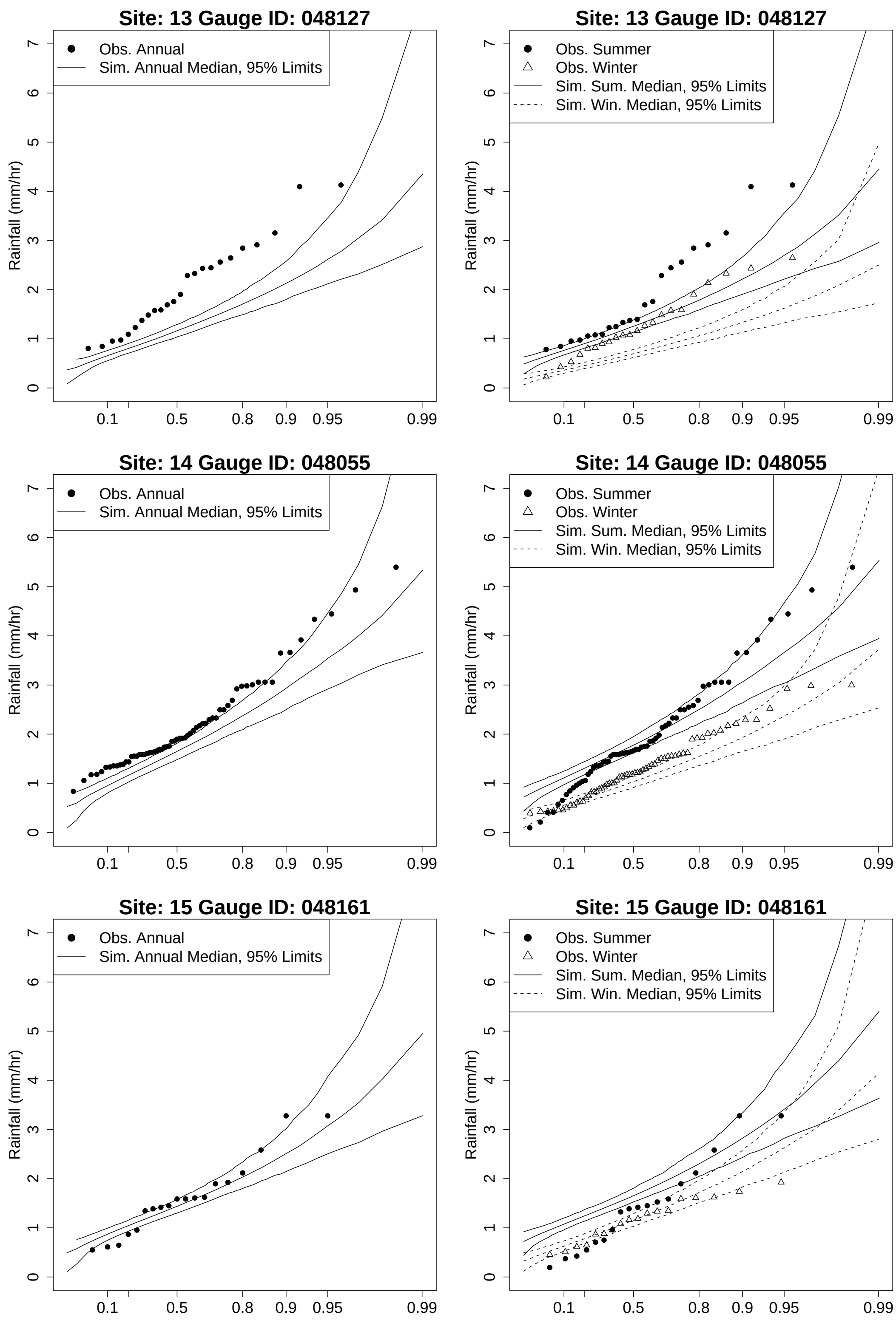

Figure B.20 L.H.S. compares observed annual extremes with the median and 95% limits of extremes from simulated daily records. R.H.S. figures compare observed 6-month seasonal extremes with simulated confidence limits. Simulated values from 1000 replicates of 100-year records. Probabilities shown using a Gumbel axis. Sites 13-15.

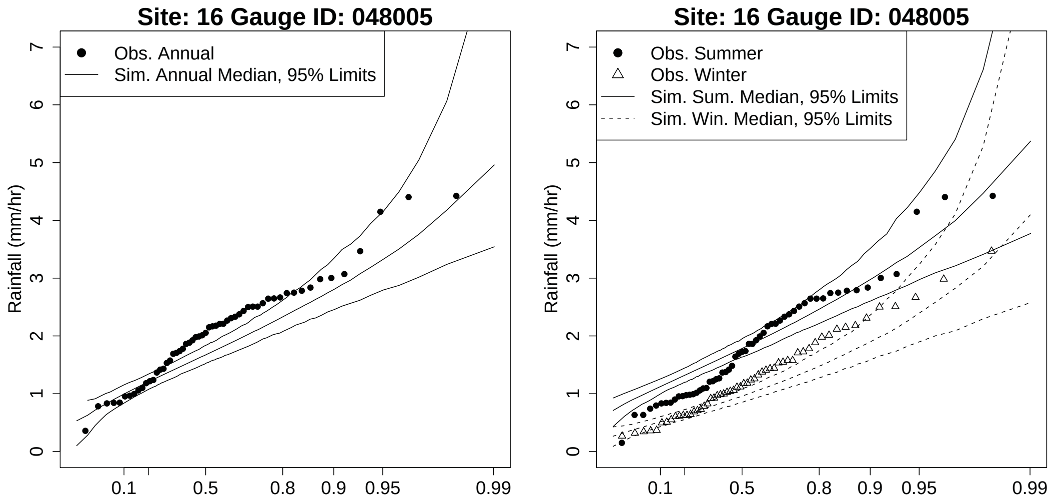

Figure B.21 L.H.S. compares observed annual extremes with the median and 95% limits of extremes from simulated daily records. R.H.S. figures compare observed 6-month seasonal extremes with simulated confidence limits. Simulated values from 1000 replicates of 100-year records. Probabilities shown using a Gumbel axis. Site 16.